مجلة الشمال
للعلوم
الأساسية والتطبيقية

دورية علمية محكمة

جامعة الحدود الشمالية
www.nbu.edu.sa & jnbas.nbu.edu.sa

طباعة - ردمد: 1658-7022
إلكتروني - ردمد: 1658-7014

2007 - 1428
جامعة الحدود الشمالية
NORTHERN BORDER UNIVERSITY

المجلد (6)
العدد (1)
مايو
2021
رمضان
1442هـ

J N B A S

مجلة الشمال للعلوم الأساسية والتطبيقية - المجلد (6) العدد (1) 1442 هـ
6(1)
Journal of the North for Basic and Applied Sciences Volume (6) Issue (1) 2021
J N B A S


بسم الله الرحمن الرحيم

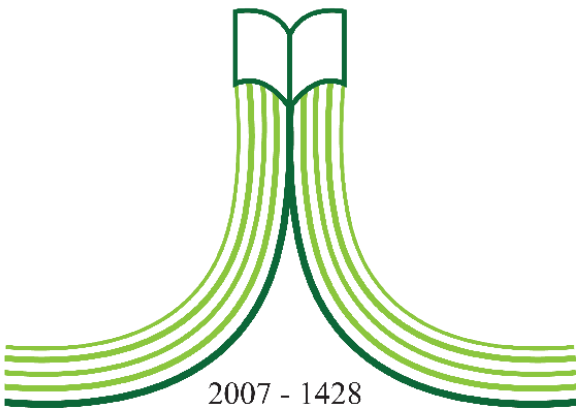
2007 - 1428
جامعة الحدود الشمالية
NORTHERN BORDER UNIVERSITY
المملكة العربية السعودية

مجلـة الشمــال
للعلوم الأساسية والتطبيقية
(JNBAS)

دورية علمية محكمة

تصدر عن
مركز النشر العلمي والتأليف والترجمة
جامعة الحدود الشمالية

المجلد السَّادس ــ العدد الأوّل

مايو 2021م ــ رمضان 1442هـ

الموقع والبريد الإلكتروني

http://jnbas.nbu.edu.sa
s.journal@nbu.edu.sa & s.journal.nbu@gmail.com

طباعة - ردمد: 1658-7022 / إلكتروني - ردمد: 1658-7014

مجلة الشمال للعلوم الأساسية والتطبيقية (JNBAS)

التعريف بالمجلة

تعنى المجلة بنشر البحوث والدراسات العلمية الأصيلة في مجال العلوم الأساسية والتطبيقية، باللغتين العربية والإنجليزية، كما تهتم بنشر جميع ما له علاقة بعرض الكتب ومراجعتها أو ترجمتها، وملخصات الرسائل العلمية، وتقارير المؤتمرات والندوات العلمية، وتصدر مرتين في السنة (مايو ـ نوفمبر).

الرؤية

الريادة في نشر البحوث العلمية المحكمة، وتصنيف المجلة ضمن أشهر الدوريات العلمية العالمية.

الرسالة

نشر البحوث العلمية المحكمة في مجال العلوم الأساسية والتطبيقية وفق معايير عالمية متميزة.

أهداف المجلة

1) أن تكون المجلة مرجعًا علميًا للباحثين في العلوم الأساسية والتطبيقية.
2) تلبية حاجة الباحثين إلى نشر بحوثهم العلمية، وإبراز مجهوداتهم البحثية على المستويات المحلية والإقليمية والعالمية.
3) المشاركة في بناء مجتمع المعرفة بنشر البحوث الرصينة التي تؤدي إلى تنمية المجتمع.
4) تغطية أعمال المؤتمرات العلمية المحكمة.

شروط قبول البحث

1) الأصالة والابتكار وسلامة المنهج والاتجاه.
2) الالتزام بالمناهج والأدوات والوسائل العلمية المتبعة في مجاله.
3) الدقة في التوثيق والمصادر والمراجع والتخريج.
4) سلامة اللغة.
5) أن يكون البحث غير منشور أو مقدم للنشر في أي مكان آخر.
6) أن يكون البحث المستل من الرسائل العلمية غير منشور أو مقدم للنشر، وأن يشير الباحث إلى أنه مستلٌ.

للمراسلة

رئيس التحرير
مجلة الشمال للعلوم الأساسية والتطبيقية (JNBAS)
جامعة الحدود الشمالية
ص.ب 1321، عرعر 91431
المملكة العربية السعودية.
هاتف : 966146615499+
فاكس: 966146614439+

الاشتراك والتبادل

مركز النشر العلمي والتأليف والترجمة
جامعة الحدود الشمالية
ص.ب. 1321، عرعر، 91431
المملكة العربية السعودية.

البريد الإلكتروني: *s.journal@nbu.edu.sa* & *s.journal.nbu@gmail.com*

الموقع الإلكتروني: *http://jnbas.nbu.edu.sa*

ISSN 1658-7022

شروط النشر

أولاً: ضوابط النص المقدم للنشر

1) ألا تزيد صفحاته عن (35) صفحة من القطع العادي (A4).
2) أن يحتوي على عنوان البحث وملخصه باللغتين العربية والإنجليزية في صفحة واحدة، بحيث لا يزيد عن (250) كلمة للملخص، وأن يتضمن البحث كلمات مفتاحية دالةٍ على التخصص الدقيق للبحث باللغتين، بحيث لا يتجاوز عددها (6) كلمات، توضع بعد نهاية كل ملخص.
3) أن يذكر اسم المؤلف وجهة عمله بعد عنوان البحث مباشرة باللغتين العربية والإنجليزية.
4) أن تقدم البحوث العربية مطبوعة بخط (Simplified Arabic)، بحجم (14) للنصوص في المتن، وبالخط نفسه بحجم (12) للهوامش.
5) أن تقدم البحوث الإنجليزية مطبوعة بخط (Times New Roman) بحجم (12) للنصوص في المتن، وبالخط نفسه بحجم (9) للهوامش.
6) كتابة البحث على وجه واحد من الصفحة، مع ترك مسافة سطر واحد بين السطور، وتكون الحواشي 2.5 سم على الجوانب الأربعة للصفحة، بما يعادل 1.00 إنش (بوصة).
7) التزام الترتيب الموضوعي الآتي:

المقدمة: تكون دالة على موضوع البحث، والهدف منه، ومنسجمة مع ما يَرِدُ في البحث من معلومات وأفكار وحقائق علمية، كما تشير باختصار إلى مشكلة البحث، وأهمية الدراسات السابقة.

العرض: يتضمن التفاصيل الأساسية لمنهجية البحث، والأدوات والطرق التي تخدم الهدف، وترتب المعلومات حسب أولويتها.

النتائج والمناقشة: يجب أن تكون واضحة موجزة، مع بيان دلالاتها دون تكرار.

الخاتمة: تتضمن تلخيصًا موجزًا للموضوع، وما توصل إليه الباحث من نتائج، مع ذكر التوصيات والمقترحات.

8) أن تدرج الرسوم البيانية والأشكال التوضيحية في النص، وترقم ترقيماً متسلسلاً، وتكتب أسماؤها والملاحظات التوضيحية أسفلها.
9) أن تدرج الجداول في النص، وترقم ترقيماً متسلسلاً، وتكتب أسماؤها أعلاها، وأما الملاحظات التوضيحية فتكتب أسفل الجدول.
10) ألا توضع الهوامش أسفل الصفحة إلا عند الضرورة فقط، ويشار إليها برقم أو نجمة، ويكون الخط فيها بحجم (12) للعربي و (9) للإنجليزي.
11) لا تنشر المجلة أدوات البحث والقياس، وتقوم بحذفها عند طباعة المجلة.
12) أن يُراعى في منهج توثيق المصادر والمراجع داخل النص نظام (APA)، وهو نظام يعتمد ذكر الاسم والتاريخ (name/year) داخل المتن، ولا يقبل نظام ترقيم المراجع داخل النص مع وضع الحاشية أسفل الصفحة، وتوضع المصادر والمراجع داخل المتن بين قوسين حسب الأمثلة الآتية: يذكر اسم عائلة المؤلف متبوعا بفاصلة، فسنة النشر، مثلا: (مجاهد، 1988م). وفي حالة الاقتباس المباشر يضاف رقم الصفحة مباشرة بعد تاريخ النشر مثلا: (خيري، 1985م، ص:33). أما إذا كان للمصدر مؤلفان فيذكران مع اتباع الخطوات السابقة مثلا: (الفالح وعياش، 1424هـ). وفي حالة وجود أكثر من مؤلفين فتذكر أسماء عوائلهم أول مرة، مثلا: (مجاهد والعودات والشيخ، 1408هـ)، وإذا تكرر الاقتباس من المصدر نفسه فيشار إلى اسم عائلة المؤلف الأول فقط، ويكتب بعده وآخرون مثل: (مجاهد وآخرون، 1408هـ)، على أن تكتب معلومات النشر كاملة في قائمة المصادر والمراجع.
13) تخرج الأحاديث والآثار على النحو الآتي:
(صحيح البخاري، ج:1، ص: 5، رقم الحديث 511).
14) توضع قائمة المصادر والمراجع في نهاية البحث مرتبة ترتيباً هجائياً حسب اسم العائلة، ووفق نظام جمعية علم النفس الأمريكية (APA) الإصدار السادس، وبحجم (12) للعربي و(9) للإنجليزي، وترتب البيانات الببليوغرافية على النحو الآتي:

- **الاقتباس من كتاب لمؤلف واحد:**

الخوجلي، أحمد. (2004م). ***مبادئ فيزياء الجوامد***. الخرطوم، السودان: عزة للنشر والتوزيع.

- **الاقتباس من كتاب لأكثر من مؤلف:**

نيوباي، تيموثي؛ ستيبتش، دونالد؛ راس، جيمس. (1434هـ/2013م). ***التقنية التعليمية للتعليم والتعلم***. الرياض، المملكة العربية السعودية: دار جامعة الملك سعود للنشر.

- **الاقتباس من دورية:**

النافع، عبداللطيف حمود. (1427هـ). أثر قيادة السيارات خارج الطرق المعبدة في الغطاء النباتي بالمنتزهات البرية: دارسة في حماية البيئة، في وسط المملكة العربية السعودية. ***المجلة السعودية في علوم الحياة***، *14*(1)، 53-72.

- **الاقتباس من رسالة ماجستير أو دكتوراه:**

القاضي، إيمان عبدالله. (1429هـ). ***النباتات الطبيعية للبيئة الساحلية بين رأسي تنورة والملوح بالمنطقة الشرقية: دراسة في الجغرافيا النباتية وحماية البيئة***. رسالة دكتوراه غير منشورة، كلية الآداب للبنات، الدمام، المملكة العربية السعودية: جامعة الملك فيصل.

- **الاقتباس من الشبكة العنكبوتية (الإنترنت):**

- الاقتباس من كتاب:

المزروعي، م.ر. و المدني، م.ف. (2010م). ***تقييم الأداء في مؤسسات التعليم العالي***. المعرِّف الرقمي (DOI:10.xxxx/xxxx-xxxxxxxx-x)، أو برتوكول نقل النصوص التشعبي (http://www...)، أو الرقم المعياري الدولي للكتاب (ISBN : 000-0- 00 - 000000-0)

– الاقتباس من مقالة في دورية:

المدني، م.ف. (2014). مفهوم الحوار في تقريب وجهات النظر. ***المجلة البريطانية لتكنولوجيا التعليم***، *11*(6)، 225-260. المعرِّف الرقمي (DOI:10.xxxx/xxxx-xxxxxxxx-x) أو برتوكول نقل النصوص التشعبي (http://onlinelibrary.wiley.com/journal/10.1111)، أو الرقم المعياري التسلسلي الدولي للمجلة - (ISSN: 1467 - 8535).

15) يلتزم الباحث بترجمة (أو رومنة) أسماء المصادر والمراجع العربية إلى اللغة الإنجليزية في قائمة المصادر والمراجع. وعلى سبيل المثال:

الجبر، سليمان. (1991م). تقويم طرق تدريس الجغرافيا ومدى اختلافها باختلاف خبرات المدرسين وجنسياتهم وتخصصاتهم في المرحلة المتوسطة بالمملكة العربية السعودية. ***مجلة جامعة الملك سعود- العلوم التربوية***، *3*(1)، 143-170.

Al-Gabr, S. (1991). The Evaluation of Geography Instruction and the Variety of its Teaching Concerning the Experience, Nationality, and the Field of Study in Intermediate Schools in Saudi Arabia *(in Arabic). Journal of King Saud University- Educational Sciences, 3*(1), 143-170.

16) تستخدم الأرقام العربية الأصلية (0، 1، 2، 3، ...) في البحث.

17) تؤول جميع حقوق النشر للمجلة في حال إرسال البحث للتحكيم وقبوله للنشر.

ثانياً: الأشياء المطلوب تسليمها

1) نسخة إلكترونية من البحث بصيغتي (WORD) و (PDF)، وترسلان على البريد الإلكتروني الآتي:

s.journal@nbu.edu.sa & s.journal.nbu@gmail.com

2) السيرة الذاتية للباحث، متضمنة اسمه باللغتين العربية والإنجليزية، وعنوان البريد الإلكتروني الحالي، ورتبته العلمية.

3) تعبئة النماذج الآتية:

أ - نموذج طلب نشر بحث في المجلة.

ب - نموذج تعهد بأن البحث غير منشور أو مقدم للنشر في مكان آخر.

ثالثاً: تنبيهات عامة

1) أصول البحث التي تصل إلى المجلة لا تردّ سواء أُنشِرَتْ أم لم تنشر.

2) الآراء الواردة في البحوث المنشورة تعبر عن وجهة نظر أصحابها.

مجلة الشمال للعلوم الأساسية والتطبيقية (JNBAS)

طباعة - ردمد: 1658-7022 إلكتروني - ردمد: 1658-7014

المجلد السادس - العدد الأول مايو 2021م - رمضان 1442هـ

المحتويات

الأبحاث العربية

الأبحاث الإنجليزية

الأبحاث باللغة العربية

المملكة العربية السعودية
جامعة الحدود الشمالية (NBU)
مجلة الشمال للعلوم الأساسية والتطبيقية (JNBAS)
طباعـــة ـ ردمد: 1658-7022 / الكتروني ـ ردمد: 1658-7014
www.nbu.edu.sa
http://jnbas.nbu.edu.sa
2007 - 1428
جامعة الحدود الشمالية
NORTHERN BORDER UNIVERSITY

فاعليـة بعـض البدائـل الطبيعيـة في مكافحـة مرض البيـاض الدقيقي على اليقطين المتسبب عن الفطر Sphaerotheca fuliginea (Schlecht.)

وليـــــد نفّـــاع [1] و نيرمين أبو فخر [2]

(قدم للنشر في 1441/02/29هـ؛ وقبل للنشر في 1442/01/15هـ)

ملخص: أجريت هذه الدراسة بهدف اختبار فاعلية مستخلصي تفل الزيتون وتفل العنب والمستحضر التجاري لحمض الساليسيلك (أسبيرين) بالمقارنة مع المبيد الفطري ثيوفانات الميثيل في الحد من الإصابة بمرض البياض الدقيقي على اليقطين Pumpkin المتسبب عن الفطر Sphaerotheca fuliginea (Schlecht). أظهرت النتائج أن استخدام مستخلص تفل الزيتون وحمض الساليسيلك أدى إلى تأخير حدوث الإصابة بالبياض الدقيقي على نباتات اليقطين، وخفض شدة الإصابة بشكل مماثل تقريباً للمبيد الفطري، حيث حققا حماية شبه تامة للنباتات خلال 12 يوماً بعد العدوى الاصطناعية، مقابل 16 يوماً عند المعاملة بالمبيد الفطري، والذي فقد فاعليته بشكل جزئي بعد 19 يوماً. بينما كان مستخلص تفل العنب الأقل فاعلية على الرغم من وجود فروق معنوية واضحة مقارنة بالمجموعة الضابطة، حيث ظهرت أولى أعراض الإصابة بعد 6 أيام من العدوى الاصطناعية، ومع ذلك كان مستوى الإصابة منخفضاً نسبياً مقارنة مع معاملة المقارنة. ويمكن ترتيب هذه المركبات تبعاً لفاعليتها في خفض شدة الإصابة كما يلي: ثيوفانات الميثيل ≤ حمض الساليسيلك ≤ مستخلص تفل الزيتون < مستخلص تفل العنب. وبالاعتماد على هذه النتائج، ونظراً للتأثير الضار للمبيدات في البيئة، يمكن أن يوصى باستخدام حمض الساليسيلك ومستخلص تفل الزيتون كبدائل آمنة ورخيصة الثمن لإدارة هذا المرض في المساحات الصغيرة والزراعات المنزلية والبيوت البلاستيكية.

كلمات مفتاحية: بياض دقيقي، قرعيات، مقاومة جهازية مكتسبة، تفل الزيتون، تفل العنب، حمض الساليسيلك.

للمراسلة:
أستاذ، قسم وقاية النبات، كلية الهندسة الزراعية، جامعة دمشق، دمشق، سوريا.

e-mail: *walid1851966@yahoo.com*

jnbas.nbu.edu.sa
DOI: 10.12816/0058339

KINGDOM OF SAUDI ARABIA
Northern Border University (NBU)
Journal of the North for Basic and Applied Sciences (JNBAS)
p- ISSN: 1658 - 7022 / **e- ISSN:** 1658 - 7014
www.nbu.edu.sa
http://jnbas.nbu.edu.sa

Effectiveness of Some Natural Alternatives in controlling pumpkin powdery mildew caused by Sphaerotheca fuliginea (Schlecht.)

Walid Naffaa[1] & Nermeen Abou Fakher[2]

(Received 29/10/2019; Accepted 03/09/2020)

Abstract: This study was conducted in order to test the efficacy of olive pomace extract (OPE), grape pomace extract (GOE) and the commercial salicylic acid / aspirin (SA) compared with methyl thiophanate fungicide to reduce powdery mildew incidence of pumpkin caused by Sphaerotheca fuliginea (Schlecht.). The results showed that OPE and SA delayed the incidence of powdery mildew on pumpkin plants, and reduced the disease severity comparably to the fungicide. They almost completely protected the plants within 12 days after artificial inoculation compared to 16 days at fungicide treatment, which was partially ineffective after 19 days. While, GPE was of less effect in this regard, although there were significant differences compared to control treatment, where the first symptoms were observed after 6 days of artificial inoculation. However, the disease severity was relatively low compared to untreated control. These compounds can be arranged according to their effectiveness in reducing the disease severity as follows: methyl thiophanate ≥ salicylic acid ≥ olive pomace extract > grape pomace extract. Based on our results and regarding the adverse effects of fungicide on the environment, use of SA and POE as environmentally safe and inexpensive agents is recommended as a valuable contribution to disease management in small areas, homegrown and greenhouses.

Keywords: Powdery mildew, Cucurbit, Systemic acquired resistance, Olive pomace extract, Grape pomace extract, Salicylic acid

jnbas.nbu.edu.sa
DOI: 10.12816/0058339

* **Corresponding Author:**

Professor Dept. of Plant Protection, Faculty of Agriculture, Damascus University, Damascus, Syria.

e-mail: *walid1851966@yahoo.com*

1. مقدمـــة

يعمد المزارعون في الكثير من القرى السورية إلى زراعة اليقطين Cucurbita moschata Duchesne ex Poir من الفصيلة القرعية Cucurbitaceae واستثماره كمصدر رزق، خاصة وأنه لا يتطلب جهداً كبيراً في العناية به، إضافة إلى فوائده، إذ يحتوي على نسب عالية من البروتين والمواد الدهنية والنشوية والألياف والفيتامينات والأحماض الأمينية ومعادن الفوسفور والبوتاسيوم والحديد والزنك والكبريت والمغنيزيوم إلى جانب الماء. كما أن بذور اليقطين تحتوي على عناصر الكربوهيدرات والبروتين وفيتامين (ب)، ويقوم اليقطين على علاج العديد من أمراض القلب وتصلب الشرايين وارتفاع الكوليسترول وضغط الدم، وذلك بسبب احتوائه على نسبة جيدة من الدهون غير المشبعة التي تساعد على طرح الكوليسترول الفائض من الدم، وأخذ ما هو مترسب منه في جميع ألياف وأنسجة الجسم (Jacobo-Valenzuela, Maróstica-Junior, Zazueta-Morales, & Gallegos-Infante, 2011; Indrianingsih, Rosyida, Apriyana, Hayatis, Nisa, Darsih, Kusumaningrum, Ratih, & Indirayati, 2019).

يعد البياض الدقيقي المتسبب عن الفطر Sphaerotheca fuliginea (Schlecht.) Pollacci, (1913) من أهم الأمراض الفطرية التي تصيب أوراق وسوق وثمار القرعيات سواء في الحقل أو في البيوت البلاستيكية (Morsy, Elham, & Gehad, 2009). وتعتمد مكافحة مرض البياض الدقيقي على القرعيات بشكل أساسي على استخدام المبيدات الفطرية، ولكن أصبحت هناك مشكلة في الحصول على مكافحة تامة وفعالة نظراً لأن مجتمعات الفطر طورت نوعاً من المقاومة ضد المبيدات الفطرية المستخدمة (De Waard, Georgopoulos, Hollomon, Ishii, Leroux, Ragsdale, & Schwinn, 1993)، إضافة إلى أن المكافحة الكيميائية لأمراض النبات تسبب غالباً تلوثاً للبيئة، وتزيد من تراكم المركبات السامة في السلسلة الغذائية للإنسان، ولذلك أصبح هناك حاجة متزايدة للبحث عن بدائل آمنة لمكافحة أمراض النبات كزراعة الأصناف المقاومة، أو استخدام مركبات لتحريض ظاهرة المقاومة المستحثة (المقاومة التحريضية) Induced resistance (IR)، وقد تم استخدام العديد من هذه المركبات بنجاح في مكافحة العديد من أمراض النبات (Yurina, Karavaev, & Solntsev, 1993؛ Ibrahim, Khafagi, Ghonim, & El-Abbasi, 2003)، وقد اشارت العديد من الأبحاث إلى أن بعض هذه المركبات الكيميائية مثل حمض السالسيليك salicylic acid (SA) وأملاح البوتاسيوم و β-amino butyric acid (βABA) تحرض المقاومة الجهازية المكتسبة Systemic acquired resistance (SAR) في النباتات ضد بعض الممرضات النباتية (Oostendorp, Kunz, Dietrich, & Staub, 2001؛ Lin, Ishizaka, & Ishii, 2009؛ Zeighaminejad, Sharifi-Sirchi, Mohamadi, & Aminai, 2016; Sharifi-Sirchi, Beheshti, Hosseinipour, & Abo-Elyousr, Hussein, Allam, وجد . Mansouri, 2011). & Hassan (2009)، أن رش نباتات البصل بحمض الساليسيلك (SA 20 µM) خفض شدة الإصابة بالفطر Stemphylium sp. المسبب للفحة الأوراق.

وتمتاز المركبات الفينولية الموجودة في ثمار الزيتون ومستخلصات أوراق الزيتون بفاعلية مضادة للطفرات وللتسرطن (Visioli, Romani, Mulinacci, Zarini, Conte, Franco, & Galli, 1999)، وبنشاط مضاد للميكروبات (Aziz, Farag, Mousa, & Abo-Zaid, 1998; Nychas, Tassou, & Board, 1990)، كما أنها تدخل في آليات المقاومة عند النباتات ضد الممرضات من بكتيريا وفطريات وفيروسات (Marsilio, Campestre, & Lanza, 2001).

لقد أظهرت العديد من الدراسات التضادية الميكروبية للماء الناتج عن عملية استخلاص زيت الزيتون من جهة (Capasso, Evidente, Schivo, Orru, Marciales, & Cristinzo, 1995)، ولمستخلص أوراق الزيتون من جهة أخرى (Markin, Duek, & Berdicevsky, 2003)، ودور حمض الساليسيلك في مقاومة العديد من أمراض النبات الفطرية (Faize & Faize, 2018؛ Subban, Subramani, Srinivasan, Johnpaul, & Chelliah, 2019)، ولكن نادرة هي الدراسات المتعلقة باستخدام مستخلص تفل الزيتون وتفل العنب في مكافحة أمراض النبات، ولهذا فقد هدف هذا البحث إلى اختبار فاعلية هذه المستخلصات النباتية إضافة إلى حمض الساليسيلك في الحد من الإصابة بمرض البياض الدقيقي على اليقطين Pumpkin.

2. المواد والطرائق

نُفّذت التجربة في أرض زراعية مساحتها (10x24=240م^2) في منطقة الكوم بمحافظة السويداء في جنوب سوريا.

1.2. تحضير الأرض للزراعة:

أجريت عملية حراثة للتربة وإزالة الحجارة منها، وتسويتها

وتقسيمها لقطعات عشوائية، عددها خمس قطعات للمعاملات الأربع (تفل الزيتون، وتفل العنب، حمض الصفصاف، ثيوفانات الميثيل)، بالإضافة لمعاملة المقارنة. مساحة كل قطاع 40 م^2 (10x24)، والمسافة بين كل قطعة والأخرى 1م، وقسّمت كل قطعة إلى ثلاث قطع تجريبية يمثل كل منها مكرر مساحة كل منها 12 م^2 (4 x 3)، والمسافة بين كل منها 50 سم. زرعت بذور اليقطين من الصنف بلدي بتاريخ 7 مايو (أيار) 2018، وذلك في ثلاثة خطوط في كل مكرر بمعدل 5 نباتات في كل خط، والمسافة بين الخط والآخر 100 سم، وبين النبات والآخر 50 سم، وبالتالي يكون عدد النباتات في كل مكرر 15 نباتاً، وعدد النباتات المزروعة في كل معاملة 45 نباتاً، و225 نباتاً في كامل التجربة. تم ري النباتات حسب الحاجة حتى انتهاء فترة التجربة.

2.2. تحضير مستخلص تفل الزيتون:

تم أخذ عينة حوالي 1 كغ من التفل الناتج عن عصر ثمار الزيتون من إحدى معاصر محافظة السويداء. تم تجفيفها عند 60 مْ، ووضعها في كيس بلاستيكي، وتخزينها بدرجة حرارة 4 مْ. أجريت عملية الاستخلاص على مرحلتين: في المرحلة الأولى، تمت إضافة الهكسان إلى الثفل الجاف بنسبة 4: 1 (v / w) لإزالة الزيت المتبقي والأصبغة، وكررت هذه العملية ثلاث مرات متتالية. في الخطوة الثانية، تمت إضافة الكحول الايثيلي 70٪ (الايثانول C2H2OH) بنسبة 6: 1 (v / w) مع التحريك المستمر والهرس بواسطة مدقة هاون خزفي على فترات متقطعة لمدة ساعتين، ثم تصفيتها بواسطة ورق ترشيح. تم تركيز المستخلص الكحولي باستخدام جهاز المبخر الدوراني حتى تبخر نصف الكمية تقريباً، وغُلف الدورق بورق القصدير لحجب الضوء، وحفظ المستخلص في البراد لحين الاستخدام (Naffaa, 2016).

3.2 تحضير مستخلص تفل العنب:

أُخذت كمية 1 كغ تقريباً من تفل العنب (صنف سلطي) من إحدى المعاصر، جُففتْ عند درجة حرارة 60 °م، ثمّ وضعت في كيس بلاستيكي عند 4 °م في البراد. أُجريَت عملية الاستخلاص بإضافة الكحول الايثيلي 70% (الايثانول C2H2OH) بنسبة 1 تفل / 5 كحول (وزن / حجم) مع التحريك المستمر والهرس بواسطة مدقة الهاون الخزفي على فترات متقطعة لمدة 60 دقيقة، ثمّ صُب المستخلص فوق ورقة ترشيح ضمن قمع مثبت فوق دورق سعة 250 مل، وتم تركيز المستخلص باستخدام جهاز المبخر الدوراني حتى تبخر نصف الكمية تقريباً، وغُلف الدورق بورق القصدير لحجب الضوء، وحفظ المستخلص في البراد لحين الاستخدام.

4.2 حمض الساليسيلك (Salicylic acid SA) :

تم استخدام المركب الدوائي التجاري اسبرين Aspirin100، حيث يحتوي كل قرص على 100 ملغ من المادة الفعالة حمض أستيل ساليسيلك acetylsalicylic acid. تم تحضير محلول حمض الساليسيلك بالماء بتركيز 0.5 غ / ليتر.

5.2 تحضير اللقاح الفطري:

جُمعت نباتات مصابة بالبياض الدقيقي بشكل طبيعي، ونُقلت الأبواغ الكونيدية بلطف بواسطة فرشاة ناعمة إلى 100 مل ماء مقطر مضافاً إليه قطرتين من التوين Tween-20. واستخدمت شريحة العد (Neubauer-improved Counting Chamber; Marienfeld, Germany) لتحديد تركيز المعلق البوغي، ثم أجريت التخفيفات المناسبة بالماء المقطر للوصول إلى التركيز 10^{6}x4 بوغاً/مل ماء (Zeighaminejad et al., 2016).

6.2 التجربة الحقلية والعدوى الاصطناعية:

تم رش السطح العلوي والسفلي لنباتات اليقطين بتاريخ 27 مايو 2018 وفق المعاملات التالية: (1) مستخلص تفل الزيتون بتركيز 10%، (2) مستخلص تفل العنب 10%، (3) حمض الساليسيلك بتركيز 0.5 غ/ليتر، (4) المبيد الفطري ثيوفانات الميثيل (توبسين 70) وفق معدل الاستخدام الموصى به، (5) الرش بالماء فقط واستخدم كشاهد غير معامل. وبعد 48 ساعة من المعاملة، أجريت العدوى الاصطناعية برش المعلق البوغي على النباتات باستخدام مرش يدوي صغير. تم أخذ ست قراءات خلال 29 يوماً، حيث تم تسجيل عدد الأوراق المصابة على السطح العلوي فقط، وعدد الأوراق المصابة على السطح السفلي فقط، وعدد الأوراق المصابة على كلا سطحي الورقة، وعدد الأوراق السليمة والأوراق

الميتة، وأخيراً حساب النسبة المئوية للأوراق المصابة وكذلك للأوراق الميتة.

7.2 التحليل الإحصائي:

أجري التحليل الإحصائي باستخدام البرنامج الإحصائي Spss15 لحساب أقل فرق معنوي (L.S.D) عند مستوى $P\leq0.05$ (Gomez & Gomez, 1984).

3. النتائج :

تمت زراعة نباتات اليقطين بقطاعات عشوائية وفق خمس معاملات وفي كل منها ثلاثة مكررات. أجريت العدوى الاصطناعية على النباتات بأبواغ الفطر Sphaerotheca fuliginea المسبب لمرض البياض الدقيقي على القرعيات، وذلك بعد 48 ساعة من معاملة النباتات بمستخلص تفل الزيتون، ومستخلص تفل العنب، وحمض الساليسيلك ومقارنتها مع المبيد الفطري ثيوفانات الميثيل، إضافة إلى معاملة المقارنة غير المعامل. أخذت ست قراءات خلال 29 يوماً.

يتضح من الجدول (1) عدم ظهور أي أعراض للإصابة على السطح العلوي بعد ستة أيام من العدوى الاصطناعية، بينما بدأت الأعراض تظهر على السطح السفلي في معاملتي تفل العنب والمقارنة، وقد وصلت أعلى نسبة مئوية للأوراق المصابة في معاملة المقارنة (15.4%)، بينما كانت 4% في معاملة مستخلص تفل العنب، ولم تسجل أي إصابة على النباتات المعاملة بمستخلص تفل الزيتون وحمض الساليسيلك والمبيد الفطري. ولم يلاحظ وجود نباتات ميتة في أي من المعاملات المختلفة. يتضح مما سبق أن الإصابة بالبياض الدقيقي على القرعيات تبدأ على السطح السفلي للأوراق، ومن ثم تنتقل إلى السطح العلوي لتعم الإصابة كلا سطحي الورقة.

جدول 1:

متوسط عدد الأوراق المصابة والميتة ونسبتها المئوية بعد 6 أيام من العدوى الاصطناعية بالفطر المسبب للبياض الدقيقي على القرعيات في كل من المعاملات المختلفة

	تفل الزيتون	تفل العنب	حمض الساليسيلك	ثيوفانات الميثيل	المعاملة المقارنة
على السطح العلوي فقط	-	-	-	-	-
على السطح السفلي فقط	-	0.2	-	-	0.17
على سطحي الورقة معاً	-	0.20	-	-	0.75
مجموع الأوراق المصابة	-	0.4	-	-	0.92
النسبة المئوية للأوراق المصابة	-	%4.0a	-	-	%15.4b
النسبة المئوية للأوراق الميتة	-	-	-	-	-

● تشير الأحرف المتشابهة لعدم وجود فروق معنوية بين المعاملات عند مستوى معنوية 5 %.

تؤكد النتائج في القراءة الثانية بعد تسعة أيام من العدوى الاصطناعية (الجدول 2) أن الأعراض لم تلاحظ أيضاً على السطح العلوي، وهذا ما يؤكد ما لوحظ في القراءة الأولى بأن الإصابة تبدأ على السطح السفلي للأوراق. كما لوحظ بدء ظهور الأعراض على النباتات في معاملتي تفل الزيتون وحمض الساليسيلك، ولكن بنسب منخفضة جداً، وهذا يشير إلى أن المعاملة بتفل الزيتون وحمض الساليسيلك أخرت ظهور أعراض الإصابة. وصل متوسط النسبة المئوية للأوراق المصابة إلى 31.7% في معاملة المقارنة، تلتها معاملة مستخلص تفل العنب 9.8%، و0.6% في معاملة مستخلص تفل الزيتون، و0.51% في معاملة حمض الساليسيلك، بينما لم تلاحظ أي إصابات في معاملة المبيد. ولم تكن الفروق معنوية بين معاملتي مستخلص تفل الزيتون ومعاملة حمض الساليسيلك والمبيد الفطري، بينما كانت الفروق معنوية بالمقارنة مع معاملة تفل العنب والمقارنة. كما يلاحظ ظهور نباتات ميتة في معاملة المقارنة فقط بنسبة مئوية 1.02%.

جدول 2:

متوسط عدد الأوراق المصابة والميتة ونسبتها المئوية بعد 9 أيام من العدوى الاصطناعية بالفطر المسبب للبياض الدقيقي على القرعيات في كل من المعاملات المختلفة

	تفل الزيتون	تفل العنب	حمض الساليسيلك	ثيوفانات الميثيل	المعاملة المقارنة
على السطح العلوي فقط	-	-	-	-	-
على السطح السفلي فقط	0.2	2.33	0.9	-	0.25
على سطحي الورقة معاً	0.33	0.33	-	-	2.33
مجموع الأوراق المصابة	0.53	2.66	0.9	-	2.58
النسبة المئوية للأوراق المصابة	%0.6a	%9.8b	%0.51a	-	%31.7c
النسبة المئوية للأوراق الميتة	-	-	-	-	%1.02

● تشير الأحرف المتشابهة لعدم وجود فروق معنوية بين المعاملات عند مستوى معنوية 5 %.

يظهر الجدول (3) أن المبيد ثيوفانات الميثيل بقي محافظاً على فاعلية عالية في حماية النباتات من الإصابة خلال 12 يوماً من العدوى وبفروق غير معنوية مع مستخلصي تفل الزيتون وحمض الساليسيلك، بينما انخفضت فاعلية مستخلص تفل العنب في حماية النباتات من الإصابة بالبياض الدقيقي، وازدادت النسبة المئوية للنباتات المصابة بشكل ملحوظ على الرغم من وجود فروق معنوية بالمقارنة مع معاملة المقارنة، فقد وصلت النسبة المئوية للأوراق المصابة إلى 3.4% و 23.3% و 1.8% في المعاملات مستخلص تفل الزيتون ومستخلص تفل العنب وحمض الساليسيلك على التوالي مقارنة مع 40.6% في معاملة المقارنة. في حين بلغ متوسط النسبة المئوية للأوراق الميتة 11.9% في معاملة تفل العنب مقابل 20.5% في معاملة المقارنة.

جدول 3:

عدد الأوراق المصابة والميتة ونسبتها المئوية بعد 12 يوماً من العدوى الاصطناعية بالفطر المسبب للبياض الدقيقي على القرعيات في كل من المعاملات المختلفة

	تفل الزيتون	تفل العنب	حمض الساليسيلك	ثيوفانات الميثيل	المعاملة المقارنة
على السطح العلوي فقط	0.20	2.07	0.27	-	-
على السطح السفلي فقط	0.8	5.0	2.07	1.33	9.50
على سطحي الورقة معاً	0.53	5.40	0.40	1.60	15.37
مجموع الأوراق المصابة	1.53	12.47	2.74	2.93	24.87
النسبة المئوية للأوراق المصابة	%3.4 a	%23.3 b	%1.8a	%0.8 a	%40.6 c
النسبة المئوية للأوراق الميتة	-a	%11.9b	-a	-a	%20.5c

● تشير الأحرف المتشابهة لعدم وجود فروق معنوية بين المعاملات عند مستوى معنوية 5 %.

حافظ المبيد ثيوفانات الميثيل على فاعلية عالية بعد 16 يوماً من العدوى، حيث لم تتجاوز النسبة المئوية للأوراق المصابة 1.6%، ولم يلاحظ وجود أوراق ميتة، كما أن المعاملة بحمض الساليسيلك قد حققت حماية جيدة أيضاً، فلم تتجاوز نسبة الأوراق الميتة 12.6%، بينما فقد مستخلص تفل الزيتون فعاليته بشكل جزئي، حيث ازدادت النسبة المئوية للأوراق المصابة لتصل إلى 20.4%، وكذلك النسبة المئوية للأوراق الميتة إلى 2.4% مقابل 1.1% في معاملة حمض الساليسيلك. بينما ازدادت الإصابة بشكل كبير في معاملة تفل العنب، إذ وصلت النسبة المئوية للأوراق المصابة إلى 37.7% ونسبة الأوراق الميتة 24% مقارنة مع 24.3% و43% في المقارنة (الجدول 4).

جدول 4:

عدد الأوراق المصابة والميتة ونسبتها المئوية بعد 16 يوماً من العدوى الاصطناعية بالفطر المسبب للبياض الدقيقي على القرعيات في كل من المعاملات المختلفة

	تفل الزيتون	تفل العنب	حمض الساليسيلك	ثيوفانات الميثيل	المعاملة المقارنة
على السطح العلوي فقط	5.47	4.47	3.27	3.53	2.23
على السطح السفلي فقط	0.47	0.87	0.80	0.73	-
على سطحي الورقة معاً	6.67	8.87	4.73	6.40	8.67
مجموع الأوراق المصابة	12.61	14.21	8.80	10.66	10.90
النسبة المئوية للأوراق المصابة	%20.4 c	%37.7 d	%12.6 b	.6 a1%	%24.3 c
النسبة المئوية للأوراق الميتة	%2.4 a	%24 b	%1.1 a	0% a	%43 c

● تشير الأحرف المتشابهة لعدم وجود فروق معنوية بين المعاملات عند مستوى معنوية 5 %.

يلاحظ من الجدول (5) زيادة ملحوظة في النسبة المئوية للأوراق الميتة، ولذلك تم اعتماد النسبة المئوية للأوراق المصابة والأوراق الميتة معاً كمؤشر لتقييم فاعلية المعاملات المختلفة في الحد من الإصابة بالبياض الدقيقي. حافظ حمض الساليسيلك على فاعلية مرتفعة نسبياً وبفروق غير معنوية مقارنة مع المعاملة بالمبيد في الحد من شدة الإصابة بالبياض الدقيقي، بينما فقد مستخلص تفل الزيتون فاعليته بشكل نسبي، إذ وصلت نسبة الأوراق المصابة والميتة معاً إلى 48.4%، مقابل 65% و78% في معاملتي مستخلص تفل العنب والمقارنة على التوالي.

جدول 5:

عدد الأوراق المصابة والميتة ونسبتها المئوية بعد 19 يوماً من العدوى الاصطناعية بالفطر المسبب للبياض الدقيقي على القرعيات في كل من المعاملات المختلفة

	تفل الزيتون	تفل العنب	حمض الساليسيلك	ثيوفانات الميثيل	المعاملة المقارنة
على السطح العلوي فقط	8.07	6.53	5.33	6.13	7.48
على السطح السفلي فقط	0.13	0.6	0.73	0.40	0.08
على سطحي الورقة معاً	6.27	7.13	6.0	7.07	2.30
مجموع الأوراق المصابة	14.47	14.26	12.06	13.60	9.86
النسبة المئوية للأوراق المصابة	%32.2c	%36.2c	%17.2a	%14.6a	%25.8b
النسبة المئوية للأوراق الميتة	%16.2 b	%28.8 c	%8.3 a	%2.3 a	%52.2 d

● تشير الأحرف المتشابهة لعدم وجود فروق معنوية بين المعاملات عند مستوى معنوية 5 %.

تظهـر نتائـج القـراءة بعـد 29 يومـاً مـن المعاملـة أن جميـع النباتـات تقريبـاً قـد ماتـت فـي معاملـة المقارنـة، حيـث وصلـت النسـبة المئويـة لـلأوراق الميتـة إلـى 96.4%، كمـا يلاحـظ ارتفـاع كبيـر فـي عـدد الأوراق الميتـة فـي معاملـة تفل العنـب (54.8%)، بينمـا حافظـت المعامـلات الأخـرى علـى مسـتوى مقبـول نسـبياً مقارنـة مـع المقارنـة، إذ وصلـت النسـبة المئويـة لـلأوراق الميتـة إلـى 29.5% و22.8% و17.1% فـي معامـلات تفـل الزيتـون وحمـض الساليسـيلك والمبيـد الفطـري علـى الترتيـب.

جدول 6:

عدد الأوراق المصابة والميتة ونسبتها المئوية بعد 29 يوماً من العدوى الاصطناعية بالفطر المسبب للبياض الدقيقي على القرعيات في كل من المعاملات المختلفة

	تفل الزيتون	تفل العنب	حمض الصفصاف	ثيوفانات الميثيل	المعاملة المقارنة
على السطح العلوي فقط	2.52	1.6	0.27	0.27	-
على السطح السفلي فقط	-	0.2	-	-	-
على سطحي الورقة معاً	9.33	7.4	13.2	10.87	0.2
مجموع الأوراق المصابة	11.85	9.2	13.47	11.14	0.2
النسبة المئوية للأوراق المصابة	%35.6	%33.9	%38	%35.4	%2.7
النسبة المئوية للأوراق الميتة	%29.5a	%54.8b	%22.8a	%17.1a	%96.4c

● تشير الأحرف المتشابهة لعدم وجود فروق معنوية بين المعاملات عند مستوى معنوية 5 %.

يبين الشكل (1a-) أن أولـى أعـراض الإصابـة بمـرض البيـاض الدقيقـي علـى أوراق نباتـات القرعيـات المعـداة اصطناعيـاً، بعـد المعاملـة بمسـتخلص تفل الزيتـون، ظهـرت بعـد 9 أيـام مـن العـدوى الاصطناعيـة وبشـكل خفيف جـداً، وظهـرت أولـى الأوراق الميتة بعد 16 يومـاً. ازدادت النسـبة المئويـة للأوراق المصابـة والأوراق الميتة مـع الزمـن، فقد ازدادت النسـبة المئوية للأوراق المصابة بشـكل كبير خـلال 16 يومـاً، وبعـد ذلـك أصبحـت ثابتة تقريبـاً، وبـكل الأحوال لم تتجـاوز نسـبتها 35.6% بعـد 29 يومـاً مـن العـدوى، كمـا أن النسـبة المئويـة لـلأوراق الميتـة وصلـت إلـى أقل مـن 30%. ويبـدو واضحـاً أن المعاملـة بمسـتخلص تفـل الزيتـون حمـت النباتـات مـن الإصابـة بشـكل تـام تقريبـا خـلال 12 يومـاً الأولـى، وحافظـت علـى مسـتوى منخفـض نسـبياً مـن الإصابـة علـى الأقل خـلال 16 يومـاً، حيـث لـم تتجـاوز النسـبة المئويـة لـلأوراق المصابـة والميتـة معـاً 22.8% .

كمـا حققـت المعاملـة بحمـض الساليسـيلك حمايـة أفضـل للنباتـات مـن مسـتخلص تفـل الزيتـون، وظهـرت أولـى الأوراق الميتـة بعـد 16 يومـاً. ولـم تتجـاوز نسـبة الأوراق المصابـة 1.8% بعـد 12 يومـاً من العـدوى، ولكـن ازدادت نسـبتها بشـكل تدريجـي لتصـل إلـى 38% وزيـادة بعـدد الأوراق الميتـة لتصـل نسـبتها المئويـة إلـى 22.8% بعـد 29 يومـاً، وقـد وصـل عـدد الأوراق المصابـة والميتـة معـاً إلـى 60.8% فـي نهايـة التجربـة (الشـكل 1- c).

أدت المعاملـة بالمبيـد الفطـري إلـى حمايـة تامـة تقريبـاً للنباتـات مـن الإصابـة بالبيـاض الدقيقـي خـلال 16 يومـاً الأولـى، إذ إن أولـى أعـراض الإصابـة ظهـرت بعـد 16 يومـاً مـن العـدوى وبشـكل طفيف جـداً. وظهـرت أولـى الأوراق الميتـة بعـد 19 يومـاً. حيـث يلاحـظ ازديـاد واضـح بالنسـبة المئويـة للأوراق المصابـة لتصـل إلـى 14.6% بعـد 19 يومـاً، ومـع فقـدان المبيـد لفعاليتـه بشـكل جزئـي ازدادت نسـبة الأوراق المصابـة بشـكل ملحـوظ خـلال العشـرة أيـام الأخيـرة، ولكـن تزامـن ذلـك مـع زيـادة بعـدد الأوراق الميتـة لتصـل نسـبتها المئويـة إلـى 17.1% بعـد 29 يومـاً، وقـد وصـل عـدد الأوراق المصابـة والميتـة معـاً إلـى حوالـي 52.5% (الشـكل 1 – d).

لقـد كان مسـتخلص تفـل العنـب الأقـل فاعليـة فـي حمايـة النباتـات مـن الإصابـة بالبيـاض الدقيقـي، فقـد بـدأت الأعـراض بالظهـور بشـكل واضـح بعـد 6 أيـام، ولكـن بنسـبة أقـل مقارنـة مـع المقارنـة، وقـد وصلـت النسـبة المئويـة لـلأوراق المصابـة إلـى 23.3% بعـد 12 يومـاً، ثـم أصبحـت ثابتـة تقريبـاً حتـى القـراءة الأخيـرة أي بعـد 29 يومـاً مـن العـدوى، حيـث وصلـت إلـى 33.9%، ورافـق ذلـك زيـادة واضحـة بعـدد الأوراق الميتـة لتصـل نسـبتها إلـى 54.8% بعـد 29 يومـاً. ويفسـر ذلـك بـأن عـدداً كبيـراً مـن الأوراق المصابـة قـد ماتـت، وهـذا يبـدو واضحـاً من خـلال الازديـاد الكبيـر بالنسـبة المئويـة لـلأوراق الميتـة خـلال العشـرة أيـام الأخيـرة (الشـكل 1 – b).

لوحظت أعراض الإصابة على نباتات المقارنة بعد 6 أيام وكانت نسبة الأوراق المصابة مرتفعة نسبياً حيث وصلت إلى 15.4% لترتفع بشكل سريع إلى 45.6% بعد 12 يوماً، ثم انخفضت بشكل مفاجئ حتى وصلت إلى 2.7% بعد 29 يوماً، ولكن من الملاحظ أيضاً ازدياد سريع لعدد الأوراق الميتة حيث وصلت نسبتها إلى 96.4% مع ملاحظة عدم وجود أوراق سليمة في نهاية هذه المرحلة (الشكل 1 – e). كما يبين الجدول (7) والشكل (2) تأثير المعاملات المختلفة في الحد من الإصابة بمرض البياض الدقيقي على اليقطين، وتطور الإصابة خلال فترة الدراسة.

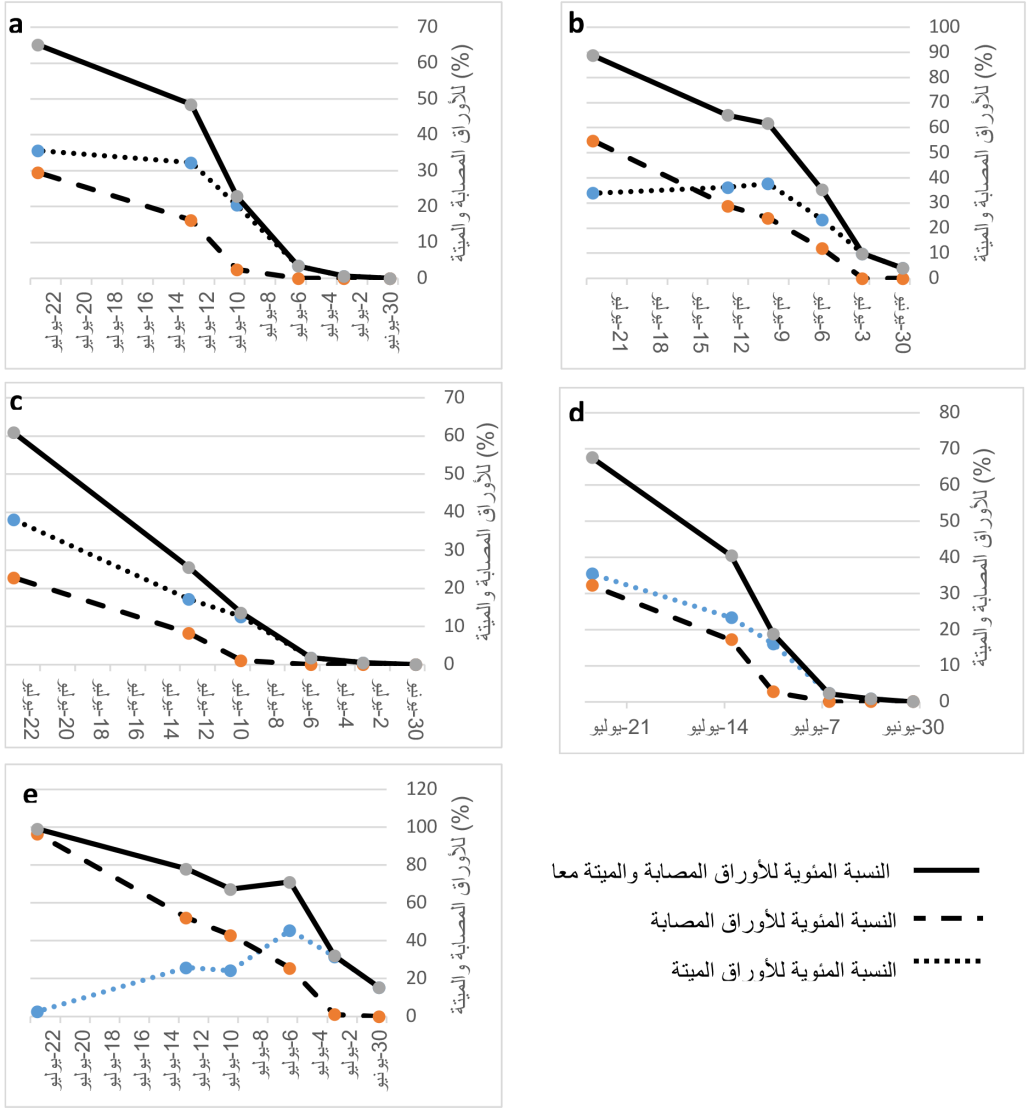

شكل 1:

تطور الإصابة بمرض البياض الدقيقي على نباتات القرعيات خلال 29 يوماً من المعاملات المختلفة: (a) تفل الزيتون، (b) تفل العنب، (c) حمض الساليسيلك، (d) ثيوفانات الميثيل، (e) المقارنة.

جدول 7:

تأثير المعاملات المختلفة في الحد من الإصابة بمرض البياض الدقيقي على القرعيات

	متوسط قراءات المعاملات المختلفة				
	تفل الزيتون	تفل العنب	حمض الصفصاف	ثيوفانات الميثيل	المقارنة
على السطح العلوي فقط	2.71	2.45	1.52	1.66	1.62
على السطح السفلي فقط	0.27	1.53	0.75	0.41	1.67
على سطحي الورقة معاً	3.86	4.89	4.06	4.32	4.93
مجموع الأوراق المصابة	6.83	8.87	6.33	6.32	8.38
النسبة المئوية للأوراق المصابة	%15.37	%24.15	%11.69	%9.4	%24.25
النسبة المئوية للأوراق الميتة	%8.02	%19.92	%5.37	%3.2	%36.35

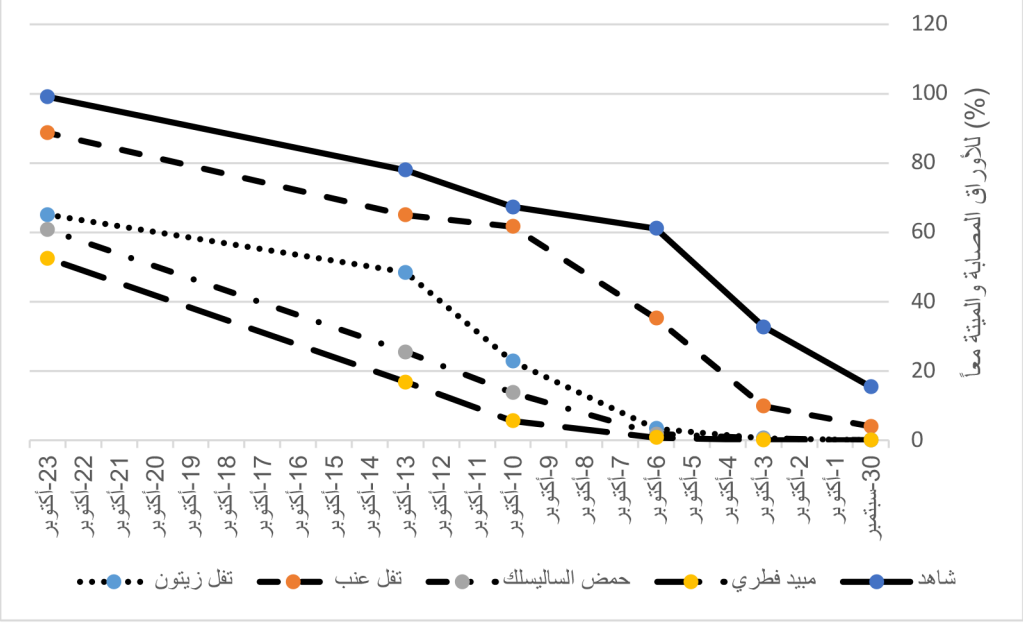

شكل 2:

تطور الإصابة بمرض البياض الدقيقي على نباتات القرعيات خلال 29 يوماً في المعاملات المختلفة بالمقارنة مع المقارنة

4. مناقشة النتائج

من الواضح أن استخدام مستخلصي تفل الزيتون والمستحضر التجاري لحمض الساليسيلك (أسبيرين) أدى إلى تأخير الإصابة بالبياض الدقيقي على نباتات اليقطين، وخفض شدة الإصابة بشكل مماثل تقريباً للمبيد الفطري على الأقل خلال 12 يوماً الأولى بعد العدوى الاصطناعية، بينما كانت فاعلية تفل العنب أقل بكثير على الرغم من وجود فروق معنوية كبيرة مقارنة مع المجموعة الضابطة. ويعزى ذلك إلى الاختلاف بآلية عمل كل من المبيد والمستخلصات النباتية وحمض الساليسيلك في خفض شدة الإصابة، إذ إن المبيد يؤثر بطريقة كيميائية على العمليات الفيزيولوجية للفطر فيوقف من تطوره، بينما مستخلص تفل

العنب وتفل الزيتون يحتويان على نسبة عالية من المركبات الفينولية المسؤولة عن آلية المقاومة عند النبات (Marsilio et al., 2001)، إذ إن مركبات oleuropein ومركبات فينولية أخرى موجودة في الزيتون قد دُرست بشكل جيد ضد العديد من البكتيريا المسؤولة عن تخمير حمض اللاكتيك ومنها Lactobacillus plantarum و L. brevis (Fleming, Walter, & Etchells, 1973)، وضد البكتيريا المرتبطة بإصابة الأمعاء عند الإنسان أو الجهاز التنفسي (Bisignano, Tomaino, Lo Cascio, Crisafi, Uccella, Saija, 1999 &). كما تتوافق نتائجنا مع تلك التي حصل عليها Winkelhausen, Pospiech, & Laufenberg (2005) حيث أبدى مستخلص تفل الزيتون فاعلية عالية في تثبيط نمو الفطريات Alternaria solani وBotrytis cinerea و Fusarium culmorum. وقد أبدى مستخلص تفل الزيتون فاعلية عالية أيضاً في مكافحة مرض تبقع أوراق البندورة المتسبب عن الفطر Alternaria alternata (Naffaa, 2016). وتتوافق هذه النتائج أيضاً مع نتائج دراسات أخرى تم فيها استخدام المستخلصات والزيوت النباتية لخفض شدة الإصابة بالبياض الدقيقي على محاصيل مختلفة، فقد استخدمت الزيوت النباتية مثل زيت بذور العنب وزيت عباد الشمس وزيت فول الصويا عند تركيز 0.1 % في مكافحة مرض البياض الدقيقي على البندورة المتسبب عن الفطر Oidium lycopersici، وقد أدت إلى خفض نسبة الإصابة بشكل معنوي، وكان زيت عباد الشمس Sunflower oil الأكثر فاعلية (Ko, Wang, Hsieh, & Ann, 2003). كما أدت معاملة نباتات القرعيات بسيليكات البوتاسيوم وبيكربونات البوتاسيوم وزيت الزيتون وفوسفات البوتاسيوم وزيت النيم إلى خفض شدة الإصابة بشكل مماثل للمبيد الفطري أزوكسي ستروبين Azoxystrobin (Pérez-Ángel, García-Estrada, Carrillo-Fasio, Angulo-Escalante, Valdez-Torres, Muy-Rangel, García-López, & Villarreal-Romero, 2010).

أظهرت هذه الدراسة أن حمض الساليسيلك كان أفضل المركبات الكيميائية المستخدمة في خفض شدة الإصابة بالبياض الدقيقي على القرعيات، وهذه النتائج تتوافق مع نتائج Ahmed (2014) وAbada حيث أدى رش نباتات البندورة بحمض الساليسيلك إلى خفض معنوي بشدة الإصابة بالبياض الدقيقي وزيادة في إنتاج الثمار ضمن ظروف البيت البلاستيكي. وقد وجد أن الانخفاض بشدة الإصابة يعزى إلى زيادة مستوى الإنزيمات بولي فينول أوكسيداز Polyphenol oxidase (PPO) و البيروكسيداز Peroxidase (PO) وفينيل آلانين أمونيا لياز Phenylalanine ammonia-lyase (PAL). أشار Farkas و Kiraly (1962) و Morkuna و Gemerek (2007) إلى أن أنزيمات البيروكسيداز تؤكسد المركبات الفينولية إلى مركبات أكثر سمية للفطريات مثل الكينين الذي يثبط إنبات الأبواغ ونمو الفطر. كما أدى استخدام المركب beta – aminobutyric acid (BABA) إلى زيادة مقاومة نباتات الكوسا Squash لمرض البياض الدقيقي المتسبب عن الفطر Podosphaera xanthii، وقد ترافق ذلك أيضاً مع زيادة في نشاط أنزيمات البيروكسيداز PO و(Zeighaminejad et al., 2016) PAL.

وعلى الرغم من إن مستخلص تفل العنب كان الأقل تأثيراً في خفض شدة الإصابة بالبياض الدقيقي، إلا أنه أدى أيضاً إلى خفض شدة الإصابة نسبياً مقارنة مع المجموعة الضابطة، علماً أن بعض الدراسات أشارت لفاعلية عالية لمستخلص تفل العنب في تثبيط نمو العديد من الفطريات، ويعزى ذلك أيضاً لاحتواء العنب بشكل عام على نسبة عالية من المركبات الفينولية، حيث 70% من هذه المركبات يبقى في التفل بعد عصر الثمار (Mazza, 1995). كما أشارت العديد من الدراسات إلى أن المركبات الفينولية في مستخلص تفل العنب تمتلك نشاطاً مضاد للأكسدة وللسرطان (Zhou & Raffoul, 2012; Xu, Burton, Kim, & Sismour, 2016)، ونشاط مضاد للجراثيم (Darra, Tannous, Mouncef, Palge, Yaghi, Vorobiev, Louka, & Maroun, 2012). ونظراً لهذه الخصائص، فإن المركبات الفينولية المستخلصة من تفل العنب بدأت تستثمر في المجال الصناعي لزيادة مدة صلاحية بعض المنتجات الغذائية استجابة للطلب المتزايد من قبل المستهلكين لإيجاد بدائل آمنة عن المواد الحافظة الكيميائية (Gyawali & Ibrahim, 2014).

5 - خاتمة:

وأخيراً يمكن ترتيب المركبات المستخدمة في هذه الدراسة تبعاً لفاعليتها في خفض شدة الإصابة بالبياض الدقيقي على اليقطين كما يلي: ثيوفانات الميثيل ≤ حمض الساليسيلك ≤ مستخلص تفل الزيتون > مستخلص تفل العنب. وفي ظل

الاهتمـام الكبيـر حاليـاً بالأثـر المتبقـي للمبيـدات فـي الغـذاء والمـاء، والحاجـة المتزايـدة لإيجـاد بدائـل آمنـة، يمكـن أن تكـون المركبـات الطبيعيـة المسـتخدمة فـي هـذا البحـث وخاصـة مسـتخلص تفـل الزيتـون وحمـض الساليسـيلك بدائـل أمنـة للبيئـة والإنسـان مـن جهـة، وقليلـة التكلفـة مـن جهـة ثانيـة، وذلـك لمكافحـة البيـاض الدقيقـي علـى القرعيـات وخاصـة فـي المسـاحات المحـدودة كالبيـوت البلاسـتيكية.

REFERENCES

Abada, K. A. & Ahmed, M. A. (2014). Effect of Combination between Bioagents and Antioxidants on Management of Tomato Powdery Mildew. Special Issue: Role of Combination Between Bioagents and Solarization on Management of Crownand Stem-Rot of Egyptian Clover. American Journal of Life Sciences, 2(6,(2-32-26.

Abo-Elyousr, K. A., Hussein, M. A. M., Allam, A. D. A., & Hassan, M. H. A. (2009). Salicylic acid induced systemic resistant on onion plants against Stemphylium vesicarium. Archives of Phytopathology and Plant Protection, 42(11), 1042–1050.

Aziz, N. H., Farag, S. E., Mousa, L. A. A., & Abo-Zaid, M. A. (1998). Comparative antibacterial and antifungal effects of some phenolic compounds. Microbios, 93(374), 43–54.

Bisignano, G., Tomaino, A., Lo Cascio, R., Crisafi, G., Uccella, N., & Saija, A. (1999). On the in-vitro antimicrobial activity of oleuropein and hydroxytyrosol, Journal of Pharmacy and Pharmacology, 51(8), 971–974.

Capasso, R., Evidente, A., Schivo, L., Orru, G., Marciales, M. A., & Cristinzo, G. (1995). Antibacterial polyphenols from olive oil mill waste waters. Journal of Applied Bacteriology, 79(4), 393398-.

Darra, N. E., Tannous, J., Mouncef, P. B., Palge, J., Yaghi, J., Vorobiev, E., Louka, N. & Maroun, R. (2012). A Comparative study on antiradical and antimicrobial properties of red grapes extracts obtained from different Vitis vinifera varieties. Food and Nutrition Sciences, 3(10), 1420–1432.

De Waard, A., Georgopoulos, S. G., Hollomon, D. W., Ishii, H., Leroux, P., Ragsdale, N. N., & Schwinn, F. J. (1993). Chemical control of plant diseases: problems and prospects. Annual Review of Phytopathology, 31, 403–423.

Faize, L. & Faize, M. (2018). Functional Analogues of Salicylic Acid and Their Use in Crop Protection. Agronomy, 8(1), 5.

Farkas, L. & Kiraly, L. (1967). Role of phenolic compounds in the physiology of plant disease and disease resistance. Phytopathologische Zeitschrift, 40, 106-150.

Fleming, H. P., Walter, Jr. W. M., & Etchells, J. L. (1973). Antimicrobial properties of oleuropein products of its hydrolysis from green olives. Journal of Applied Microbiology, 26(5), 777–782.

Gomez, K. A. & Gomez, A. A. (1984). Statistical Procedure for Agricultural Research. John Wiley and Sons, New York.

Gyawali, R. & Ibrahim, S. A. (2014). Natural products as antimicrobial agents. Food Control, 46, 412–429.

Ibrahim, A. S., Khafagi, Y. S., Ghonim, A. M., & El-Abbasi, I. H. (2003). Integrated management of powdery mildew on cantaloupe (Cucumis melo L. var. cantaloupensis). Egyptian Journal of applied science,18, 521–531.

Indrianingsih, A. W., Rosyida, V. T., Apriyana, W., Hayatis, N., Nisa, K., Darsih, C., Kusumaningrum, A., Ratih, D., & Indirayati, N. (2019). Comparisons of antioxidant activities of two varieties of pumpkin (Cucurbita moschata and Cucurbita maxima) extracts. IOP Conference Series: Earth and Environmental Science, 251.

Jacobo-Valenzuela, N., Maróstica-Junior, M. R., Zazueta-Morales, J. J., & Gallegos-Infante, J. A. (2011). Physicochemical, technological properties, and health-benefits of Cucurbita moschata Duchense vs. Cehualca A Review. Food Research International, 44(9), 25872593-.

Ko, W. H., Wang, S. Y., Hsieh, T. F., & Ann, P. J. (2003). Effects of Sunflower Oil on Tomato Powdery Mildew Caused by Oidium neolycopersici. Journal of Phytopathology, 151 (3), 144- 148.

Lin, T., Ishizaka, M., & Ishii, H. (2009). Acibenzolar-s-methyl-induced systemic resistance against anthracnose and powdery mildew diseases on cucumber plants without accumulation of phytoalexins. Journal of Phytopathology, 157(1), 40–50.

Markin, D., Duek, L., & Berdicevsky, I. (2003). In vitro antimicrobial activity of olive leaves. Mycoses, 46(3-136-132 ,(4.

Marsilio, V., Campestre, C., & Lanza, B. (2001). Phenolic compounds change during California-style ripe olive processing. Food Chemistry, 74(1), 55–60.

Mazza, G. (1995). Anthocyanins in grape and grape

products. Critical Reviews in Food Science and Nutrition, 35(4), 341–371.

Morkunas, I. & Gemerek, J. (2007). The possible involvement of peroxidase in defense of yellow lupine embryo axes against Fusarium oxysporum. Journal of Plant Physiology, 164(2), 497506-.

Morsy, S. M., Elham, A. D., & Gehad, M. M. (2009). Effect of garlic and onion extracts or their intercropping on suppressing damping-off and powdery mildew diseases and growth characteristics of cucumber. Egyptian journal of phytopathology, 37(1), 35–46.

Naffaa, W. (2016). Antifungal activity of olive pomace extract and its effectiveness against tomato leaf spot disease. Journal of the North for Basic and Applied Sciences, 1 (1), 59 – 68.

Nychas, G. J. E., Tassou, S. C., & Board, R. G. (1990). Phenolic extract from olives: inhibition of Staphylococcus aureus, Lett. Applied Microbiology, 10(5), 217–220.

Oostendorp, M., Kunz, W., Dietrich, B., & Staub, T. (2001). Induced disease resistance in plants by chemicals. European Journal of Plant Pathology, 107(1), 19–28.

Pérez-Ángel, R., García-Estrada, R. S., Carrillo-Fasio, J. A., Angulo-Escalante, M. Á., Valdez-Torres, J. B., Muy-Rangel, M. D., García-López, A. M., & Villarreal-Romero, M. (2010). Powdery Mildew (Sphaerotheca fuliginea Schlechtend: Fr, Pollaci) Control with Vegetable Oils and Mineral Salts on Cucumber Growing in Greenhouse in Sinaloa, México. Revista Mexicana de Fitopatología, 28(1), 1724-

Sharifi-Sirchi, G.R., Beheshti, B., Hosseinipour, A., & Mansouri, M. (2011). Priming against Asiatic citrus canker and monitoring of PR genes expression during resistance induction. African Journal of Biotechnology, 10(19), 38183823-.

Subban, K., Subramani, R., Srinivasan, V. P. M., Johnpaul, M., & Chelliah, J. (2019). Salicylic acid as an effective elicitor for improved taxol production in endophytic fungus Pestalotiopsis microspora. PLoS ONE 14(2), e0212736. https://doi.org/10.1371/journal.pone.0212736.

Visioli, F., Romani, A., Mulinacci, N., Zarini, S. Conte, D., Franco, F., & Galli C. (1999). Antioxidant and other biological activities of olive mill waste waters. Journal of Agricultural and Food Chemistry, 47(8), 3397–3401.

Winkelhausen, E., Pospiech, R., & Laufenberg. G. (2005). Antifungal activity of phenolic compounds extracted from dried olive pomace. Bulletin of the Chemists and Technologists of Macedonia, 24(1), 41–46.

Xu, Y., Burton, S., Kim, C. & Sismour, E. (2016). Phenolic compounds, antioxidant, and antibacterial properties of pomace extracts from four Virginia-grown grape varieties. Food Science & Nutrition, 4(1), 125 – 133.

Yurina, T. P., Karavaev, V. A., & Solntsev, M. K. (1993). Characteristics of metabolism in two cucumber cultivars with different resistance to powdery mildew. Russian Journal of Plant Physiology, 40(2), 197–202.

Zeighaminejad, R., Sharifi-Sirchi, G. R., Mohamadi, H., & Aminai, M. M. (2016). Induction of resistance against powdery mildew by Beta aminobutyric acid in squash. Journal of Applied Botany and Food Quality, 89, 176 – 182.

Zhou, K. & Raffoul, J. J. (2012). Potential anticancer properties of grape antioxidants. Journal of Oncology, 5, 18-. doi:10.1155803294/2012/.

in diabetes. The Journal of Clinical Endocrinology & Metabolism, 101(9), 3401-3408.

Sagna, M. B., Diallo, A., Sarr, P. S., Ndiaye, O., Goffner, D., & Guisse, A. (2014). Biochemical composition and nutritional value of Balanites aegyptiaca (L.) Del fruit pulps from Northern Ferlo in Senegal. African Journal of Biotechnology, 13(2), 336-342.

Sena, C. M., Pereira, A. M., & Seiça, R. (2013). Endothelial dysfunction—a major mediator of diabetic vascular disease. Biochimica et Biophysica Acta (BBA)-Molecular Basis of Disease, 1832(12), 2216-2231.

Versari, D., Daghini, E., Virdis, A., Ghiadoni, L., & Taddei, S. (2009). Endothelial dysfunction as a target for prevention of cardiovascular disease. Diabetes care, 32(suppl 2), S314-S321.

Zafar, M., Naqvi, S. N.-u.-H., Ahmed, M., & Kaimkhani, Z. A. (2009). Altered Liver Morphology and Enzymes in Streptozotocin Induced Diabetic Rats. International Journal of Morphology, 27(3). https://scholar.google.com/citations

Zeid, I. M. A., Al-Thobaiti, S. A., Almalki, D. A., Ali, S. S., & Umar, A. (2019). Global Journal of Medicinal Plant Research. Global Journal of Medicinal Plant Research, 7(1), 1-6.

in diabetes. The Journal of Clinical Endocrinology & Metabolism, 101(9), 3401-3408.

Sagna, M. B., Diallo, A., Sarr, P. S., Ndiaye, O., Goffner, D., & Guisse, A. (2014). Biochemical composition and nutritional value of Balanites aegyptiaca (L.) Del fruit pulps from Northern Ferlo in Senegal. African Journal of Biotechnology, 13(2), 336-342.

Sena, C. M., Pereira, A. M., & Seiça, R. (2013). Endothelial dysfunction—a major mediator of diabetic vascular disease. Biochimica et Biophysica Acta (BBA)-Molecular Basis of Disease, 1832(12), 2216-2231.

Versari, D., Daghini, E., Virdis, A., Ghiadoni, L., & Taddei, S. (2009). Endothelial dysfunction as a target for prevention of cardiovascular disease. Diabetes care, 32(suppl 2), S314-S321.

Zafar, M., Naqvi, S. N.-u.-H., Ahmed, M., & Kaimkhani, Z. A. (2009). Altered Liver Morphology and Enzymes in Streptozotocin Induced Diabetic Rats. International Journal of Morphology, 27(3). https://scholar.google.com/citations

Zeid, I. M. A., Al-Thobaiti, S. A., Almalki, D. A., Ali, S. S., & Umar, A. (2019). Global Journal of Medicinal Plant Research. Global Journal of Medicinal Plant Research, 7(1), 1-6.

balanites aegyptiaca on antioxidant defense system against adriamycin-induced cardiac toxicity in experimental mice. Egyptian Journal of Biochemistry & Molecular Biology, 28(1).

Giacco, F., & Brownlee, M. (2010). Oxidative stress and diabetic complications. Circulation research, 107(9), 1058-1070.

Gnoula, C., Mégalizzi, V., De Nève, N., Sauvage, S., Ribaucour, F., Guissou, P., Duez, P., Dubois, J., Ingrassia, L., & Lefranc, F. (2008). Balanitin-6 and-7: diosgenyl saponins isolated from Balanites aegyptiaca Del. display significant anti-tumor activity in vitro and in vivo. International journal of oncology, 32(1), 5-15.

Hassan MD, A. Z., Mary M. (2020). Effect of Balanites aegyptiaca Fruit-pericarp Extract on Fructose Induced Hyperglycemia and Hyperlipidemia in Rats Asian J Biotechnol 12, 87-96.

Hegab, I. I. (2018). Ameliorative effect of apelin on streptozotocin-induced diabetes and its associated cardiac hypertrophy. Alexandria journal of medicine, 54(2), 119-127.

Helal, E. G., El-Wahab, A., Samia, M., El Refaey, H., & Mohammad, A. A. (2013). Antidiabetic and antihyperlipidemic effect of Balanites aegyptiaca seeds (aqueous extract) on diabetic rats. The Egyptian Journal of Hospital Medicine, 52(1), 725-739.

Hussain, S. A. M., Velusamy, S., & Muthusamy, J. (2019). Balanites aegyptiaca (L.) Del. for dermatophytoses: Ascertaining the efficacy and mode of action through experimental and computational approaches. Informatics in Medicine Unlocked, 15, 100177.

Kamel, M. (1991). Study of Balanites aegyptiaca Del. and Salvadora persica l. Reputed to Have Hypoglycemic Effects: Department of Pharmacognosy, Faculty of Pharmacy, Assiut, Egypt.

Leon, B. M., & Maddox, T. M. (2015). Diabetes and cardiovascular disease: Epidemiology, biological mechanisms, treatment recommendations and future research. World journal of diabetes, 6(13), 1246.

Li, P.-J., Jin, T., Luo, D.-H., Shen, T., Mai, D.-M., Hu, W.-H., & Mo, H.-Y. (2015). Effect of prolonged radiotherapy treatment time on survival outcomes after intensity-modulated radiation therapy in nasopharyngeal carcinoma. PloS one, 10(10), e0141332.

Li, X., Xu, Z., Jiang, Z., Sun, L., Ji, J., Miao, J., Zhang, X., Li, X., Huang, S., & Wang, T. (2014). Hypoglycemic effect of catalpol on high-fat diet/streptozotocin-induced diabetic mice by increasing skeletal muscle mitochondrial biogenesis. Acta Biochim Biophys Sin, 46(9), 738-748.

Majithiya, J. B., & Balaraman, R. (2006). Metformin reduces blood pressure and restores endothelial function in aorta of streptozotocin-induced diabetic rats. Life sciences, 78(22), 2615-2624.

Mao, Y., Hu, Y., Feng, W., Yu, L., Li, P., Cai, B., Li, C., & Guan, H. (2020). Effects and mechanisms of PSS-loaded nanoparticles on coronary microcirculation dysfunction in streptozotocin-induced diabetic cardiomyopathy rats. Biomedicine & Pharmacotherapy, 121, 109280.

Nadro, M., & Samson, F. (2014). The effects of Balanite aegyptiaca kernel cake as supplement on alloxan-induced diabetes mellitus in rats. Journal of Applied Pharmaceutical Science, 4(10), 058-061.

Nayak, N., & Padhy, R. N. (2017). GC-MS Analysis of Bioactive Compounds and Host-toxicity Studies of Azolla caroliniana Symbiotic with the Cyanobacterium Anabaena azollae. Indian journal of pharmaceutical education and research, 51(2), S24-S33.

Oki, Y., Kawai, M., Minai, K., Ogawa, K., Inoue, Y., Morimoto, S., Tanaka, T., Nagoshi, T., Ogawa, T., & Yoshimura, M. (2019). High serum uric acid is highly associated with a reduced left ventricular ejection fraction rather than increased plasma B-type natriuretic peptide in patients with cardiovascular diseases. Scientific reports, 9(1), 1-12.

Palmieri, V., Capaldo, B., Russo, C., Iaccarino, M., Pezzullo, S., Quintavalle, G., Di Minno, G., Riccardi, G., & Celentano, A. (2008). Uncomplicated type 1 diabetes and preclinical left ventricular myocardial dysfunction: insights from echocardiography and exercise cardiac performance evaluation. Diabetes research and clinical practice, 79(2), 262-268.

Patel, S. S., & Goyal, R. K. (2011). Cardioprotective effects of gallic acid in diabetes-induced myocardial dysfunction in rats. Pharmacognosy research, 3(4), 239-245.

Picchi, A., Capobianco, S., Qiu, T., Focardi, M., Zou, X., Cao, J.-M., & Zhang, C. (2010). Coronary microvascular dysfunction in diabetes mellitus: a review. World Journal of Cardiology, 2(11), 377-390.

Rajesh, M., Mukhopadhyay, P., Bátkai, S., Patel, V., Saito, K., Matsumoto, S., Kashiwaya, Y., Horváth, B., Mukhopadhyay, B., & Becker, L. (2010). Cannabidiol attenuates cardiac dysfunction, oxidative stress, fibrosis, and inflammatory and cell death signaling pathways in diabetic cardiomyopathy. Journal of the American College of Cardiology, 56(25), 2115-2125.

Roustit, M., Loader, J., Deusenbery, C., Baltzis, D., & Veves, A. (2016). Endothelial dysfunction as a link between cardiovascular risk factors and peripheral neuropathy

namide, polyphenols and/or flavonoids, which possess antioxidant properties (Hussain et al., 2019). The kernel extract contains also many saturated and poly unsaturated fatty acids that have a beneficial effect on protection against cardiovascular diseases (Ander et al., 2003).

In summary, to the best of the authors' knowledge, this study could be considered the first study to report the protective effect of B. aegyptiaca kernel extract oral administration for 6 weeks against cardiac dysfunction associated with diabetes mellitus. The protective mechanism was most probably lying in its hypoglycaemic and its antioxidant effects that led to preserving the structure and functions of coronary blood vessels and cardiac muscles. Further studies are recommended with estimation of oxidative stress markers in cardiac and coronary artery homogenates and also using specific stains of coronary blood vessels to detect various protective effects of B. aegyptiaca kernel extract.

Conflicts of interest: None.
Financial support and sponsorship: None.

ACKNOWLEDGEMENT

The author would like to thanks Professor Soad Shaker Ali, Professor in Department Anatomy, Faculty of Medicine, King Abdulaziz University, Jeddah, Saudi Arabia for her kind support in reading and interpretation of the histology part of the study.

REFERENCES

Abdul-Ghani, M., DeFronzo, R. A., Del Prato, S., Chilton, R., Singh, R., & Ryder, R. E. (2017). Cardiovascular disease and type 2 diabetes: has the dawn of a new era arrived? Diabetes Care, 40(7), 813-820.

Abou Khalil, N. S., Abou-Elhamd, A. S., Wasfy, S. I., El Mileegy, I. M., Hamed, M. Y., & Ageely, H. M. (2016). Antidiabetic and antioxidant impacts of desert date (Balanites aegyptiaca) and parsley (Petroselinum sativum) aqueous extracts: lessons from experimental rats. Journal of Diabetes Research, 2016, 8408326.

Al-Thobaiti, S. A., & Zeid, I. M. A. (2019). Antidiabetic potential of Balanites aegyptiaca kernel, flesh and their combination against streptozotocin-induced hyperglycemia in male rats. Tropical Journal of Pharmaceutical Research, 18(2), 263-271.

Ander, B. P., Dupasquier, C. M., Prociuk, M. A., & Pierce, G. N. (2003). Polyunsaturated fatty acids and their effects on cardiovascular disease. Experimental & Clinical Cardiology, 8(4), 164-172.

Aouacheri, O., Saka, S., Krim, M., Messaadia, A., & Maidi, I. (2015). The investigation of the oxidative stress-related parameters in type 2 diabetes mellitus. Canadian journal of diabetes, 39(1), 44-49.

Bailey, C. J. (2017). Metformin: historical overview. Diabetologia, 60(9), 1566-1576.

Baragob, A. E. A., AlMalki, W. H., Shahid, I., Bakhdhar, F. A., Bafhaid, H. S., & Eldeen, O. M. I. (2014). The hypoglycemic effect of the aqueous extract of the fruits of Balanites aegypticea in Alloxan-induced diabetic rats. Pharmacognosy research, 6(1), 1-5.

Baynes, H. W. (2015). Classification, pathophysiology, diagnosis and management of diabetes mellitus. J diabetes metab, 6(5), 1-9.

Bertoluci, M. C., Cé, G. V., da Silva, A. M., Wainstein, M. V., Boff, W., & Puñales, M. (2015). Endothelial dysfunction as a predictor of cardiovascular disease in type 1 diabetes. World journal of diabetes, 6(5), 679-692.

Chothani, D. L., & Vaghasiya, H. (2011). A review on Balanites aegyptiaca Del (desert date): phytochemical constituents, traditional uses, and pharmacological activity. Pharmacognosy reviews, 5(9), 55-62.

Collaboration, E. R. F. (2010). Diabetes mellitus, fasting blood glucose concentration, and risk of vascular disease: a collaborative meta-analysis of 102 prospective studies. The Lancet, 375(9733), 2215-2222.

De, S., Dey, A., Babu, A. S., & Aneela, S. (2013). Phytochemical and GC–MS analysis of bioactive compounds of Sphaeranthus amaranthoides Burm. Pharmacognosy Journal, 5(6), 265-268.

Dokken, B. B. (2008). The pathophysiology of cardiovascular disease and diabetes: beyond blood pressure and lipids. Diabetes Spectrum, 21(3), 160-165.

Einarson, T. R., Acs, A., Ludwig, C., & Panton, U. H. (2018). Prevalence of cardiovascular disease in type 2 diabetes: a systematic literature review of scientific evidence from across the world in 2007–2017. Cardiovascular diabetology, 17(1), 83.

El Masry, S. A., Ebeed, M. M., El Sayed, I. H., Nasr, M. Y., & El Halafawy, K. A. (2010). Protective effect of

4. DISCUSSION

Diabetes mellitus is one of the most critical disorder that cause cardiovascular diseases and its seriousness effects and increases in mortality rate among these patients (Abdul-Ghani et al., 2017; Leon and Maddox, 2015). Therefore, it was essential to search for medication against these diabetic complications. The present research examined if B. aegyptiaca kernel extract prevents cardiovascular and coronary vessel alterations associated with STZ produced diabetes in rats. In the current study, the results demonstrated protective effect of the B. aegyptiaca kernel extract against cardiac damage associated with diabetes mellitus caused by STZ in rats. Treating diabetic rats with B. aegyptiaca kernel extract also reduced cardiac enzymes (CK-MB and troponin I) relative to the non-treated diabetic rats. Meanwhile, metformin treated diabetic rats showed insignificant decreased in cardiac enzyme levels versus control. In addition, administration of the extract resulted in protecting the coronary artery and heart muscles against the pathological changes associated with diabetes.

In agreement with this study results a previous study showed protective effect of B. aegyptiaca extract against adriamycin-induced cardiotoxicity, where their results demonstrated that the extract preserved level of different heart enzymes (lactate dehydrogenase, glutamate oxaloacetate transaminase, creatine phosphokinase, glutamate pyruvate transaminase) at their normal levels (El Masry et al., 2010). Insignificant changes in cardiac enzymes in diabetic rats treated with metformin could be explained by the fact that metformin improve insulin action and sensitivity in diabetic human and animals especially in skeletal muscles and improved lipid profiles in diabetics (Bailey, 2017; Majithiya and Balaraman, 2006). So its beneficial actions on the heart may need longer duration to occur.

Research studies attributed most cardiac complications associated with diabetes to hyperglycaemia. It was noticed that the risk of developing cardiovascular complications increases with an increase in fasting blood glucose levels even before it reaches the diagnostic standard of diabetes (Collaboration, 2010; Einarson et al., 2018; Li et al., 2015). This work showed hypoglycaemic effect of B. aegyptiaca extract, which is like metformin action. Similar studies have recently reported antidiabetic activity of several B. aegyptiaca parts (Abou Khalil et al., 2016; Al-Thobaiti and Zeid, 2019; Helal et al., 2013). Therefore, it may be one of the mechanisms behind its protective effect against cardiac damage in this study.

Endothelial dysfunction is one of underlying causes of cardiovascular complication in diabetics (Bertoluci et al., 2015; Roustit et al., 2016; Sena et al., 2013; Versari et al., 2009) . In the present study, it was found that treatment with B. aegyptiaca kernel extract has improved the endothelial integrity and thickness of coronary vessels, which will ensure normal perfusion to the heart muscle, normal contractile function and protection against overload work and hypertrophy and this was reflected her by the improvement in the function of the heart and its enzymes with B. aegyptiaca kernel extract. Previously, a strong relationship between increased blood glucose and increased products of oxidative stress, as well as a decrease in antioxidant enzymes, was documented. It was also found that there a correlation between oxidative stress and deteriorating cardiovascular functions (Aouacheri et al., 2015; Giacco and Brownlee, 2010; Mao et al., 2020; Picchi et al., 2010).

The findings of the present study demonstrated that the use of B. aegyptiaca kernel extract had reduced malondialdehyde as an indication of oxidative stress while increasing the serum level of CAT enzyme. In a similar study, it was found that the B. aegyptiaca kernel extract raised antioxidant enzymes (CAT, glutathione peroxidase, and superoxide dismutase) and reduced lipid oxidation products as one of the preventative mechanisms against adriamycin-induced cardiac toxicity (El Masry et al., 2010).

Published research proved that B. aegyptiaca kernel extracts contain approximately 23 bioactive compounds that identified through chromatography (De et al., 2013). Among these substances was 3-0-methyl-D-glucose, which showed anti-toxic activity against STZ in previous research (Nayak and Padhy, 2017) besides the presence of 9-octadece-

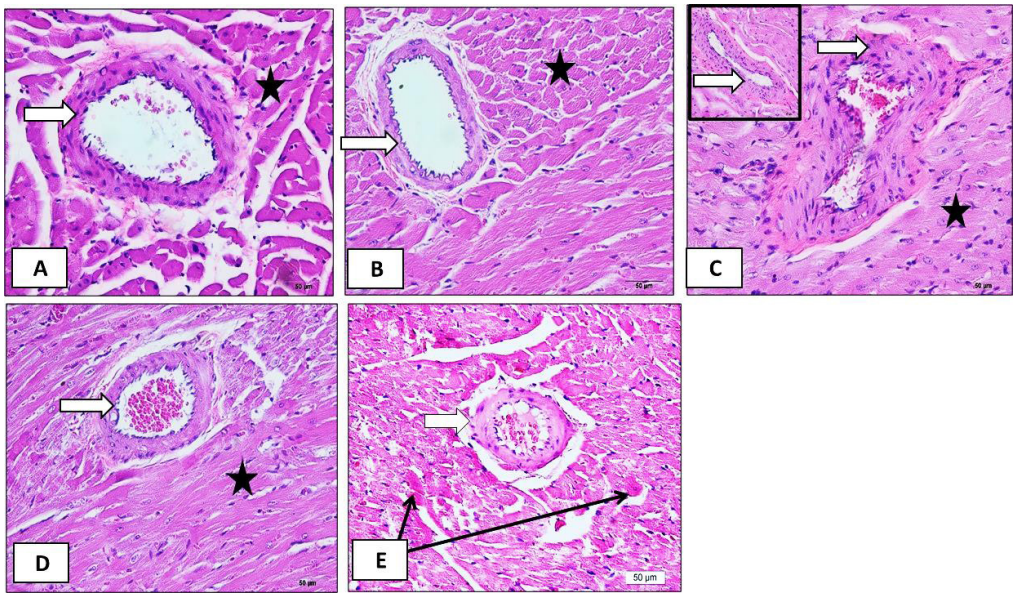

Figure 1. Effect of B. aegyptiaca kernel extract and metformin treatment on coronary artery wall thickness (white arrows) and nearby cardiac muscle fibers (stars) examined in the different study groups. A: Control section showed normal arterial wall thickness and spaced normal size muscle fibers; B: B. aegyptiaca section showed apparently normal coronary artery wall thickness and cardiac muscle histology; C: Diabetes section showed marked deformity, increased coronary artery with thickened wall with narrow lumen and hypertrophy of cardiac muscles and presence of BRCs in lumen; D: Diabetes + B. aegyptiaca section showed preserved coronary artery and cardiac muscle histology and presence of BRCs in lumen; E: Diabetes + metformin section showed nearly normal coronary artery wall thickness and presence of small amount of BRCs in lumen while the nearby cardiac muscles still showed few dark apoptotic fibers (black arrows).

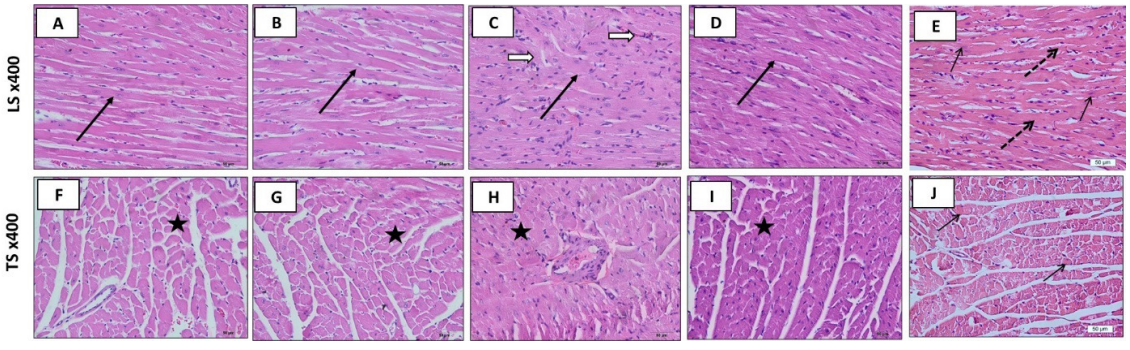

Figure 2. Effect of B. aegyptiaca kernel extract and metformin treatment on cardiac muscle fibers pathology [longitudinal (LS, arrows) and transverse (TS, stars) stained by H and E] examined in the different study groups. A and F: Control section showed normal sizes and spacing of muscle fibers with central active vesicular nuclei in myocytes surrounded by few fibroblasts and connective tissue nuclei; B and G: B. aegyptiaca section showed no apparent changes in cardiac muscle fibers histology; C and H: Diabetes section showed marked deformity, decreased spacing mostly due to hypertrophy of cardiac muscle fibers. There is an apparent increase in nuclei of connective tissue around hypertrophied cardiac muscle fibers; D: Diabetes + B. aegyptiaca section showed preserved cardiac muscle fibers histology which looked more similar to control; E: Diabetes + metformin section showed nearly normal cardiac muscle fibers with some increase in nuclei of connective tissue surrounding the muscle fibers/which showed some focal hypertrophy in some regions (dotted arrows).

3.3 Effect of B. aegyptiaca kernel extract and metformin treatment on serum malondialdehyde concentration catalase enzyme activity

Control and B. aegyptiaca groups showed an average serum MDA level with no significant differences relative to each other. The serum MDA concentration of the diabetic rats was significantly increased versus control rats ($p < 0.001$). Serum MDA concentrations of diabetic rats treated with both B. aegyptiaca kernel extract and metformin were significantly decreased versus diabetic rats ($p < 0.001$, and $p = 0.01$, respectively) but still significantly higher than control rats ($p < 0.001$ for both). Serum CAT activity level was significantly increased in B. aegyptiaca group versus control ($p = 0.05$). The serum CAT concentration of the diabetic group was significantly decreased relative to the control group ($p < 0.001$). B. aegyptiaca kernel extract and metformin-treated groups showed a significantly increased serum CAT concentration relative to the diabetic rats ($p < 0.001$ for both) that reached nearly the control level (Table 3).

Table 3. Effect of B. aegyptiaca kernel extract and metformin treatment on serum levels of malondialdehyde (MDA) concentration and catalase (CAT) enzyme activity.

Groups	**MDA** (nmol/ml)	**CAT** (IU/L)
Control	0.202±0.159	98.00±11.28
B. aegyptiaca	0.094±0.009	113.00±2.28*
Diabetes	0.865±0.042***	64.00±13.71***
Diabetes + B. aegyptiaca	0.530±0.205$^{***, \#\#\#}$	102.17±3.31$^{\#\#\#}$
Diabetes + metformin	0.618±0.169$^{***, \#\#}$	92.33±11.18$^{\#\#\#}$

Data were expressed as mean +/- standard deviation. *: Significance versus control; #: significance versus diabetes. *: significance <0.05, ##: significance <0.01, *: significance <0.001.**

3.4 Effect of B. aegyptiaca kernel extract and metformin treatment on coronary vessels and cardiac muscle histopathology

The control and B. aegyptiaca groups showed apparently normal coronary artery wall thickness and cardiac muscle histology with no observed differences relative to each other. The diabetic group showed marked deformity, thickened coronary artery wall and narrowing of the lumen with apparent hypertrophy of cardiac muscles. Treatment of the diabetes rats with B. aegyptiaca kernel extract preserved the coronary artery and cardiac muscle histology. Diabetes treated with metformin-treated groups showed nearly normal coronary atery wall thickness and few dark apoptotic cardiac muscle fibers (Figure 1).
Figure 2 showed longitudinal and transverse sections of cardiac muscle stained with H and E for all groups. The control and B. aegyptiaca groups showed normal sizes and spacing of muscle fibers with central active vesicular nuclei surrounded by few fibroblasts and connective tissue nuclei. The diabetic group showed marked deformity, decreased spacing of cardiac fibers, mostly due to cardiac muscle hypertrophy. There is an apparent increase in nuclei of connective tissue around the hypertrophied fibers. Treatment of the diabetes rats with B. aegyptiaca kernel extract preserved the cardiac muscle histology, which looked more similar to control. Diabetics treated with metformin-treated group showed nearly normal cardiac fibers with some increase in nuclei of connective tissue surrounding the muscles which showed focal hypertrophy in some regions.

determined by ANOVA followed by Tukey's test.

3. RESULTS

3.1 Effect of B. aegyptiaca kernel extract and metformin treatment on fasting blood glucose level

The control and B. aegyptiaca groups showed normal fasting serum glucose levels with no significant differences between them. Diabetes induction significantly ($p < 0.001$) raised the fasting glucose level relative to the control group. B. aegyptiaca kernel extract-treated and metformin-treated groups showed significantly decreased fasting serum glucose concentration relative to diabetic group ($p < 0.001$) but still significantly higher than control group ($p < 0.001$) (Table 1).

Table 1. Effect of B. aegyptiaca kernel extract and metformin treatment on fasting blood glucose levels (mg/dl) measured in different study groups.

Groups	**Fasting blood glucose** (mg/dl)
Control	85.17±3.49
B. aegyptiaca	91.67±6.68
Diabetes	371.67±29.94***
Diabetes + B. aegyptiaca	135.83±33.46***, ###
Diabetes + metformin	148.17±30.00***, ###

Data were expressed as mean +/- standard deviation. *: Significance versus control; #: significance versus diabetes. *: significance <0.001.**

3.2 Effect of B. aegyptiaca kernel extract and metformin treatment on serum cardiac function markers concentration

The control and B. aegyptiaca groups showed normal serum troponin I and CK-MB concentration with no significant differences relative to each other. The serum troponin I and CK-MB concentrations of the diabetic group were significantly elevated versus control group ($p < 0.001$ for both). Serum troponin I and CK-MB concentrations of B. aegyptiaca kernel extract-treated diabetic rats were significantly decreased versus diabetes group ($p < 0.001$ for both). Conversely, serum troponin I and CK-MB concentrations of the metformin-treated diabetic group were non-significantly changed relative to the diabetic rats but still significantly higher than control ($p < 0.001$ for both) (Table 2).

Table 2. Effect of B. aegyptiaca kernel extract and metformin treatment on serum cardiac function markers measured in the different study groups.

Groups	**Troponin** (ng/ml)	**CK-MB** (IU/L)
Control	0.099±0.026	46.33±3.50
B. aegyptiaca	0.143±0.063	44.83±1412
Diabetes	0.348±0.069***	71.67±6.92***
Diabetes + B. aegyptiaca	0.165±0.059###	36.17±4.07###
Diabetes + metformin	0.353±0.063***	73.50±13.84***

Data were expressed as mean +/- standard deviation. *: Significance versus control; #: significance versus diabetes. *: significance <0.001.**

stoppered flask and maintained for 3 days at ambient temperature. The mixture was then evaporated using a rotary evaporator. Finally, full drying of the methanolic extract was performed via the freeze-drying technique (De et al., 2013).

2.4 Animals

Thirty male Wister rats weighing 180–240 g obtained from the Mansour Scientific Research and Development Foundation, Saudi Arabia. Rats were allowed for 7 days acclimatization at ambient temperature. Rats could ate rodent food and drank water freely. The ethics committee of King Fahd Medical Research Centre approved the experimental designs and the animal handling protocol of this study.

2.5 Experimental designs

Rats were classified into five groups ($n = 6$). Group I (control), injected intraperitoneally (i.p.) with citrate buffer (0.05 M, pH 4.5). Group II (B. aegyptiaca), injected orally (p.o.) with B. aegyptiaca kernel extract (650 mg/kg) (De et al., 2013). Diabetes was produced in the remaining 3 groups by injecting one dose (45 mg/kg i.p) of STZ (Zafar et al., 2009). Diabetic rats were then classified as follows: Group III (Diabetes). Group IV (Diabetes + B. aegyptiaca), ingested orally (p.o.) with B. aegyptiaca kernel extract (650 mg/kg) via oral gavage (De et al., 2013). Group V: (Diabetes + metformin), ingested (200 mg/kg p.o.) with metformin via oral gavage (Li et al., 2014). Duration of the experiment and treatment with both B. aegyptiaca and metformin was 6 weeks.

2.6 Blood sampling and heart dissection

After 6 weeks from the start of the treatments, the blood samples were collected from the ether anesthetized rats from the retro-orbital plexus, then sera were isolated and stored at -80 °C until biochemical tests were performed. After that, the hearts were dissected out, cut as cross segments and kept in a neutral solution of 10% formalin for further histopathological processing.

2.7 Estimation of serum blood glucose level

Fasting serum blood glucose levels were assessed after 6 weeks of diabetes induction with STZ using the colorimetric kit of Reactivos GPL, Barcelona, Spain, according to the manufacture instruction.

2.8 Estimation of serum cardiac function markers concentration

Serum troponin I and creatine phosphokinase (CK-MB) concentrations were assessed after 6 weeks of diabetes induction with STZ using the ELISA kit of MyBioSource, USA, according to the manufacture instruction.

2.9 Estimation of serum oxidative stress markers concentration

Serum malondialdehyde (MDA) concentrations as oxidative stress marker and catalase (CAT) enzyme activity as anti-oxidative stress marker were assessed after 6 weeks of diabetes induction with STZ using the ELISA kit of MyBioSource, USA, according to the manufacture instruction.

2.10 Histopathological examination of the heart muscle and coronaries

Hearts preserved in formalin were processed in ascending degrees of isopropyl alcohol and then cleared in xylene embedded in waxy blocks, cut into thin sections (3-5 mm), stained with Haematoxylin and Eosin (H & E), and examined under a light microscope by a blind pathologist to determine pathological changes associated with diabetes and its amelioration by different treatments. The sections were photographed, and a representative photo from each group was presented.

2.11 Statistical calculation

The results of this study were offered as mean ± standard deviation. SPSS software version 22, Armonk, was utilized to perform the statistical calculation. The statistical variation between groups was

1. INTRODUCTION

Diabetes mellitus (DM) is a metabolic condition distinguished by a persistent increased blood glucose levels induced by either insulin insufficiency, insulin resistance, or sometimes both (Baynes, 2015). DM cause cardiovascular diseases, including cardiomyopathy. Diabetic-induced cardiomyopathy (DIC) is a case of ventricular hypofunction that compromised most DM patients. The condition is not necessarily associated with elevated blood pressure or coronary artery disorders (Palmieri et al., 2008) . DIC is characterized by various structure deformities including cardiac muscle hypertrophy, inflammation, fibrosis, and apoptosis. At the beginning of DIC, the patients suffer diastolic dysfunction that progresses to systolic dysfunction and end by heart failure (Oki et al., 2019). The mechanism behind DIC is not yet defined. However, elevated blood glucose, dyslipidaemia, as well as indicators of oxidative stress, may be risk factors for occurrence of DIC (Dokken, 2008; Hegab, 2018; Rajesh et al., 2010). Therefore, the use of antidiabetic treatments, anti-lipidemic, and antioxidants supplements may show a protective action against cardiac damage in experimentally induced diabetes mellitus (Patel and Goyal, 2011).

Balanites aegyptiaca (B. aegyptiaca, family Zygophyllaceae) is a widely spread African plant and in Saudi Arabia has many medicinal uses. The fruit flesh's is utilized in Egyptian popular medicine in diabetes mellitus management (Gnoula et al., 2008; Kamel, 1991). Numerous previous and recent studies have demonstrated the hypoglycaemic and antioxidants activity of different parts of B. aegyptiaca fruits and their extracts in animals diabetic models (Abou Khalil et al., 2016; Al-Thobaiti and Zeid, 2019; Baragob et al., 2014; Nadro and Samson, 2014). In a recent study, researchers demonstrated the hypoglycaemic and hypolipidemic effects of B. aegyptiaca fruit epicarp ethanolic extract in fructose-induced diabetic rat's model (Hassan MD, 2020). Besides, it has been proven in a recent study that methanolic extracts of various parts of B. aegyptiaca fruit have hypolipidemic and antioxidant effects against streptozotocin (STZ)-induced diabetes mellitus in rats (Zeid et al., 2019). B. aegyptiaca fruit had many nutritional values as it contains abundant amounts of carbohydrates and many beneficial monounsaturated fatty acids (Sagna et al., 2014). The fruits of the plant also contain many active substances such as flavonoids, sterols, cardiac glycosides, saponins, fatty acids, and tannins (Chothani and Vaghasiya, 2011). Leaves of B. aegyptiaca contain furanocoumarin, saponin, and flavonoids as 3-glucoside, 3-rutinoside, quercetin 3-glucoside, quercetin-3-rutinoside, 3-7-diglucoside and 3-rhamnogalactoside of isorhamnetin (Chothani and Vaghasiya, 2011).

To the best of authors' knowledge, there is no published research on the effect of B. aegyptiaca against diabetic cardiovascular complications. This experimental study aimed to investigate the possible protective action of B. aegyptiaca kernel extract on coronary artery and cardiac muscles alterations caused by STZ-induced diabetes mellitus in rats.

2. MATERIALS AND METHODS

2.1 Drugs and chemicals

STZ was obtained from Sigma, USA. A solution of STZ was prepared freshly at 20 mg/ml in citrate buffer at pH 4.5 and used within 1 hour. Metformin (Glucophage, 500 mg metformin) Merck Santé, France, was obtained from Nahdi Pharmacy, Jeddah, Kingdom of Saudi Arabia and dissolved in distal water.

2.2 Plant material

B. aegyptiaca fruits were purchased from a domestic market in Jeddah, Kingdom of Saudi Arabia. The fruits were documented and authenticated by Dr. Elfeel A. "Meteorology, Environment, and Arid Land Agriculture College, University of King Abdulaziz, Saudi Arabia".

2.3 Preparation of the plant extract

Five hundred g of B. aegyptiaca kernel powder was mixed with two litters of 70% methanol in a

المملكة العربية السعودية
جامعة الحدود الشمالية (NBU)
مجلة الشمال للعلوم الأساسية والتطبيقية (JNBAS)
طباعة - ردمد: 7022-1658 / الكتروني - ردمد: 7014-1658
www.nbu.edu.sa
http://jnbas.nbu.edu.sa

حماية مستخلص بلانيت إيجيبتياكا (بلح الصحراء) من اعتلال عضلة القلب الناجم عن داء السكري في الجرذان: دراسة نسيجية وتحليلية

عبير خالد عبدالله الأنصاري[1]*، ساعد عايض الثبيتي[2]

(قدم للنشر في 1441/12/26هـ؛ وقبل للنشر في 1442/07/16هـ)

ملخص: يؤثر داء السكري على عضلة القلب. بلانيت إيجيبتياكا) بلح الصحراء) نبات أفريقي يوجد في المملكة العربية السعودية، شائع له العديد من الاستخدامات الطبية، بما في ذلك مضاد لداء السكرى. هدفت هذه الدراسه إلى معرفة التأثير الوقائي المحتمل لمستخلص بلانيت إيجيبتياكا على أمراض القلب المرتبطة بداء السكري في الجرذان. تم استخدام ثلاثين من ذكور جرذان ويستر وزنهم يتراوح بين 180-240 جرام. قسمت العينة الى 5 مجموعات متساوية. المجموعة الأولى (المجموعة الضابطة)، المجموعة الثانية (بلانيت إيجيبتياكا) ، المجموعة الثالثة (السكري)، المجموعة الرابعة (السكري + بلانيت إيجيبتياكا)، المجموعة الخامسة: (السكري + الميتفورمين). تم إحداث داء السكري في المجموعات الثالثة والرابعة والخامسة عن طريق حقن جرعة واحدة من الستربتوزيتوسين (45 مجم/كجم (. كانت التجربة ومدة العلاج مع كل من بلانيت إيجيبتياكا والميتفورمين 6 أسابيع. وجد انخفاض بسكر الدم ومستويات السيرم لإنزيمات القلب و المالونياليدهيد وزيادة نشاط إنزيم الكاتلاز في السيرم فى الفئران المصابة بمرض السكر التي عولجت بمستخلص بلانيت إيجيبتياكا بشكل ملحوظ. حافظ مستخلص بلانيت إيجيبتياكا على الحالة النسيجية الطبيعية للشريان التاجي وعضلة القلب في الجرذان المصابة بداء السكري. في الختام نستنتج أن مستخلص بلانيت إيجيبتياكا له تأثير وقائي ضد ضعف عضله القلب المرتبط بداء السكري المستحث تجريبياً فى الجرذان عن طريق تقليل نسبة السكر في الدم، وتحسين نسيج الأوعية الدموية التاجية وذلك بواسطه زياده مضادات الأكسدة.

كلمات مفتاحية: مضادات الأكسدة، مستخلص بلانيت إيجيبتياكا، سكر الدم، إنزيمات القلب، الأنسجة المرضية.

* للمراسلة:
1. أستاذ مساعد، قسم التربية الاسرية ، كلية التربية، جامعة ام القرى، ص ب: 715، رمز بريدي: 21955، مكة المكرمة، المملكة العربية السعودية.
2. قسم الأحياء، الكلية الجامعية بتربة، جامعة الطائف، المملكة العربية السعودية.

e-mail akansari@uqu.edu.sa

jnbas.nbu.edu.sa
DOI: 10.12816/0058338

KINGDOM OF SAUDI ARABIA
Northern Border University (NBU)
Journal of the North for Basic and Applied Sciences (JNBAS)
p- ISSN: 1658 - 7022 / **e- ISSN:** 1658 - 7014
www.nbu.edu.sa
http://jnbas.nbu.edu.sa

Balanites Aegyptiaca Kernel Extract (Desert Date) Protects Against Diabetes-Induced Cardiomyopathy in Rats: A Histological and Biochemical Study

Abeer Khalid Abdullah Alansari[1*], Saed Ayidh Al-Thobaiti[2]

(Received 16/08/2020; Accepted 28/02/2021)

Abstract: Diabetes mellitus had harmful effects on the cardiac muscle. Balanites aegyptiaca (B. aegyptiaca) is common African and planted in Saudi Arabia has many medicinal activities, including antidiabetic. This study aimed to investigate possible protective effect of B. aegyptiaca kernel extract on cardiac diseases associated with diabetes in rats. Thirty male Wister rats (180–240 g) were sorted into 5 groups. Group I (control), Group II (B. aegyptiaca), Group III (Diabetes), Group IV (Diabetes+B. aegyptiaca), and Group V: (Diabetes+metformin). Diabetes was produced in groups III, IV, and V by injecting one dose of STZ (45 mg/kg). Experiment and treatment duration with both B. aegyptiaca and metformin was 6 weeks. Diabetic rats treated with B. aegyptiaca kernel extract significantly decreased fasting blood glucose, serum levels of troponin I, creatine kinase MB (CK-MB), and malondialdehyde. Administration of B. aegyptiaca extract to diabetic rats significantly increased serum catalase enzyme activity. B. aegyptiaca extract preserved normal histological status of coronary artery and cardiac muscle in diabetic rats. In conclusion, B. aegyptiaca kernel extract has protective effect against cardiac dysfunction associated with experimentally induced diabetes via decreasing fasting blood glucose, improving coronary blood vessels histology via an antioxidant mechanism.

Keywords: Antioxidant. Balanites aegyptiaca. Blood glucose. Cardiac enzymes. Histopathology.

* **Corresponding Author:**

1. Assistant Professor, Dept., Home Science Education Faculty Faculty of Education., University, Umm Al-Qura University P.O. Box: 715, Code:21955, Makkah al mukarramah, Kingdom of Saudi Arabia.
2. Department of Biology, University College of Turabah, Taif University, Saudi Arabia

e-mail akansari@uqu.edu.sa

jnbas.nbu.edu.sa

DOI: 10.12816/0058338

(amaranths) and Conyza/Erigeron (fleabanes) naturalised in the Asian-Pacific region," in Proceedings of the 6th Asian-Pacific Weed Scial Socity Conference, Jakarta: Asian-Pacific Weed Science Society, 87–95.

Milović, M. (2004). Naturalised species from the genus Conyza Less. (Asteraceae) in Croatia. – Acta Bot. Croat., 63(2),

4. CONCLUSIONS AND RECOMMENDATIONS

All observed populations of the *E. canadensis* were reproductive and spread, without the intervention by humans, which suggests that the species may be considered naturalized (Richardson, Pyšek, Rejmánek, Barbour, Dane Pe netta & West, 2000). Personal observations to the locality of the species show that it is rapidly spreading. The plant has a strong and faster competitive advantage against local plant species (Djurdjević et al., 2011).

E. canadensis can be economically important e.g medicinal, source of oil etc. (Burkill, 1985; Cambie, and Ash, 1994; Pawlaczyk et al., 2011; Weaver, 2001). The economic exploitation of this plant may reduce its spread and may help in controlling and managing it for the benefit of the homeland and the citizen. Uprooting the plant in its seedling stage which starts in July will help in controlling and limiting its spread.

REFERENCES

Anzalone, B. (1964). Un nuovo Erigeron nella Flora Italiana. Ann. Bot. (Roma), 28, 25–39.

Brouillet L, Desmet P, Coursol F, Meades SJ, Favreau M, Anions M, Bélisle P, Gendreau C, Shorthouse D, and contributors (2010+). Database of Vascular Plants of Canada (VASCAN). Retrieved from: http://data.canadensys.net/vascan and http://www.gbif.org/dataset/3f8a1297-3259-4700-91fc-acc4170b27ce. doi: http://doi.org/10.3897/phytokeys.25.3100

Burkill, H. M. (1985). Entry for Lasiurus hirsutus (Forssk.) Boiss. [family POACEAE]. In: The useful plants of West tropical Africa, 2nd edition. Royal Botanic Gardens, Kew, UK. http://plants.jstor.org/upwta/2_580

Cambie, R.C. & Ash, J. (1994). Fijian Medicinal Plants. Csiro Publishing, Raj., 18, 1414 AH- Science-365 pages. https://doi.org/10.1021/np960466o. ISBN: 0-643-05404-9.

Cronquist, A. (1976). Conyza Less. In TUTIN et al. (Eds.), Flora Europaea.Vol.4, Cambridge University Press, Cambridge. ISBN: 0-521-087171.

David, J. K. & Nesom, G. L. (2012). *Erigeron canadensis*, in Jepson Flora Project (eds.) Jepson Flora.

Djurdjević, L. M., Mitrović, G., Gajić, S., Jarić, O., Kostić, L.& Oberan, P. P. (2011). An allelopathic investigation of the domination of the introduced invasive Conyza canadensis L. Flora (Jena), 206(11), 921-927.

Funk, V.A., Bayer, R.J., Keeley, S., Chan, R., Watson, L. & Gemeinholzer, B. (2005). Everywhere but Antarctica: using a supertree to understand the diversity and distribution of the Compositae. Biol. Skr., 55, 343–374.

Greuter, W. (2006–2009). Compositae (pro parte majore). In: Greuter, W. & Raab-Straube, E. von (Eds), Compositae. Euro+Med Plantbase the information resource for Euro-Mediterranean plant diversity. Retrieved at 13.04.2020, from: http://www.emplantbase.org/home.html

Greuter, W. (2008). Compositae. – In: Greuter, W. & Raab-Straube, E. von. (eds), Med-Checklist. A critical inventory of vascular plants of the circum-Mediterranean countries. 2. Dicotyledones (Compositae). OPTIMA Secretariat, Palermo, Med-Checklist Trust of OPTIMA, Géneve, and Euro+Med Plantbase Secretariat, Berlin.

Greuter, W. (2003). The Euro+Med treatment of Asteraceae (Compositae): generic concepts and required new names. – Willdenowia, 33(1), 45–47.

HAYEK, A. (1931). Prodromus Florae peninsulae Balcanicae, 2. Dahlem bei Berlin

Jeffrey, C. (2007). Compositae: Introduction with key to tribes. Pages 61–87 in Families and Genera of Vascular Plants, Vol. VIII, Flowering Plants, Eudicots, Asterales (J. W. Kadereit and C. Jeffrey, (Eds.). Berlin: Springer-Verlag.

Kissmann, K. & Groth, D. (1999). Plantas Infestantes e Nocivas (2nd ed.). São Paulo: BASF Brasileira.

Lust, J. (2014). The Herb Book: The Most Complete Catalog of Herbs Ever Published. Courier Corporation, Raj. 11, 1435 AH - Nature - 640 pages.

Marochio, C. A., Bevilaqua, M. R. R., Takano, H. K., Mangolim, C. A., Oliveira Junior, R. S. & Machado, M. F. P. S. (2017). Genetic admixture in species of Conyza (Asteraceae) as revealed by microsatellite markers. Acta Sci. Agron. 39, 437–445. doi: 10.4025/actasciagron.v39i4.32947.

Melzer, H. (1996). Neues zur Flora von Steiermark, XXXV. Mitt. naturwiss. Verein Steiermark 126, 99–104.

Michael, P.W. (1977). Some weedy species of Amaranthus

3.3. Phenology

E. canadensis L. has been seen from June to February. Flowering periods was from August to October. The seedling stage in Albaha start in July and flowering starts rapidly at the beginning of August until the end of October, few species seen flowering at the end of December.

E. canadensis L. is only found in Albaha region with relatively cold habitats, and altitudes more than 2000 m. above sea level (Fig. 1). Its habitat also could be sunny, warm environments (Vladimirov, 2009; Wu, 2009). Considering the present scattered distribution and abundance of *E. canadensis* in Albaha region, has probably been introduced at least a decade ago and looks like a highly invasive plant, the limited localities in Albaha region suggest also that it is introduced recently.

The number of *E. canadensis* increased significantly in the recorded locations where they were seen in the year 2016. In the same habitat, E. bonariensis is also seen, the two species are very similar and often difficult to distinguish between them. The two species differ from each other in the form of the inflorescence, phyllaries, and leaves.

E. canadensis expected to spread noticeably in several habitats, making it an aggressive invasive weed and requires rapid action to control it. Internationally, the species is a difficult weed to control. In some country, E. bonariensis is first discovered and reported as an exotic herb in the environment and then became a challenging weed to control (Wang et al., 2018), the same situation may apply to *E. canadensis*. Chemical control e.g. glyphosate and glufosinate-ammonium was used worldwide to control the species (Weaver, 2001, Sansom et al., 2013). *E. canadensis* is also mentioned in many references as a problem weed in crop production because of its resistance to glyphosate and other herbicides (Van Gessel, 2001; Weaver, 2001).

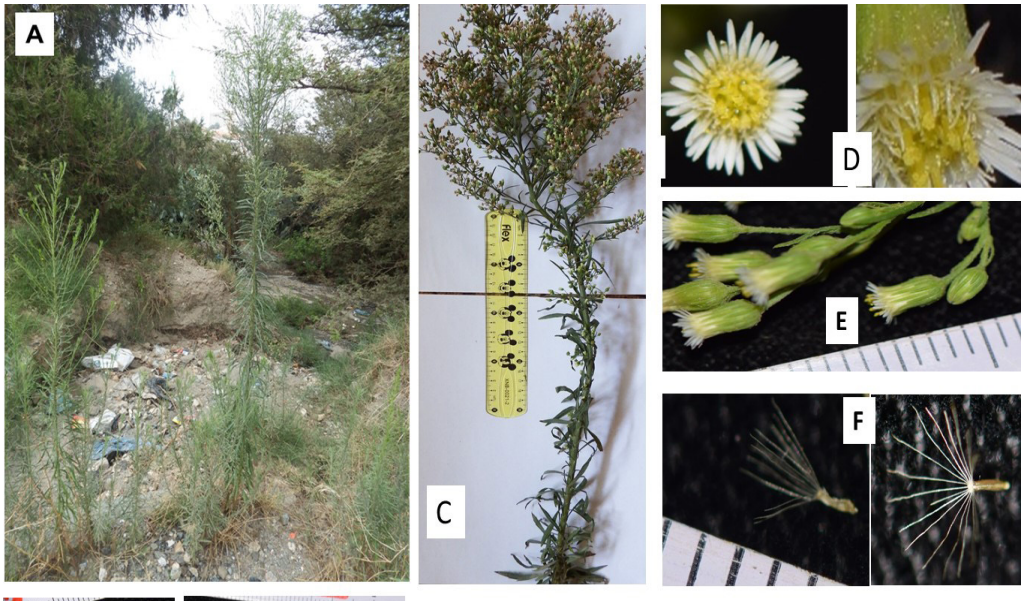

Fig. 2. The plant sample Erigeron canadensis. A: Plant habit, B: Leaves, C: Inflorescences, D: the flower showing the style branches. E: Capitulum, F: cypsela with pappus.
Photos by Dr. Nageeb and Dr. Abdul Wali in 2016

Table 1. Explored Plant Distribution in Albaha region, Saudi Arabia:

Lat.	Long.	Location	Altitude	Habitat	Area
19.850318	41.60031	Baljurashi	2039	road side	Al Shatibah
19.85048	41.599697	Baljurashi	2042	road side	Al Shatibah
19.853416	41.598313	Baljurashi	2033	disturbed site	Al Shatebah
19.849504	41.583829	Baljurashi	2024	natural habitat dominated by *Acacia origena*	Shkran Park
19.98910	41.534656	Al-Baha	2153	Terraces	Wadi Fiq
19.862071	41.571513	Baljurashi	2036	neglected fields	Shkran
19.84081	41.59193	Baljurashi	2070	road side	Shkran

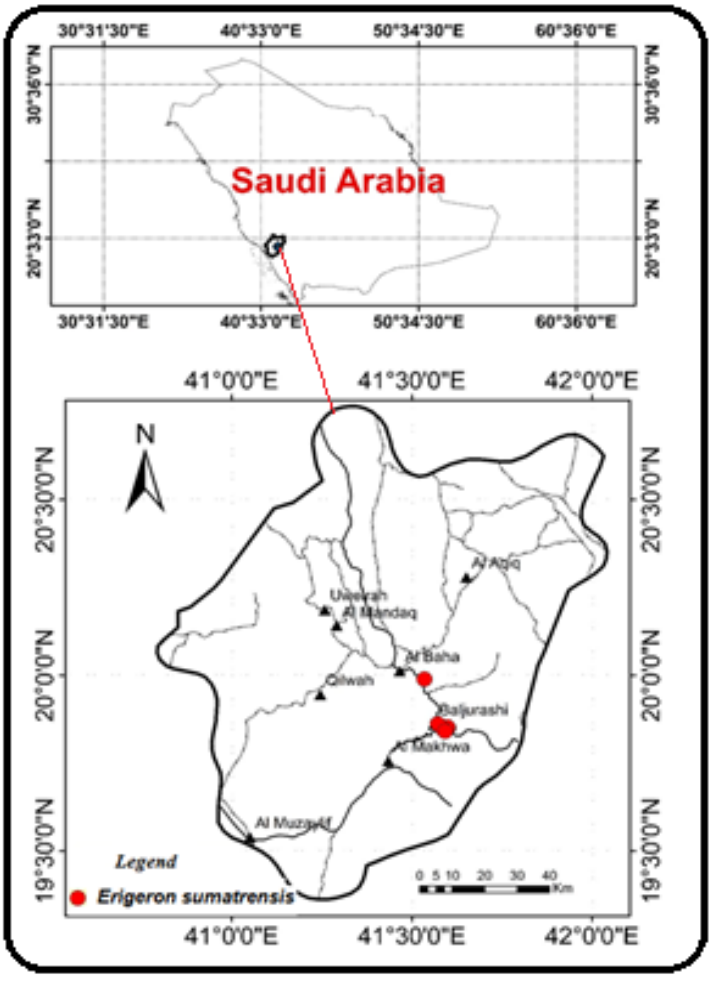

Figure 1: Distribution of Erigeron canadensis in Albaha region, Saudi Arabia.

1.3. Vernacular names

Barrilla, Canada fleabane, Horseweed, Smooth horseweed, Pinillo (Brouillet, Desmet, Coursol, Meades, Favreau, Anions, Bélisle, Gendreau, Shorthouse, and contributors, 2010).

2. MATERIALS AND METHODS

Plant specimens of *E. canadensis* was collected from different parts of Albaha region, SW Saudi Arabia (Figure 1) during fieldwork, mainly between July and February in particular in 2016. Morphological features were noted and recorded of the collected herbarium specimens and then were compared with the information available on the targeted plant in the books and published research (e.g. Yan et al., 2020; Djurdjević et al., 2011; David & Nesom, 2012; Lust, 2014). Herbarium specimens were deposited in the Herbarium of Albaha University, Department of Biology, Balhurashi, Saudi Arabia, and the Herbarium of Royal Botanic Garden of Edinburgh (RBGE), UK. Under reference "Al-Khulaidi, 24/12. 2016". Plants photographs that show habit description and the plants main parts are given in (Figure 2) to facilitate its identification. Distribution map of the species was prepared by using geographic information system (GIS.

The taxonomic key for plant identification is reported below; in addition to E. bonariensis, the species that usually to be confused with E. sumatrensis (Šida, 2003; Wurzell, 1988).

1a. Ligulate florets present, white, 0.5-1mm length; involucral bracts glabrous or scattered pubescent……..……..……..…….*E. canadensis*

1b. Ligulate florets absent or short, not more than 0.5mm, often with reddish apex; involucral bracts usually hirsute……..……..……2

2a Inflorescence diamond-shaped; ligules short, ca.0.5mm length, head 3-7mm length……E. sumatrensis

2b Inflorescence cone-shaped, elongate branches overlapping the main axis; ligules absent; head 7-10mm length……..……..…….E. bonariensis

3. RESULTS AND DISCUSSION

3.1. Plant Taxonomic Classification

The accepted name in well authentic Taxonomic web sites and publications is *E. canadensis* (Yan, et al, 2020) still some references and websites is using the name C. canadensis (Michael, 1977). On 1 May 1753, the species was named by Linnaeus, in Species Plantarum, as *Erigeron canadensis* L., Sp. Pl. 2: 863 (1753), the plant name has been changed in Bulletin of the Torrey Botanical Club. New York, 1943 by Cronquist to C. canadensis (L.) Cronquist, Bull. Torrey Bot. Club 70: 632 (1943). Although the accepted name in trustable sites and studies is *E. canadensis*, still some references and websites prefer to use the name C. canadensis.

3.2. Plant Description

An annual, erect herb up to 2 m tall, much branched in the upper part. Leaves dense and crowded along the entire length of the stem and appearing whorled, alternate, simple, base oblanceolate to linear- lanceolate, apex acute, withered at anthesis, persistent, margins entire usually with fine white hair, the upper leaves are smaller, linear to lanceolate, sub-entire to entire, sparsely hirsute, grey on both surfaces, sessile. The lower leaves toothed in particular towards the apex. Inflorescence, heads in panicle-like clusters with many small flowers individually stalked; capitula small, 2–4 mm in diameter, flowers many on short branches near the top of the main stem; involucre 3--4 mm, 2--3 mm diameter, phyllaries, smooth, to sparse sort white hairs, the outer ones are green to red brown, lanceolate to linear, inner bracts longer, linear, yellowish green to reddish. Ray florets white, many, less than 1 mm. Disk florets, yellowish-green disk. Cypsela beakless, grey-brown less than 2 mm with 2 to 3 mm long white simple papuse.

1. INTRODUCTION

The family Asteraceae family covers more than 32000 species of plants species that are belong to more than 1900 genera, the family is widespread worldwide (Jeffrey, 2007), except in Antarctica (Funk, Bayer, Keeley, Chan, Watson & Gemeinholzer, 2005), about 200 species of Erigeron genera and about 50 species of Conyza genera are distributed almost throughout the world (Kissmann & Groth 1999; Sansom, Saborido & Dubois, 2013; Milović, 2004; Cronquist, 1976; Yan, Feng, Zhao, Feng, Zhu, Qu and Wang, 2020).

Erigeron canadensis L. (= Conyza canadensis (L.) Cronquist), horseweed is an annual species, up to 2 m. the species is native to North America and widely distributed as invasive species to many countries in the world (Pruski & Sancho, 2006; Thebaud & Abbott, 1995). The plant also known as horseweed or Canadian horseweed herb

In the recent treatment of Asteraceae (Compositae) for the MedChecklist and Euro+Med Plant Base projects (Greuter, 2006–2009, 2008) most species of Conyza genus have been included in Erigeron genus

Erigeron bonariensis and *E. canadensis* often occur in the same habitat and sites. Identification confusion between *E. canadensis*, E. bonariensis Erigeron sumatrensis, and other Erigeron (Conyza) species are common (Michael, 1977; Marochio, Bevilaqua, Takano, Mangolim, Oliveira Junior & Machado, 2017; Wu, 2009). This due to the morphological and ecological resemblance and the lack of a proper literature (Anzalone, 1964; Melzer, 1996; Poldini and Kaligari, 2000). Identification was also made extremely difficult because of the occurrence of hybrids, mostly between *E. canadensis* and E. bonariensis (Rohiena, 1923; Hayek, 1931; Anzalone, 1964; Cronquist, 1976; Stace, 1997). By following taxonomic treatment of *E. canadensis* based on the concept proposed by Greuter (2003), the newly recorded species is an accepted name. Identification of *E. canadensis* was based on morphological features described by Yan, et al 2020; Djurdjević, Mitrović, Gajić, Jarić, Kostić & Oberan, 2011; David & Nesom, 2012; Lust, 2014.

On 1 May 1753, the species was named by Linnaeus, in Species Plantarum, as *E. canadensis* L. Sp. Pl. 2: 863 (1753), the plant name has been changed in Bulletin of the Torrey Botanical Club. New York, 1943 by Cronquist to C. canadensis (L.) Cronquist, Bull. Torrey Bot. Club 70: 632 (1943).

The study aims to survey and explore the new unknown plant species so that enhance the flora of the Saudi Arabia.

1.1. Plant Classification (Penev, 2019):

Classification:

Kingdom	Plantae
Phylum	Tracheophyta
Class	Magnoliopsida
Order	Asterales
Family	Asteraceae
Genus	Erigeron

Accepted scientific name: *Erigeron canadensis* L.

1.2. Synonyms

Aster canadensis (L.) E. H. L. Krause (Deutschl. Fl. (Sturm), ed. 2. 13: 59, pl. 10 (1905).

Caenotus canadensis (L.) Rafin., Fl. Tellur. 2: 50 (1837), nom. inval.

Caenotus pusillus Raf., Fl. Tellur. 2: 50 (1837).

Conyza canadensis (L.) Cronq., Bull. Torrey Bot. Club 70: 632 (1943).

Conyza canadensis var. incisa P. D. Sell, Fl. Gr. Brit. Ireland 4: 555 (459) (2006).

Conyza canadensis var. obovoidea P. D. Sell, Gr. Brit. Ireland 4: 555 (459) (2006).

Conyza canadensis var. pusilla (Nutt.) Cronquist, Bull. Torrey Bot. Club 74: 150 (1947).

Conyza canadensis var. robusta P. D. Sell, Fl. Gr. Brit. Ireland 4: 556 (459) (2006).

Conyza canadensis var. simplex P. D. Sell

Conyza parva Cronq. (Synonym) Conyza parva Cronq.

Erigeron paniculatus Lam., Fl. Gr. Brit. Ireland 4: 555 (459) (2006).

Leptilon pusillum (Nutt.) Britt, Torreya 14: 198 (1914).

Marsea canadensis (L.) Badillo, Bol. Soc. Venez. Ci. Nat. 10: 256 (1946).

المملكة العربية السعودية
جامعة الحدود الشمالية (NBU)
مجلة الشمال للعلوم الأساسية والتطبيقية (JNBAS)
طباعـــة ـ ردمد: 1658-7022 / الكتروني ـ ردمد: 1658-7014
www.nbu.edu.sa
http://jnbas.nbu.edu.sa

حشيشـــة الجبـــل أو العشـــبة الكنديـــة *Erigeron canadensis* L. (العائلـــة النجميـــة) تســـجيل جديـــد لقائمـــة نباتـــات شـــبه الجزيـــرة العربيـــة

عبد الولي أحمد الخليدي[1,2]، نجيب علي الصغير[1،2] وفاتن زبير فلمبان[3]

(قدم للنشر في 1441/12/03هـ؛ وقبل للنشر في 1442/03/24هـ)

ملخص: تتميز شبه الجزيرة العربية بنباتات غنية جدًا، ولا تزال نباتات شبه الجزيرة العربية غير مستكشفة جيدًا. تم إجراء العمل الميداني لمسح الفلورا في عام 2016 في المناطق المرتفعة من منطقة الباحة الممتدة بين حوالة جنوب شرق الباحة حتى منطقة دوس وما حولها شمال غرب الباحة بهدف التحقيق في الأنواع النباتية غير المعروفة، وذلك لتعزيز نباتات الباحة وشبه الجزيرة العربية بأنواع نباتية جديدة.. تقوم هذه الدراسة بتوثيق نبات جديد لم يرد ذكره ضمن نباتات شبه الجزيرة العربية وهو حشيشة الجبل أو العشبة الكندية. *Erigeron canadensis* L. = *Conyza canadensis* (L.) Cronquist. يتبع النبات الفصيلة النجمية Asteraceae. تم جمع هذا النوع في عام 2016 من المرتفعات العالية الواقعة في منطقة الباحة، المملكة العربية السعودية. وبما أنه لم يوثق في وقت سابق ضمن نباتات شبه الجزيرة العربية، لذلك يعتبر هذا النبات إضافة جديدة لنبات شبه الجزيرة العربية.

كلمات مفتاحية: الجزيرة العربية، العائلة النجمية حشيشة الجبل (العشبة الكندية)، الحياة النباتية، تسجيل جديد

*** للمراسلة:**
أستاذ مشارك، قسم الأحياء، كلية العلوم والآداب، جامعة الباحة، ص ب: 1988، رمز بريدي: 61008، الباحة، المملكة العربية السعودية.

e-mail: abdulwali20@gmail.com

jnbas.nbu.edu.sa
DOI: 10.12816/0058337

KINGDOM OF SAUDI ARABIA
Northern Border University (NBU)
Journal of the North for Basic and Applied Sciences (JNBAS)
p- ISSN: 1658 - 7022 / **e- ISSN:** 1658 - 7014
www.nbu.edu.sa
http://jnbas.nbu.edu.sa

Erigeron canadensis L. (Asteraceae): A New Record to the Flora of the Arabian Peninsula

Abdul Wali A. Al-Khulaidi[1],2 Nageeb A. Al-Sagheer1,2 and Faten Z. Filimban3

(Received 24/07/2020; Accepted 09/11/2020)

Abstract The Arabian Peninsula characterized by very rich flora, the flora of the Arabian Peninsula is still not explored well. Field work was conducted in 2016 in high altitude areas of Albaha region, between Hawalah (SE Albaha region) and Dos and surrounding areas (NW Albaha region) to investigate the unknown plant species so that to enhance the flora of Albaha and Arabian Peninsula with new plant species. This paper is reporting and documenting newly record of *Erigeron canadensis* L. = *Conyza canadensis* (L.) Cronquist (Asteraceae) to the flora of the Arabian Peninsula. The species was collected from high altitude mountains of Albaha region, Saudi Arabia in 2016. Since it has not been reported earlier from flora of the Arabian Peninsula, therefore, the recorded plant will be an addition to the flora of the Arabian Peninsula.

Keywords: Arabian Peninsula, Asteraceae, *Erigeron canadensis*, Flora, New record

* **Corresponding Author:**

Associate Professor, Dept. of Biology, Faculty of Science and Arts, Albaha University, P.O. Box: 1988, Code: 61008, Albaha, Kingdom of Saudi Arabia.

e-mail: abdulwali20@gmail.com

jnbas.nbu.edu.sa

DOI: 10.12816/0058337

Azmi M., & Malik A. (2001). Optimum Tilt Angle and Orientation for Solar Collector in Brunei Darussalam. Renewable Energy, Elsevier, 24(2), 223-234.

Lim, C. S. (2004). The universal sun chart. Proceedings of the 8th Korea-Russia International Symposium on Science and Technology, KORUS 2004, 2, pp. 307-310.

El-Sebaii, A.A., Al-Hazmi, F.S., Al-Ghamdi, A.A., Yaghmour, S.J. (2010). Global direct and diffuse solar radiation on horizontal and tilted surfaces in Jeddah, Saudi Arabia. Applied Energy, 87(2), 568-576.

Jenkins Alejandro. (2012). The Sun's position in the sky. European Journal of Physics. 34 (3), 633. DOI: 10.1088/0143-0807/34/3/633.

Yadav, A.K., & Chandel, S.S. (2013). Tilt angle optimization to maximize incident solar radiation: A review Renewable and Sustainable Energy Reviews, 23(C), 503-513. DOI: 10.1016/j.rser.2013.02.027.

Bortolini, M., Gamberi, M., Graziani, A., Manzini, R., Mora, C. (2013). Multi-location model for the estimation of the horizontal daily diffuse fraction of solar radiation in Europe. Energy Conversion and Management, (67), 208-216.

Kazimierski, S.M. (2015). Qualities of Solar Incidence Diagram. Energy Procedia, (70), 737-744.

Ng, K. (2016). Prediction Methods in Solar Sunspots Cycles. Scientific Reports 6(1), 21028. DOI: 10.1038/srep21028

Messenger, R., Goswami, D.Y. (2017). Photovoltaics fundamentals, technology and application. In D. Y. Goswami and F. Kreith (Eds.), Energy Conversion (2nd ed. pp. 765-795). Taylor & Francis Group: CRC Press. ISBN: 978-1-4665-8482-2.

Bakirci, K. (2018). Investigation of solar energy potential on inclined surfaces. Environmental Progress and Sustainable Energy, 37(1), 524-532. Doi:10.1002/ep.12680.

Ursula Eicker. (2005). Solar Technologies for Buildings. Solar Technologies for Buildings. Wiley. ISBN: 9780471486374.

Kalogirou, S., Solar Energy Engineering, (2009), Academic Press.

The University of Oregon, Retrieved at 2019 from: http://www.susdesign.com/sunposition

The University of Oregon, Retrieved at 2019 from: http://solardata.uoregon.edu/ SoftwareTools.html

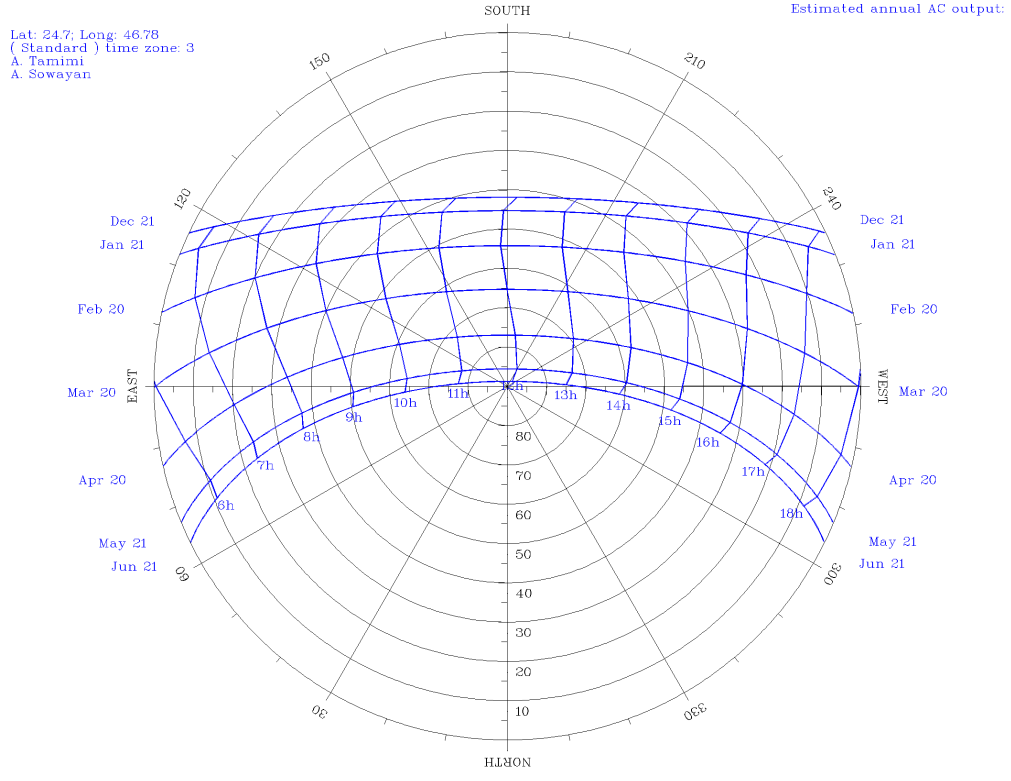

Figure 12: The Yearly Monthly Average Polar Sun Chart of Year 2019 for Riyadh, Saudi Arabia (local standard clock time), Retrieved at 2019 from: http://www.susdesign.com/sunposition.

Conclusions:

Available yearly monthly average sun charts of Riyadh assist in determining the sun's elevation angle α and azimuth angle ɣs over certain location for a day. These angles are very essential parameters in calculating the amount of collected solar energy by a solar system under specific sun's path. The sun chart and SunPosition softwares proved to be quick and accurate tools to predict most of essential solar parameters, and have been used extensively by academics, researchers, and design professionals due to their accuracy and ease of use.

Also, the apparent sun paths can be used to assess the effect of shade on the performance of solar systems in Riyadh, and assess the extent of over shading caused by neighboring tall objects which block the sun path over Riyadh, thus reducing the performance of solar systems. Solar systems are mounted at a fixed tilt angle of inclination under a wide variability in sun's paths at the considered location. The solar systems intended for winter heating alone benefits from the higher tilt angles relative to the average sun's path than those which are used in summer season. This is due to variation of sun's paths over Riyadh from winter to summer as indicated in Figures (9-12). Thus, it is increasingly important to know and understand the effect of the apparent sun's paths on the design and performance of solar-energy collecting systems.

REFERENCES:

Duffie, J. A., & Beckman, W.A. (2013). Solar Engineering of Thermal Processes (4th ed.). John Wiley & Sons.

Yogi Goswami D., Kreith F., & Kreider J. (2000). Principles of Solar Energy Engineering (2nd ed.). Taylor & Francis. ISBN: 978-1560327141.

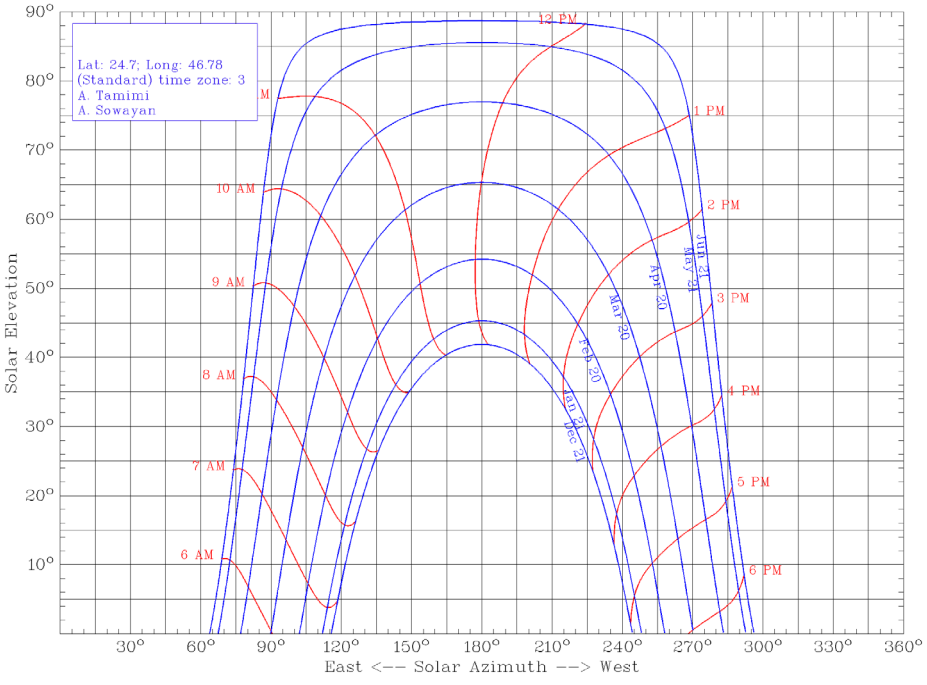

Figure 10: The Yearly Monthly Average Cartesian Sun Chart of Year 2019 for Riyadh, Saudi Arabia (local standard clock time), Retrieved at 2019 from: http://www.susdesign.com/sunposition.

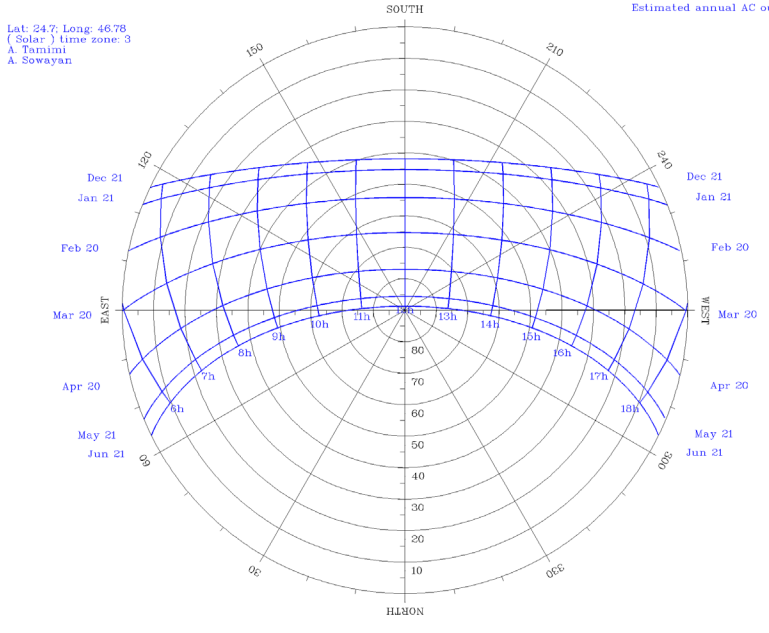

Figure 11: The Yearly Monthly Average Polar Sun Chart of Year 2019 for Riyadh, Saudi Arabia (local solar time), Retrieved at 2019 from: http://www.susdesign.com/sunposition

has an azimuth orientation of 180o.

Designers and architectural engineers pay particular attention to building orientation with respect to the yearly monthly average sun paths to minimize heating and cooling loads requirements. For homes located in the northern hemisphere, as in Riyadh, Kingdom of Saudi Arabia, the south-facing side of the home should be oriented due south to receive maximum solar radiation from the low sun's elevation at its low southerly inclined sun paths during the winter season. The home southern exposure should be clear from large and tall objects which block the solar radiation coming from the low sun's elevation at its daily sun path. Thus, reducing heating load requirements during the cold winter seasons.

The summer sun paths are higher overhead than the winter sun paths. Thus, roof overhangs at Riyadh's building should be designed with respect to the high sun's elevation at its summer path to reduce heat gain in the summer season. Consequently, reducing cooling load requirements during the hot summer seasons.

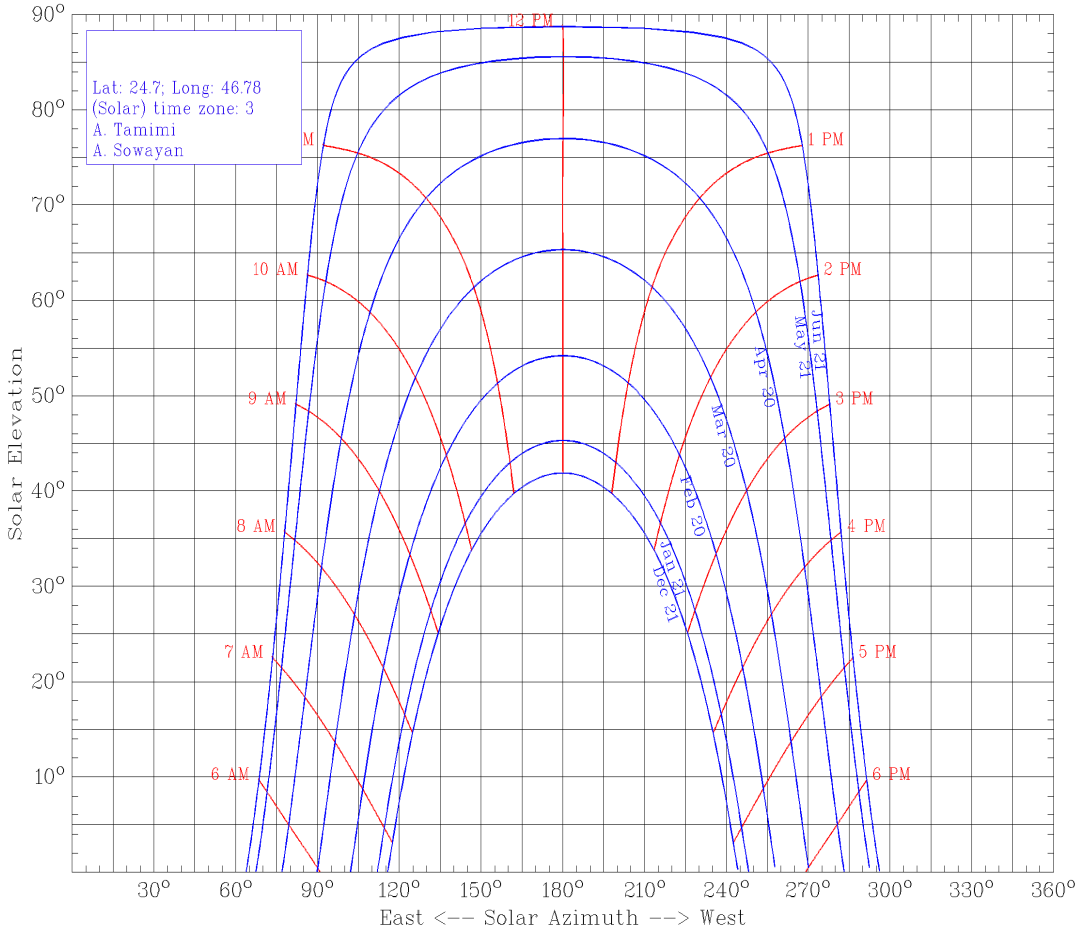

Figure 9: The Yearly Monthly Average Cartesian Sun Chart of Year 2019 for Riyadh, Saudi Arabia (local solar time), Retrieved at 2019 from: http://www.susdesign.com/sunposition

Polar sun paths Figure (11) and (12) are based on a circle where the sun elevation (altitude angles) are represented by smaller and smaller circles as the elevation increases, that is the larger the circle is the smaller is the sun elevation. The azimuth angle increases clockwise from 0° to 360° east to west around the upper half of the circle, and counter clockwise from 0° to 360° east to west around the lower half of the circle. Sun paths are drawn in east-west direction on the surface of the sun elevation circles.

Sun paths for any location on earth surface can be drawn on Cartesian or polar co-ordinates for every day in the year from sunrise to sunset on hourly basis, thus generating approximately 30 graphs per month and 365 graphs per year. This large number of curves on the same graph will create crowdedness of close parallel curves which makes the graphs difficult to read or interpolate. The variation of those paths from day to day is slight, but is noticeable from month to month in the year. Therefore, the number can be shortened to twelve monthly average sun paths for every location per year when the average day of the month 20/21 is used in calculations.

There is similarity of sun paths for any two corresponding months in the year per latitude, due to the symmetrical apparent movement of the sun about solstice, thus it is enough to plot sun paths for one half of the year (seven months were considered). Non-mentioned months have similar sun paths as their corresponding months in the year. Thus, seven sun paths were created for seven cases; 21 December, 21 January, 20 February, 20 March, 20 April, 21 May, and 21 June.

The generated seven monthly average sun paths were compiled in one graph at an acceptable level of crowdedness to create one yearly monthly average sun chart Riyadh as indicated in Figure (9) for the Cartesian sun charts using local solar time, Figure (10) for the Cartesian sun charts using local clock time, Figure (11) for the polar sun charts using local solar time, and Figure (12) for the polar sun charts using local clock time. The yearly monthly average sun charts look similar at the first glance for any location on earth, but close examination of those charts results in considerable differences in time and angle values.

The position of the sun at any time of a day, during any month of a year and for any location on earth can be abstracted by the sun path. It is a plot of the sun's altitude versus azimuth at different times throughout a given day. Generally, the seasonal positions of the sun are known in general terms. The sun is directly over the equator about March 21, the vernal equinox. It appears farther north each day until it reaches its zenith above the Tropic of Cancer about June 21 (the summer solstice in northern latitudes). Then, the sun appears a little more southerly each day, rising above the Equator about September 21 (the autumnal equinox) and reaching its most southerly point over the Tropic of Capricorn about December 21 (winter solstice).

There is a considerable difference between the yearly monthly average sun charts created with local solar time parameter and those with local clock time parameter (local standard time). Solar noon always (12 noon) lies exactly at solar azimuth angle of 180 in the middle of the sun chart when local solar time is used as a parameter as shown in Figure (9). This is not the case for the sun chart with local clock time (local standard time) as parameter where the hour lines are shifted for longitude and EoT corrections as shown in Figure (10).

The determination of the yearly monthly average apparent Cartesian and polar sun charts can be used to rapidly predict the incidence angle at any location and time during the year, and assist in realizing the sun's apparent position at any location through the daytime sky at any location in a year as shown in Figures. (11) and (12). The Stereographic Figures (11) and (12) show the position of the Sun at a given time frame (solar time and standard clock time) for the city of Riyadh. In these figures, there are four lines, which are: azimuth lines, altitude lines, date and months lines, and hour lines. The azimuth lines originated from the center to the edge of the chart with an increment of 30o, on the other hand, the altitude lines are represented as concentric circles with an increment of 10o. In these figures the intensity of the Sun can be identified all year long. The polar sun path chart shown in Figures (11) and (12)

Table (1) shows the values of declination angle δ and Equation of time EoT at the average day of the month 20/21of year 2019. In this table should be noted that, the values of the considered parameters have two values for some cells. The values in these cells when they printed in bold italic text, they represent the hand calculations using the MS-Excel software. If the cell in these tables has only one value, this means that the values obtained from the calculations performed in this study and the values obtained from the considered software (The University of Oregon, 2019) are identical.

Table 1: Values of declination angle δ and EoT at the average day of the month 20/21of year 2019 for Riyadh (Φ = 24.7° N, L=46.78° E)

Average day of the Month	Declination Angle *δ* Degrees	*EoT* Minutes
21-Jan	-19.88 ***-20.07***	-11.28 ***-11.29***
21-Feb	-10.53 ***-10.532***	-13.63 ***-13.627***
21-Mar	0.27	-7.24
21-Apr	11.89	1.26
21-May	20.2 ***20.18***	3.43
21-Jun	23.44	-1.74
21-Jul	20.45 ***20.44***	-6.41 ***-6.406***
21-Aug	12.08	-3.18
21-Sep	0.67 ***0.66***	6.87
21-Oct	-10.72	15.34
21-Nov	-19.93 ***-19.92***	14.18 ***14.17***
21-Dec	-23.44	2

Cartesian sun paths Figure (9) and (10) were constructed by plotting solar elevation (solar altitude angle α) versus the solar azimuth angle γs for the location under consideration. Parameters are the average day of every month of year 2019 at which this work was conducted, and the values of constant local solar time or constant local clock time (constant local standard time).

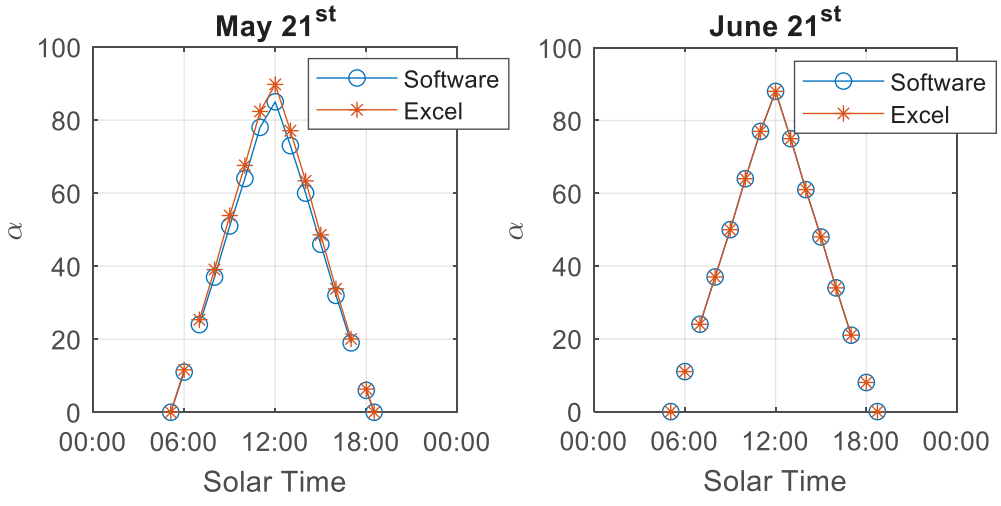

Figure 7: Solar elevation angle α at the average day of the months of May and June of year 2019 for Riyadh ((Φ = 24.7° N, L=46.78° E).

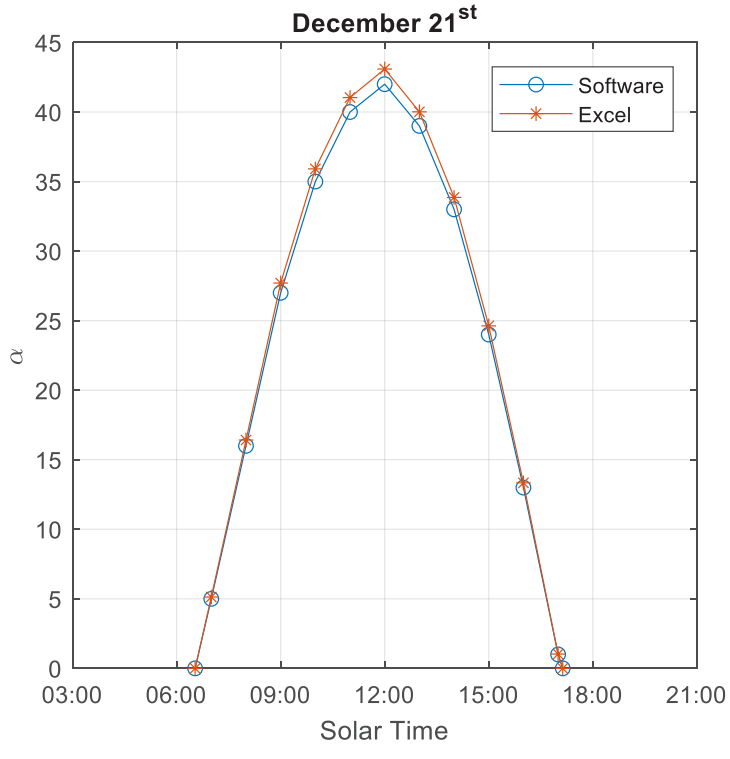

Figure 8: Solar elevation angle α at the average day of the month of December of year 2019 for Riyadh ((Φ = 24.7° N, L=46.78° E).

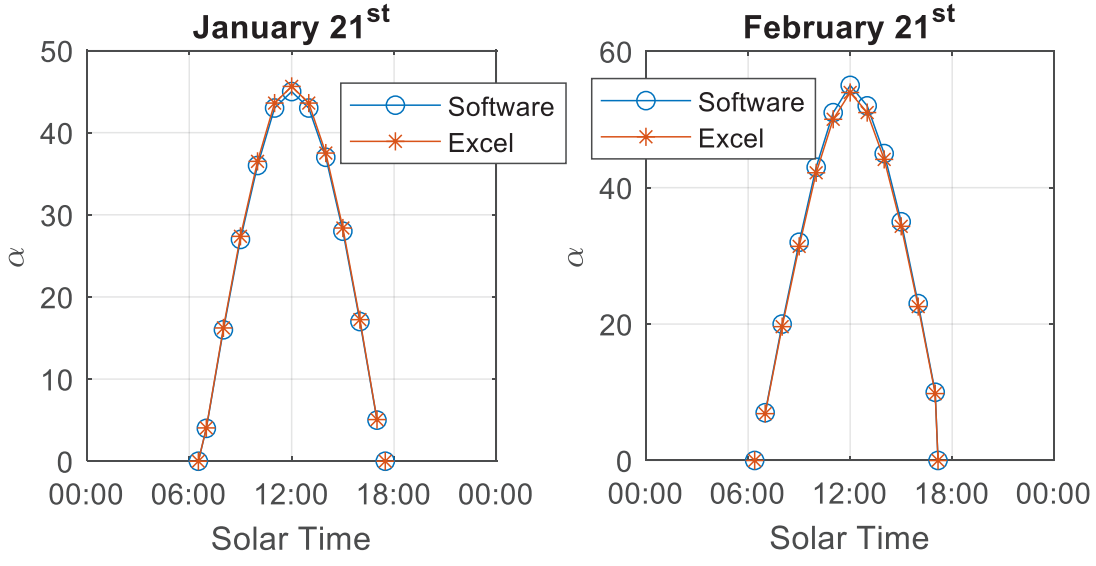

Figure 5: Solar elevation angle α at the average day of the months of January and February of year 2019 for Riyadh ((Φ = 24.7° N, L=46.78° E).

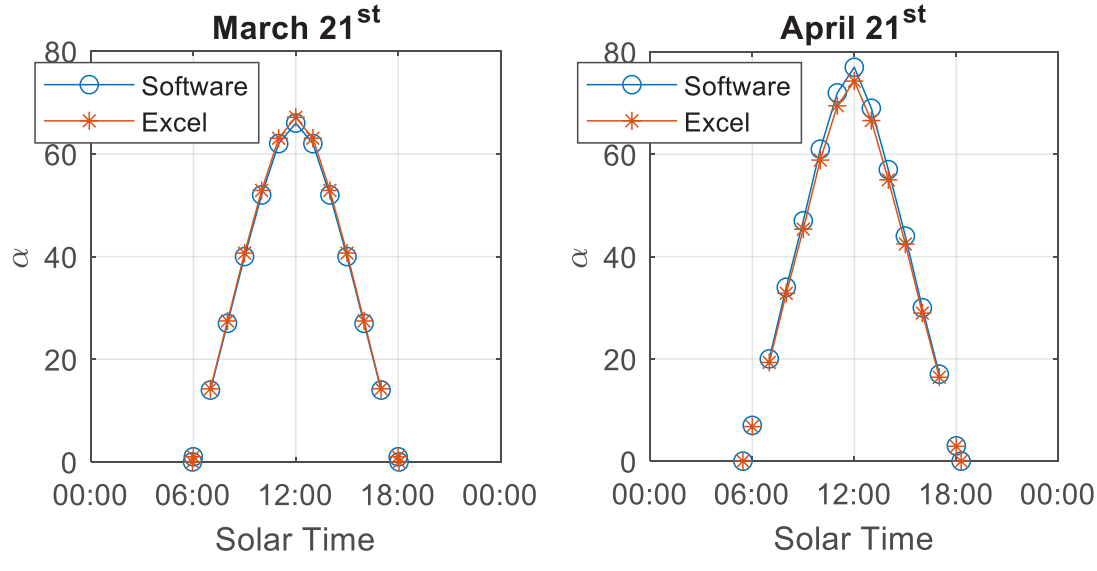

Figure 6: Solar elevation angle α at the average day of the months of March and April of year 2019 for Riyadh ((Φ = 24.7° N, L=46.78° E).

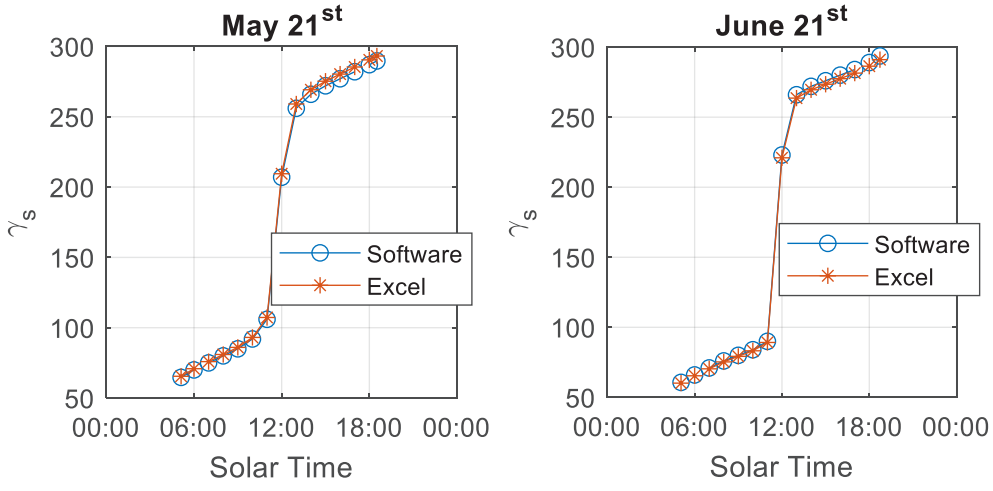

Figure 3: Solar azimuth angle γs at the average day of the months of May and June of year 2019 for Riyadh (Φ = 24.7° N, L=46.78° E).

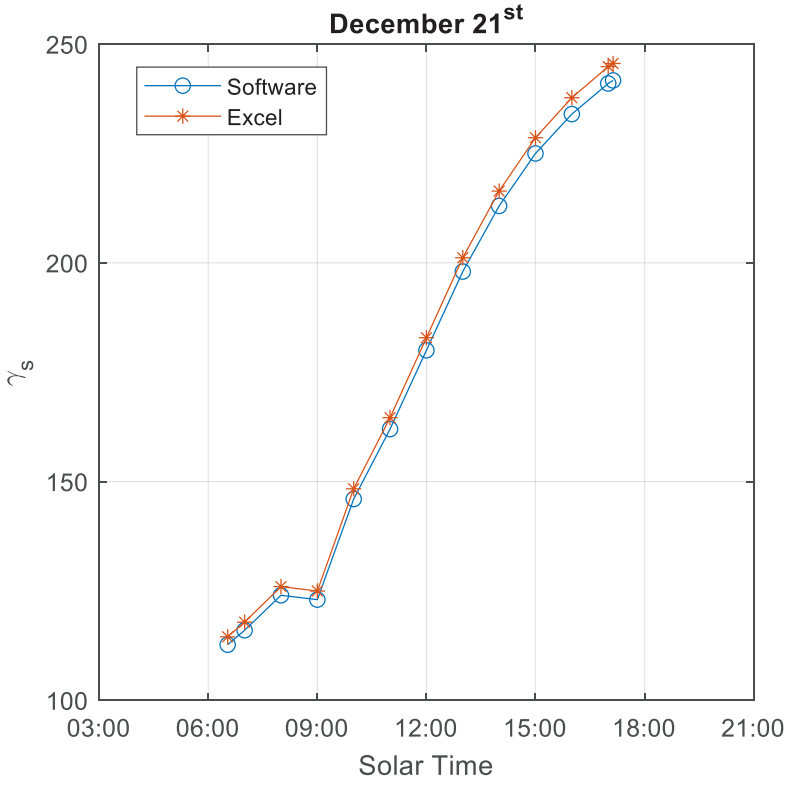

Figure 4: Solar azimuth angle γs at the average day of the month of December of year 2019 for Riyadh (Φ = 24.7° N, L=46.78° E).

Figures (1) to (4) show the azimuth angle for seven months of the year 2019. In these figures a full agreement between the curves that were achieved from the SunPosition software and our Excel calculations. It can be concluded from these figures that the azimuth angle increases as the time advances during the day. Also at noon time the azimuth angle tends to be constant. The altitude or solar elevation angle α shown in Figures (5) to (8) is always maximum during noon time all year long in Riyadh, Saudi Arabia. It forms a parabolic shape that starts to increase in the morning until noon time then it decreases as the day progress toward the sunset.

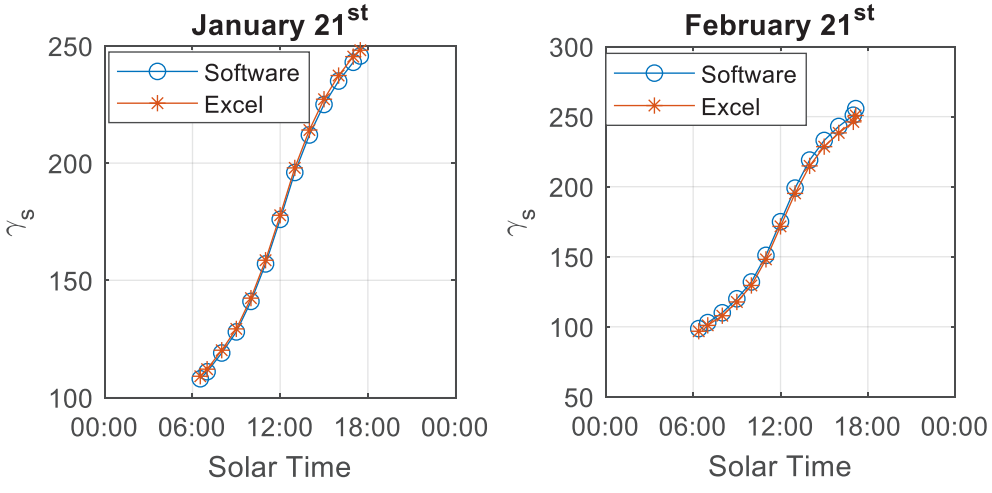

Figure 1: Solar azimuth angle γs at the average day of the months of January and February of year 2019 for Riyadh (Φ = 24.7° N, L=46.78° E).

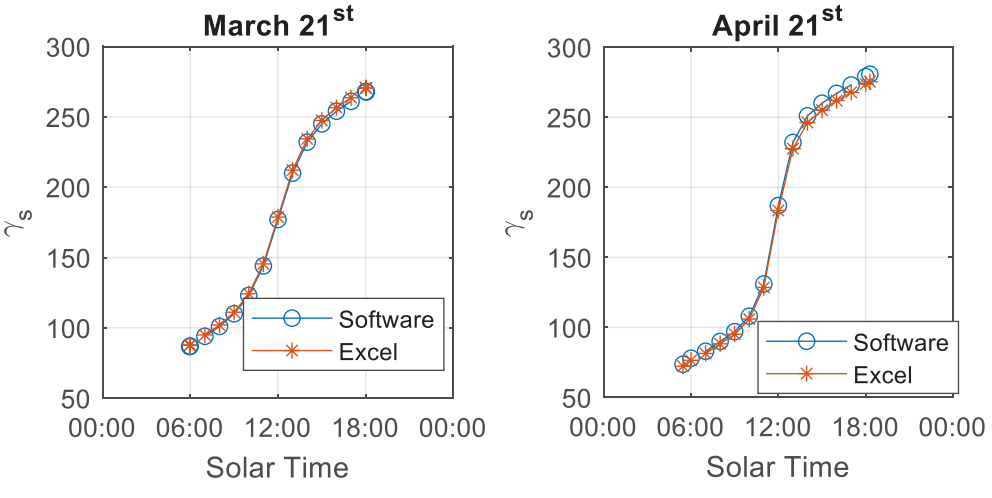

Figure 2: Solar azimuth angle γs at the average day of the months of March and April of year 2019 for Riyadh (Φ = 24.7° N, L=46.78° E).

cal solar time into local clock time correction factors must be included to compensate for the following aspects:
The difference between the standard longitude of the time zone and the local longitude multiplied by 4. This is due to earth rotation which takes one degree of longitude per four minutes,
Daylight saving time if applied,
Equation of Time (EoT): to compensate for the irregularity in earth rotation around the sun. This factor is available in the literature of solar energy as correlations, tables, and charts [1,14].
Thus, the relationship between local solar time and local clock time is given by:

$$\text{Local solar time} = \text{Local clock time} + 4 \times (L_{std} - L_{local}) + EoT \quad (12)$$

where:

L_{std} is the local standard longitude measured in degrees for the local time zone, which runs through the center of each time zone,
L_{local} is the local longitude of the location under consideration, East= +ve, and West= -ve, and EoT is the equation of time adjustment in minutes.

The apparent sun paths are determined by the sun's elevation (altitude angle α) and solar azimuth angle γ_s over a day as seen from a specific location. The sun's elevation α of the sun at certain horizontal location measures the height of the sun in the sky from the horizon, and compliments the zenith angle of the sun θ_z. The solar azimuth angle γ_s indicates the direction of the sun projection on a horizontal plane from due south. It varies in the range of 180° to -180°, east has negative values while west has positive values. Due north has an azimuth angle value of 0.0° while due south has an azimuth angle value of 180°. The values of the solar azimuth angle γ_s is given by the absolute value of the following equation (Duffie & Beckman, 2013):

$$\gamma_s = \pm 1 \cos^{-1}\left[\frac{\{\cos\theta_z \sin\emptyset - \sin\delta\}}{\sin\theta_z}\right], \quad (13)$$

3. Results and Discussion:

The applied software to create the sun path charts, both Cartesian and polar, was developed by researchers at the University of Oregon, USA after several years of research [15, 16]. The use of this software is free at the website of the University of Oregon (Solar Radiation Monitoring Laboratory). This software allows using either local solar time or local clock time (local standard time).
Sun position in the sky is determined by knowing both the sun elevation (altitude angle α) and the solar azimuth angle γs. These two angles can be calculated from equations (4) and (13) by hand calculator or by the Excel software. These parameters are strongly related to the location parameters, latitude and longitude L.

There are several sites from the common-knowledge domain on the web, including that of the University of Oregon/USA which addresses calculating the sun position in the sky from the equations 2-13 [1, 13, 14]. The adopted softwares were SunPosition softwares due to their accuracy and ease of use. Calculations were checked for accuracy by hand and Excel spreadsheet calculations. The results were in full agreement with those predicted by the sun chart and the SunPosition softwares [15, 16].
SunPosition software was used to calculate the declination angle δ, EoT, solar azimuth angle γs and sun elevation in the sky (altitude angle α) for the average day of the month of year 2019 for Riyadh, Kingdom of Saudi Arabia. The results of calculations are presented in Figures (1-8), which are almost identical to the results obtained from the SunPosition software.

$$T_{sr} = 12 - \frac{1}{15}\cos^{-1}(-\tan \emptyset \tan \delta) \text{ in hours before solar noon} \quad (8)$$

In the same analysis, the incidence angle at sunset of a horizontal surface $\theta_{ss} = 90°$, thus substituting in equation (3) yields the value of sunset hour angle ω_{ss} as follows:

$$\omega_{ss} = \frac{1}{15}\cos^{-1}(-\tan \emptyset \tan \delta) \text{ in hours of solar time} \quad (9)$$

The day length is denoted by T_d, and is given by degrees or hours of solar time by:

$$T_d = \omega_{sr} + \omega_{ss} \text{ in degree} \quad (10)$$

Or

$$T_d = \frac{1}{15}(\omega_{sr} + \omega_{ss}) \text{ in hours of solar time} \quad (11)$$

At any time during the day at any location of particular latitude the declination angle ∅ and hour angle ω are fixed. It is customary to express the date during the day throughout the year in terms of n (the Jolian number of the day during the year starting the count January 1), and thus as an integer of 1-365 is used in the previous equations. The average day of the month is taken to be day 20/21 of each month. The sun's elevation (altitude angle) and solar azimuth angles can be calculated easily from the previous equations (2-11) if the number of the day in the year n, the location parameter (latitude), and the hour angle ω (time during the day) are determined prior of calculations.
There are two important ways to describe time when calculating solar angles:

1. Local solar time:

The local solar time is a system of time based on the daily cycle of the sun, that is the time according to the position of the sun in the sky relative to one specific location on the ground. In solar time, the sun is always due south (or north) at exactly solar noon. This means that someone a few miles east or west of the location under consideration in the same country will have a slightly different solar noon than that at this location, although the local clock time is probably the same.
The velocity of the earth varies as it moves through its elliptical orbit around the sun; therefore, the correction factor known as the equation of time (EoT) should be taken into consideration. There are available correlations, graphs and tables in the literature to predict the value of EoT in minutes. This correction factor (EoT) compensate for the irregularity in earth motion around the sun in its elliptical orbit [1,13].

2. Local clock time:

The local solar time is the artificial time observed or measured by any time measuring device, as hand watches, clocks or any standard time measuring device which are used in everyday life. This time is usually called standard local time relative to a reference time zone (Greenwich Mean Time, GMT), since it standardizes time values to suit the practical needs of various countries. Local clock time or standard local time is related to the local standard longitude of the time zone of the location under consideration.
This time allows people living in different locations of different time zones in the world to realize their times during day and night, or to easily convert standard local time from one location to another. Daylight saving time is an arbitrary time which has no technical background and its use varies widely from country to country, but it can be implemented if local clock time (local standard time) is adjusted by +1 according to the time zone and the local energy demand.
Local solar time differs from local clock time (local standard time). All calculations in solar energy conversion must be first expressed in local solar time, then conversion to local clock time (local standard time) takes place. For the purpose of converting lo-

$$\cos\theta = \sin\delta\sin\phi\cos\beta - \sin\delta\cos\phi\sin\beta\cos\gamma + \cos\delta\cos\phi\cos\beta\cos\omega + \cos\delta\sin\phi\sin\beta + \cos\delta\sin\beta\sin\gamma\sin\omega \quad (1)$$

The values of declination angle δ at the average day of the month depend on the Julian number of the day in the year n starting count January 1. Calculations of δ are made by the following equation (Duffie & Beckman, 2013):

$$\delta \approx 23.45\sin\left(\frac{360\times(284+n)}{365}\right), \quad (2)$$

where $1 \leq n \leq 365$

The angle of incidence θ at any horizontal surface on the ground during the day is called the zenith angle of the sun and is denoted by θ_z. It complements the sun's elevation (altitude angle α) which varies from $0.0°$ at both sunrise and sunset to $90°$ at due solar noon. For horizontal surface $\beta=0.0$, thus Equation (1) yields:

$$\cos\theta_z = \sin\emptyset\sin\delta + \cos\emptyset\cos\delta\cos\omega = \cos(90-\alpha) = \sin\alpha, \quad (3)$$

upon rearrangement;

$$\alpha = \sin^{-1}\{\sin\emptyset\sin\delta + \cos\emptyset\cos\delta\cos\omega\}, \quad (4)$$

The incidence angle at sunrise of a horizontal surface $\theta_{sr} = 90^o$, thus substituting in equation (3) yields the value of sunrise hour angle ω_{sr} as follows:

$$0.0 = \sin\emptyset\sin\delta + \cos\emptyset\cos\delta\cos\omega_{sr} \quad (5)$$

Rearrangement of Equation (5), yields:

$$\cos\omega_{sr} = \frac{\sin\emptyset\sin\delta}{\cos\emptyset\cos\delta} = -\tan\emptyset\tan\delta \quad (6)$$

Thus;

$$\omega_{sr} = \cos^{-1}(-\tan\emptyset\tan\delta) \text{ in degrees before solar noon} \quad (7)$$

Or,

$$\omega_{sr} = \frac{1}{15}\cos^{-1}(-\tan\emptyset\tan\delta) \text{ in hours before solar time} \quad (8)$$

The solar time at sunrise is measured east from12 solar noon time and denoted by T_{sr} as follows:

and diffuse solar radiation on a horizontal surface, the number of bright sunshine hours, mean daily ambient temperature, maximum and minimum ambient temperatures, relative humidity. Empirical correlations for estimating the diffuse solar radiation incident on horizontal surfaces have been proposed. It is found in this study that at Jeddah, the solar energy devices have to be tilted to face south with a tilt angle equals the latitude of the place in order to achieve the best performance all year round El-Sebaii et al. (2010).

The position of the sun in the sky was derived as a function of time and the observer's geographic coordinates in Jenkins Alejandro, (2012). The method was based on applying rotation matrices to vectors describing points on the celestial sphere. The altitude of the sun was plotted to illustrate results in this study by computing the dates of the city of Manhattan in New York City when sunset aligns with the east-west streets for the sun position in the sky at a given hour of the day Jenkins Alejandro, (2012).

The tilt angle of a solar energy system is one of the important parameters for capturing maximum solar radiation falling on the solar panels. This angle is site specific as it depends on the daily, monthly and yearly path of the sun. The accurate determination of the optimum tilt angle for the location of interest is essential for maximum energy production by the system (Yadav, & Chandel, 2013). Yadav, & Chandel, (2013) had provided updated status of research and applications of various methods for determining solar panel tilt angle using different optimization techniques. The study had showed that for maximum energy gain, the optimum tilt angle for solar systems must be determined accurately for each location.

Design of energy systems based on the solar source needs an hourly and daily solar radiation data measurements. A multi-location model to estimate the expected profiles of the horizontal daily diffuse component of solar radiation has been presented by Bortolini, Gamberi, Graziani, Manzini, & Mora. (2013). Achieved results in this study showed the effectiveness of adopting a multi-location approach to estimate solar radiation components on the horizontal surface instead of developing several single location models. This is due to the increase of the geographical range of applicability without a significant decrease of the accuracy. It should be noted that the effect of seasonality on solar irradiance has been considered to develop summer and winter scenarios together with annual models Bortolini et al. (2013).

The solar incidence diagram has been presented as an alternative to the solar position chart (Kazimierski, 2015). The diagram consists of curves of the solar incidence angle plotted against the solar azimuth angle. In this study, the point of reference was located on the vertical wall of a building, facing East (Kazimierski, 2015).

The total number of sunspots in a solar cycle and the maximum averaged monthly sunspots number Rz(max) have been investigated in Ng, (2016). They were both shown to be statistically related to the geomagnetic activity index in the prior solar cycle. Also the Sun's electromagnetic dipole is moving toward the Sun's Equator during a solar cycle (Ng, 2016).

Sun path prediction was first introduced by companies dealing with building design to provide a relatively simple method of determining the apparent sun paths during the year. Few authors of solar books treated the subject for different latitudes as a service to the architectural and engineers who work in the field of solar energy (Messenger, & Goswami, 2017). The f-chart method for solar energy application has been presented by Bakirci, (2018). It was shown in this study that the increase in the annual fractions of the surface with the optimum tilt angle is nearly 21% (Bakirci, 2018). The solar panel in this study is based on horizontal surface of different tilt angles.

2. Methodology and Governing Equations

The general equation that relates the sun position in the sky to other solar angles is expressed by the angle of incidence θ of beam radiation at which solar radiation strikes an inclined surface on the ground with any angle of inclination β. The incidence angle depends on the apparent sun position in the sky, and is given by (Duffie & Beckman, 2013):

NOMENCLATURES:

L Longitude of a location [Degrees]
n The Julian number of the day in the year
T_d Day length [Degrees or solar time hours]
T_{sr} Time of sunrise [Degrees or solar time hours]
T_{ss} Time of sunset [Degrees or solar time hours]
Greek Letters:
α Altitude angle of the sun over horizontal [Degrees]
β Angle of inclination on horizontal [Degrees]
γ Surface azimuth angle [Degrees]
γ_s Sun azimuth angle [Degrees]
Θ Angle of incidence on any surface [Degrees]
Θ_{sr} Angle of incidence on a horizontal surface at sunrise [Degrees]
Θ_{ss} Angle of incidence on a horizontal surface at sunset [Degrees]
Θ_z Angle of incidence on a horizontal surface [Degrees]
δ Declination angle of earth axis [Degrees]
Φ Latitude angle of the location under consideration [Degrees]
ω Solar hour angle [Degrees or solar time hours]
ω_{sr} Sunrise hour angle of a horizontal surface [Degrees or solar time hours]
ω_{ss} Sunset hour angle of a horizontal surface [Degrees or solar time hours]

1. INTRODUCTION

Sun charts simplify the complex geometry of the hourly sun's position in the sky relative to an observer on the ground at hourly intervals based on local solar time or local clock time. Such charts usually present sun azimuth γ_s and altitude angle α based on average latitude for a given location, and on a longitude relative to the standard meridian of the time zone under consideration (Duffie & Beckman, 2013). The solar azimuth angle γs indicates the direction of the sun in the horizontal plane for a given location. It should be noted that the azimuth and altitude angles (γ_s, α) cannot be interpolated linearly. The collected solar energy by a surface varies during the day due to the variation in the apparent sun position, the inclination angle β, and the conditions of cloud cover (Duffie & Beckman, 2013). Apparent sun paths can be drawn either in Cartesian (rectangular) co-ordinates or polar (circular) co-ordinates. Cartesian co-ordinates mainly depend on solar elevation angle α and solar azimuth angle γs for any day and time of the year. The solar elevation angle α is plotted on y-axis while the solar azimuth angle γ_s is plotted on the x-axis. Polar co-ordinates are based on a circle where the solar elevation is denoted on various concentric circles while the solar azimuth is denoted by values going around the circle.

The inclination angle of a flat-plate solar collector at specific geographical location was discussed by other researchers. The effect of this angle was presented in a general graph for certain locations but without any model to predict its optimum value under a specific sun path (Duffie & Beckman, 2013). The maximum daily amount of solar irradiation which can be received at any given location will be that which falls on a flat surface when oriented normally to the sun's rays, so that it can receive maximum levels of direct, reflected and diffuse radiation during the whole day. For maximum solar energy collection, flat-plate solar collecting systems should be installed facing south at optimum angles of orientation, and the sun path is almost close to perpendicular at solar noon throughout the year (Yogi, Goswami, Kreith, & Kreider, 2000).

Estimation of the global solar radiation on a tilted surface was utilized to determine the optimum inclination angle and orientation of a flat-plate solar collector on a daily basis for specific period. The results revealed that changing the inclination angle 12 times in a year to match the sun paths maintains approximately the total amount of solar radiation near its maximum value (Azmi, & Malik, 2001). Lim, (2004) incorporated a universal sun chart which used concept of the 'solar cross', a cross with the single sun path and multiple earth positions.

Many measured data in El-Sebaii, Al-Hazmi, Al-Ghamdi, & Yaghmour, (2010) have been analyzed for Jeddah (lat. 21°42″37″N, long. 39°11″12″E), Saudi Arabia, during the period (1996-2007). The data in this study include global

المملكة العربية السعودية
جامعة الحدود الشمالية (NBU)
مجلة الشمال للعلوم الأساسية والتطبيقية (JNBAS)
طباعـــة - ردمد: 7022-1658 / الكتروني - ردمد: 7014-1658
www.nbu.edu.sa
http://jnbas.nbu.edu.sa

التنبـؤ بمخططـات الشـمس الديكارتيـة والقطبيـة الظاهـرة لمدينـة الريـاض، المملكـة العربيـة السـعودية

أحمد صالح الصويان[1] و عبد الرحمن التميمي[2]

(قدم للنشر في 1441/08/27هـ؛ وقبل للنشر في 1442/01/15هـ)

ملخص: يعد توفر المخططات البيانية السنوية/الشهرية للشمس من المعلومات المهمة جدًا للمهندسين المعماريين والباحثين في تصميم المباني وفي مجال تطبيقات تظليل للطاقة الشمسية. عادةً ما تُستخدم العلاقات المثلثية لحساب الزوايا الشمسية اللازمة لرسم مخططات الشمس الظاهرة. و يمكن استخدام برامج متاحة على الشبكة العنكبوتية الإنترنت لرسم هذه المخططات مباشرة. وهذه البرامج تم تطويرها من قبل مؤسسات تعمل في أبحاث الطاقة الشمسية. بالرغم من أن هذه البرامج متاحة مجانًا للمعرفة العامة، إلا أنه لم يتم القيام بأي جهد للتحقق من دقتها وصلاحيتها. هذه الدراسة أجريت على مدينة الرياض بالمملكة العربية السعودية بواسطة العلاقات المثلثية وتم مقارنة نتائجها بأحد البرامج المتاحة على الشبكة العنكبوتية الإنترنت، وهو البرنامج المصمم من جامعة أوريجون بالولايات المتحدة الأمريكية. وأشارت النتائج ان مخرجات البرامج المتاحة جيدة مقارنة بالنتائج التي تم الحصول عليها من العلاقات المثلثية. وأوضحت الدراسة أن الانحراف في النتائج بين العلاقات المثلثية والبرامج المتاحة كان في حدود ± 1٪.

كلمات مفتاحية: ديكارتي، قطبي، مسار الشمس، مخطط الشمس، موقع الشمس، الطاقة الشمسية.

* للمراسلة:
1. أستاذ مشارك، قسم الهندسة الميكانيكية، كلية الهنسة، جامعة الإمام محمد بن سعود الإسلامية، ص ب:5701، رمز بريدي: 11432، الرياض، المملكة العربية السعودية.
2. أستاذ، قسم الهندسة الكيميائية، كلية الهنسة، الجامعةالأردنية للعلوم والتكنولوجيا، اربيد، الأردن.

email: assowayan@imamu.edu.sa

jnbas.nbu.edu.sa
DOI: 10.12816/0058336

KINGDOM OF SAUDI ARABIA
Northern Border University (NBU)
Journal of the North for Basic and Applied Sciences (JNBAS)
p- ISSN: 1658 - 7022 / **e- ISSN:** 1658 - 7014
www.nbu.edu.sa
http://jnbas.nbu.edu.sa

Comparative Prediction of Apparent Cartesian and Polar Sun Charts for Riyadh, Kingdom of Saudi Arabia

Ahmed S. Sowayan[1] & A. Tamimi[2]

(Received 21/04/2020; Accepted 03/09/2020)

Abstract: The availability of the yearly/monthly average sun charts is a very useful piece of information for architectural engineers and researchers in passive building design and shading of solar applications. Usually, trigonometric relationships are used to calculate the solar angles needed to draw the apparent sun charts. Also, available software programs can be used to directly draw these charts in a very short time. These programs were developed by recognized solar research institutions. These programs are available free from common-knowledge domain on the web. However, no previous work was done to check their accuracy and validity. A comparative study indicated that the available software programs are as good as direct calculations obtained from trigonometric relationships. This study was conducted for the city of Riyadh, Kingdom of Saudi Arabia. The calculations indicated that the deviation in results between trigonometric relationships and the available programs was within ±1 %.

Keywords: Cartesian, Polar, Sun Path, Sun Chart, Sun Position, Solar Energy.

jnbas.nbu.edu.sa

DOI: 10.12816/0058336

* **Corresponding Author:**

1. Associate Professor, Dept. of Mechanical Engineering, College of Engineering, Al Imam Mohammad ibn Saud Islamic University (IMSIU), P.O. Box: 5701, Code:11432, Riyadh, Kingdom of Saudi Arabia.
2. Professor, Dept. of Chemical Engineering, College of Engineering, Jordan University of Science and Technology, Irbid, Jordan.

email: assowayan@imamu.edu.sa

https://doi.org/10.1109/WDDC.2007.4339387

Picco, V., Erricolo, D., & Lo Monte, L. (2010). Experimental validation of RF tomography. Symposium Digest - 20th URSI International Symposium on Electromagnetic Theory, EMTS 2010, 243–244.

Qiu, C., Liang, B., Han, F., Liu, H., Zhu, C., Liu, N., … Liu, Q. H. (2019). Multifrequency 3-D Inversion of GREATEM Data by BCGS-FFT-BIM. IEEE Transactions on Geoscience and Remote Sensing, 57(4), 2439–2448. https://doi.org/10.1109/TGRS.2018.2873363

Sato, M. (2009). Principles of mine detection by ground-penetrating radar. In Anti-personnel Landmine Detection for Humanitarian Demining: The Current Situation and Future Direction for Japanese Research and Development (pp. 19–26). https://doi.org/10.1007/978-1-84882-346-4_2

Vitebskiy, S., Carin, L., Ressler, M. A., & Le, F. H. (1997). Ultra-wideband, short-pulse ground-penetrating radar: simulation and measurement. IEEE Transactions on Geoscience and Remote Sensing, 35(3), 762–772. https://doi.org/10.1109/36.581999

Wicks, M. C. (2007). RF Tomography with Application to Ground Penetrating Radar. 2007 Conference Record of the Forty-First Asilomar Conference on Signals, Systems and Computer, 2017–2022. https://doi.org/10.1109/ACSSC.2007.4487591

Zhdanov, M., & Hursan, G. (2000). 3D electromagnetic inversion based on quasi-analytical approximation. Inverse Problems, 16(5), 1297–1322. https://doi.org/10.1088/0266-5611/16/5/311

Zhou, C., & Liu, L. (2000). Radar-diffraction tomography using the modified quasi-linear approximation. IEEE Transactions on Geoscience and Remote Sensing, 38(1), 404–415. https://doi.org/10.1109/36.823936

Magazine, 18(2), 3–6. https://doi.org/10.1109/MAES.2003.1183861

Carevic, D. (2000). Clutter reduction and target detection in ground-penetrating radar data using wavelets. Subsurface Sensing Technologies and Applications, 101–118. https://doi.org/10.1117/12.357117

Chew, W. C., & Wang, Y. M. (1990). Reconstruction of two-dimensional permittivity distribution using the distorted Born iterative method. IEEE Transactions on Medical Imaging, 9(2), 218–225. https://doi.org/10.1109/42.56334

Cui, T. J., Aydiner, A. A., Chew, W. C., Wright, D. L., & Smith, D. V. (2003). Three-dimensional imaging of buried objects in very lossy earth by inversion of VETEM data. IEEE Transactions on Geoscience and Remote Sensing, 41(10), 2197–2210. https://doi.org/10.1109/TGRS.2003.815974

Cui, T. J., Qin, Y., Ye, Y., Wu, J., Wang, G. L., & Chew, W. C. (2005). High-order inversion formulas for 3D buried dielectric objects. IEEE Antennas and Propagation Society, AP-S International Symposium (Digest), 131–134. https://doi.org/10.1109/APS.2005.1551754

Desai, M. D., & Jenkins, W. K. (1992). Convolution Backprojection Image Reconstruction for Spotlight Mode Synthetic Aperture Radar. IEEE Transactions on Image Processing, 1(4), 505–517. https://doi.org/10.1109/83.199920

Fornaro, G., Lombardini, F., & Serafino, F. (2005). Three-dimensional multipass SAR focusing: Experiments with long-term spaceborne data. IEEE Transactions on Geoscience and Remote Sensing, 43(4), 702–714. https://doi.org/10.1109/TGRS.2005.843567

Gao, G., & Torres-Verdin, C. (2006). High-Order Generalized Extended Born Approximation for Electromagnetic Scattering. IEEE Transactions on Antennas and Propagation, 54(4), 1243–1256. https://doi.org/10.1109/TAP.2006.872671

Gurbuz, A. C. (2012). Determination of background distribution for ground-penetrating radar data. IEEE Geoscience and Remote Sensing Letters, 9(4), 544–548. https://doi.org/10.1109/LGRS.2011.2174137

Guzel, Y., Tran, T. M., Wicks, M. C., & Monte, L. Lo. (2015). RF Tomography for Ground Penetrating Radar : Simulation and Experimentation. IEE International Radar Conference, 1–5.

Han, F., Zhuo, J., Liu, N., Liu, Y., Liu, H., & Liu, Q. H. (2019). Fast Solution of Electromagnetic Scattering for 3-D Inhomogeneous Anisotropic Objects Embedded in Layered Uniaxial Media by the BCGS-FFT Method. IEEE Transactions on Antennas and Propagation, 67(3), 1748–1759. https://doi.org/10.1109/TAP.2018.2883682

Karlovšek, J., Scheuermann, A., & Willimas, D. J. (2012). Investigation of voids and cavities in Bored Tunnels using GPR. 2012 14th International Conference on Ground Penetrating Radar (GPR), 496–501. https://doi.org/10.1109/icgpr.2012.6254916

Kasban, H., Zahran, O., Elaraby, S. M., El-Kordy, M., & Abd El-Samie, F. E. (2010). A comparative study of landmine detection techniques. Sensing and Imaging, 11, 89–112. https://doi.org/10.1007/s11220-010-0054-x

Lo Monte, L., Erricolo, D., Picco, V., Soldovieri, F., & Wicks, M. C. (2009). Distributed RF tomography for tunnel detection: Suitable inversion schemes. National Aerospace and Electronics Conference, Proceedings of the IEEE, 182–189. https://doi.org/10.1109/NAECON.2009.5426629

Lo Monte, L., Erricolo, D., Soldovieri, F., & Wicks, M. C. (2010). RF tomography for below-ground imaging of extended areas and close-in sensing. IEEE Geoscience and Remote Sensing Letters, 7(3), 496–500. https://doi.org/10.1109/LGRS.2009.2039918

Lo Monte, L., Patton, L. K., & Wicks, M. C. (2010). Direct-path mitigation for underground imaging in RF tomography. Proceedings - 2010 12th International Conference on Electromagnetics in Advanced Applications, ICEAA'10, (1), 27–30. https://doi.org/10.1109/ICGPR.2010.5550225

Meincke, P. (2001). Linear GPR inversion for lossy soil and a planar air-soil interface. IEEE Transactions on Geoscience and Remote Sensing, 39(12), 2713–2721. https://doi.org/10.1109/36.975005

Monte, L. L., Soldovieri, F., Akduman, I., & Wicks, M. C. (2010). Imaging under irregular terrain using RF tomography and numerical green functions. Antennas and Propagation Society International Symposium (APSURSI), 2010 IEEE, (1), 1–4. https://doi.org/10.1109/APS.2010.5561678

Monte, L. Lo, Erricolo, D., Soldovieri, F., & Wicks, M. C. (2010). Radio frequency tomography for tunnel detection. IEEE Transactions on Geoscience and Remote Sensing, 48(3 PART 1), 1128–1137. https://doi.org/10.1109/TGRS.2009.2029341

Norgard, J., Wicks, M. C., Baldygo, W., Magde, K., Moore, W., Drozd, A., & Musselman, R. (2007). Distributed/embedded sub-surface sensors for imaging buried objects with reduced mutual coupling and suppressed electromagnetic emissions. 2007 International Waveform Diversity and Design Conference, WDD, 93–97.

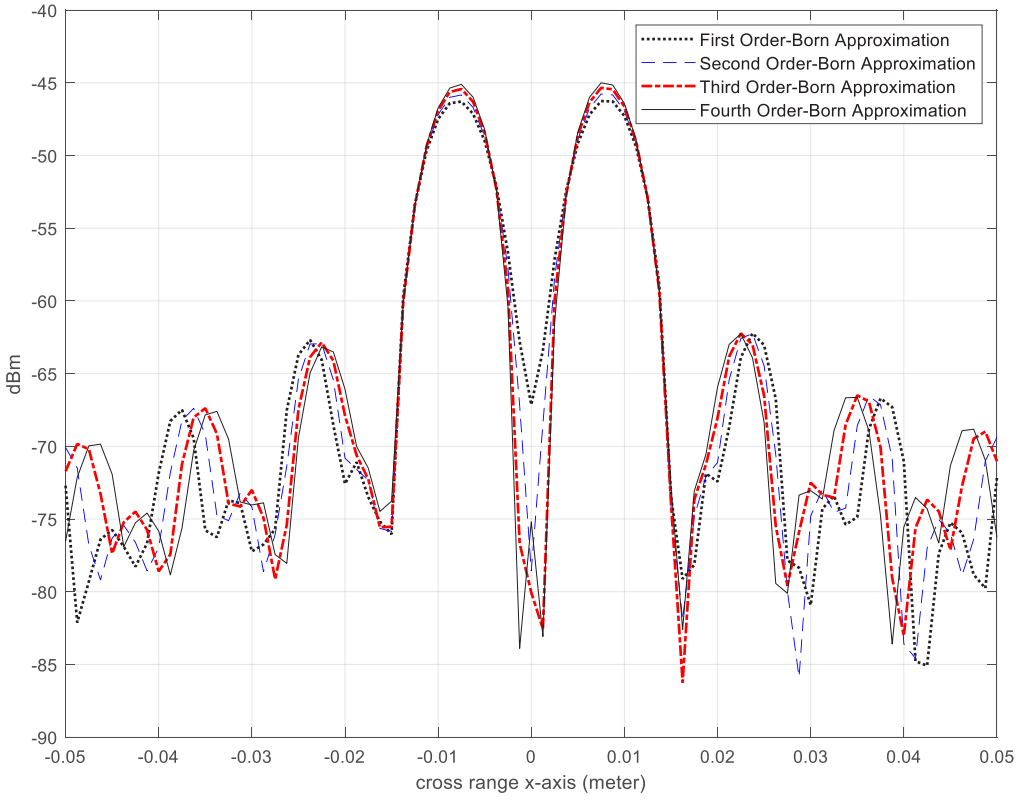

Figure 4: the cross-range of x-axis at each iteration.

4. CONCLUSION

Combining GPR and RFT concepts provides an improved resolution of target imagery when detecting landmines and another unexploded ordinance. Target sensing was improved with adjustments to the transmitter/receiver deployment. Inverse scattering of a first-order Born approximation was employed for the resolution of the linear unknown dielectric profile. We used the object profile function to calculate and update the incident field at each iteration. This numerical solution's outcomes demonstrate an accurate interpretation of the scattered field to derive an image of the target. Propagation attenuation and losses are reduced through the use of an ultra-narrowband frequency, which leads to a reduction of the resolution.

REFERENCE

Afsari, A., Abbosh, A. M., & Rahmat-Samii, Y. (2019). Modified Born Iterative Method in Medical Electromagnetic Tomography Using Magnetic Field Fluctuation Contrast Source Operator. IEEE Transactions on Microwave Theory and Techniques, 67(1), 454–463. https://doi.org/10.1109/TMTT.2018.2876228

Ambrosanio, M., Bevacqua, M. T., Isernia, T., & Pascazio, V. (2019). The Tomographic Approach to Ground-Penetrating Radar for Underground Exploration and Monitoring: A More User-Friendly and Unconventional Method for Subsurface Investigation. IEEE Signal Processing Magazine, 36(4), 62–73. https://doi.org/10.1109/MSP.2019.2909433

Baker, C. J., & Hume, A. L. (2003). Netted radar sensing. IEEE Aerospace and Electronic Systems

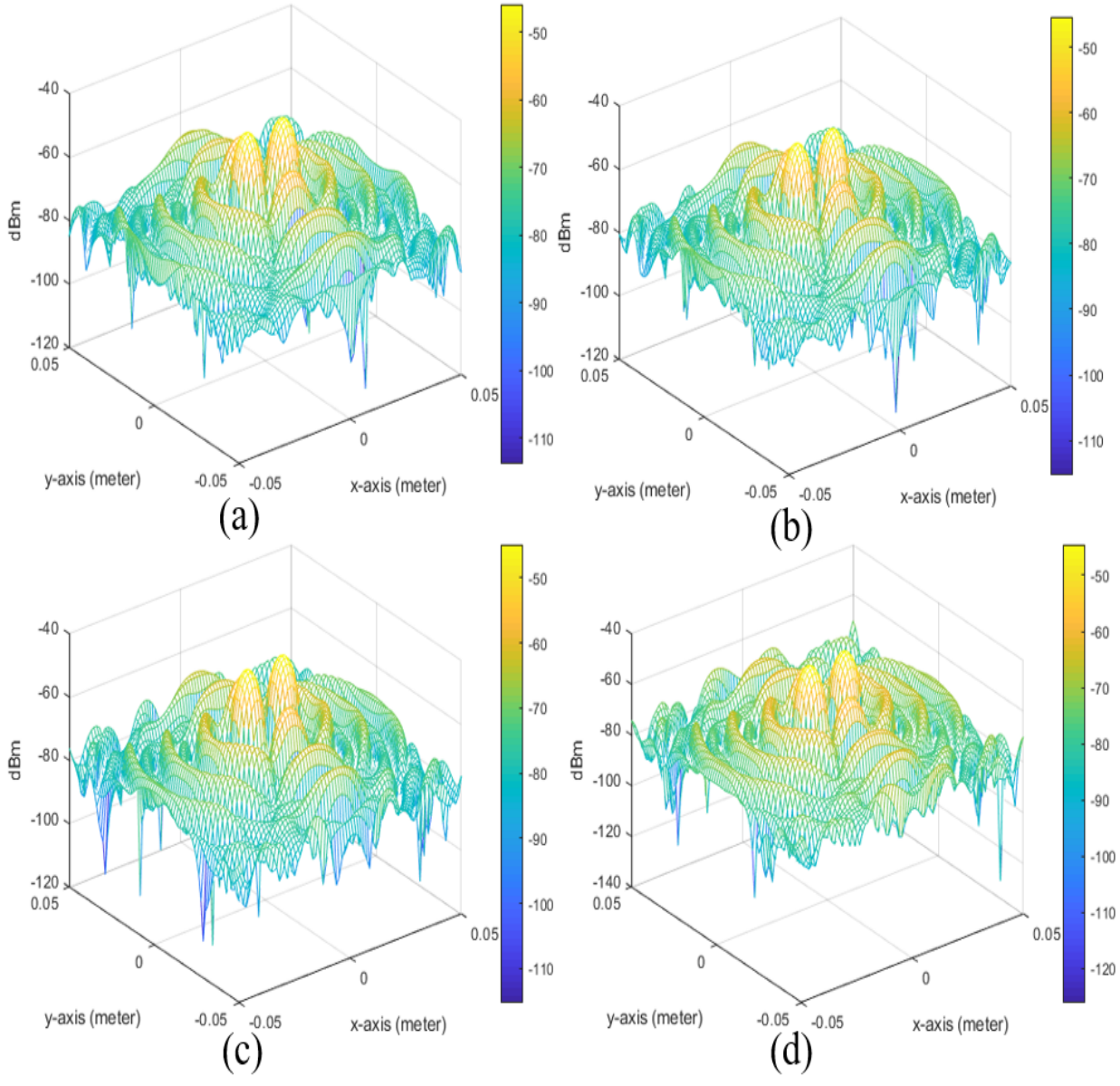

Figure 3: (a) First order Born Approximation power distribution of the measurement domain.
(b) Second-order Born Approximation power distribution of the measurement domain.
(c) Third-order Born Approximation power distribution of the measurement domain.
(d) Fourth-order Born Approximation power distribution of the measurement domain.

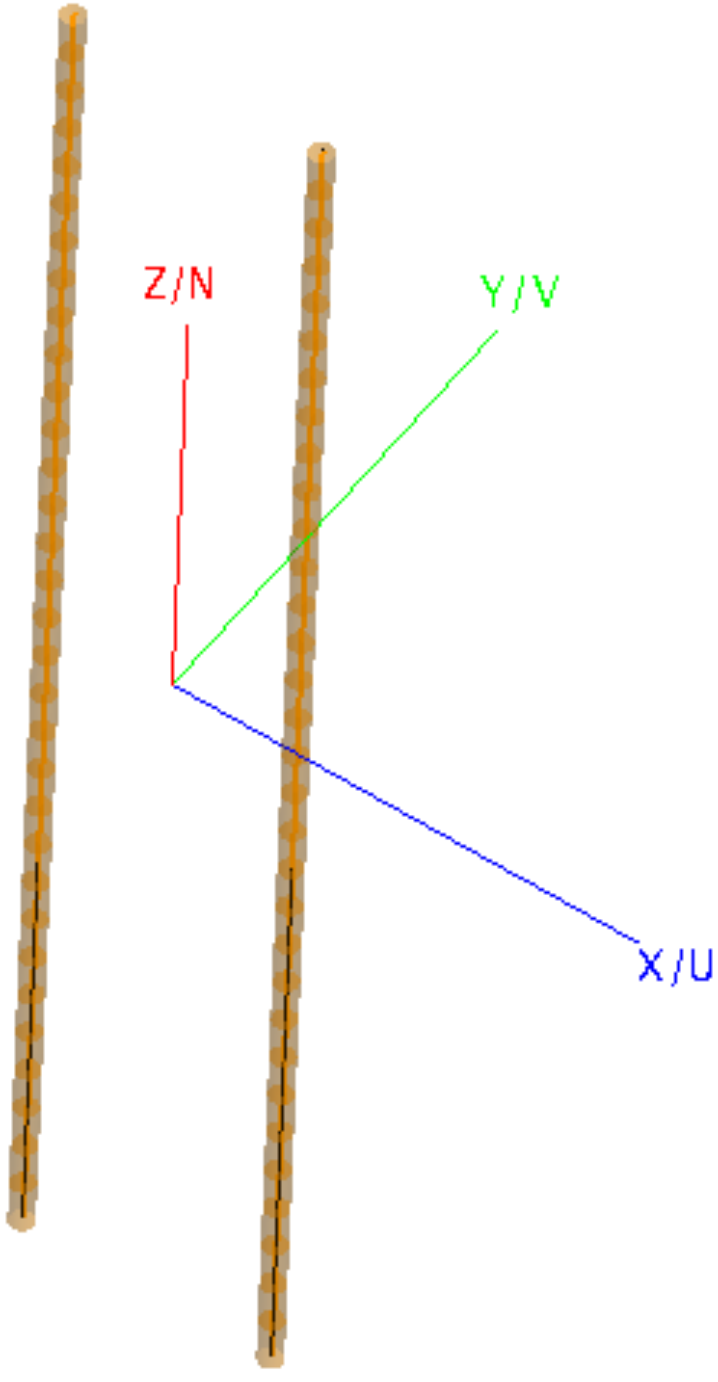

Figure 2: The two thin wires placed 0.8 cm and -0.8 cm along the x-axis.

measurement domain. The distance, from the center of the measurement domain to the transmitters and the receivers placed rounded, were 40 cm and 200 cm, respectively. The objects at the measurement domain are two thin wires, and the two wires are placed at 0.8 cm and -0.8 cm from the center along the x-axis, as shown in Figure 2. The measurement domain was reconstructed with size 5×5 cm discrete into 81×81 pixels at xy-plan. The pixel dimension is 0.1249 cm. The reconstructed domain xy-plan was simulated at z=0. The linear operator matrix L consists of 969×6561 components of the calculated electric field response at each pixel location due to the transmitter's location and the receiver under first-order Born approximation to keep the linearity of the inversion using conjugate gradient algorithm. The process was repeated after we obtained the object profile function, and then we calculated the second-order Born approximation. The object profile function was updated at each iteration of the algorithm until we sufficiently obtain the desired resolution of the resolution's improvement reached the peak. The power distribution of the measurement domain at each iteration is shown in Figure 3, starting from First order Born approximation to the fourth-order Born approximation. This First Order Born Approximation has less resolution to distinguish the two peaks where its distance kept the same comparing with higher orders. The noise to peak ratio test has employed to analyze the improvement of processing the data with higher order Born approximation. By notice that, the second order is the process of the first order result as solution of the ill-posed matrix solution. Table 1 is shown the improvement of the noise to peak ratio where we can notice the fourth order Born approximation has better performance comparing to lower orders.

Table 1: The Signal to Noise Ratio of the Measurement Domain

	Born Approximation Order	Signal-to-Noise Ratio (dB)
1	First Order Born Approximation	20.5070
2	Second Order Born Approximation	20.8222
3	Third Order Born Approximation	21.1109
4	Fourth Order Born Approximation	21.3739

The conjugate gradient's computational cost is $O(TNMP^2)$, with the number of iterations T equaling four, P is the number of pixels, and N and M are the numbers of the transmitters and receivers. Figure 4 illustrates reconstructed results employing both First-Order Born Approximation and Higher-Order Born Approximation. It may be observed that there is less background noise with the higher-order approximation than with the first-order approximation, where clearly we can distinguish the two peaks without overlapping. The proposed algorithm has a significant noise reduction compared to conventional methods (first-order Born approximation). Generally, the object function derived from the higher-order approximation is a closer match to the ideal.

in which,

$$\boldsymbol{A^{q+1}}(\boldsymbol{r_m^r}) = k_0^2 \iiint_{V_i} \hat{\mathrm{a}}_{\mathrm{m}}^{\mathrm{r}} \cdot \bar{\mathbf{G}}(\boldsymbol{r_m^r}, \mathbf{r}') \cdot \boldsymbol{X_q}^{-1}(\boldsymbol{r}')\tau_\delta{}^q(\mathbf{r}')d\mathbf{r}' \tag{29}$$

$$\begin{bmatrix} A_1^{q+1} \\ \vdots \\ A_M^{q+1} \end{bmatrix} = \begin{bmatrix} \bar{\mathbf{G}}_{\mathbf{11}}(\mathbf{r_1^r}, \mathbf{r_1}) & \dots & \bar{\mathbf{G}}_{\mathbf{1P}}(\mathbf{r_1^r}, \mathbf{r_P}) \\ \vdots & \ddots & \vdots \\ \bar{\mathbf{G}}_{\boldsymbol{M1}}(\boldsymbol{r_m^r}, \mathbf{r_1}) & \dots & \bar{\mathbf{G}}_{\boldsymbol{MP}}(\boldsymbol{r_m^r}, \mathbf{r_P}) \end{bmatrix} \begin{bmatrix} X_1^q \\ \vdots \\ X_M^q \end{bmatrix}^{-1} \begin{bmatrix} \tau_\delta{}^q(\mathbf{r_1}) \\ \vdots \\ \tau_\delta{}^q(r_P) \end{bmatrix} \tag{30}$$

where, q = 0,1,2,3 …

As the 3×3 matrix in Eq.(17) is small in size, it is easy for the reflectivity coefficient to be inverted and thus obtain the total electric field $\mathbf{E}(\mathbf{r}', \boldsymbol{r_n^t})$. Nevertheless, the evaluation of the matrix element $\boldsymbol{A^q}(\boldsymbol{r_m^r})$ may be extremely rapid if we employ the component form:

$$\boldsymbol{A^{q+1}}(\boldsymbol{r_m^r}) = k_0^2 \sum \iiint_{V_i} \hat{\mathrm{a}}_{\mathrm{m}}^{\mathrm{r}} \cdot \bar{\mathbf{G}}(\boldsymbol{r_m^r}, \mathbf{r}') \cdot [\boldsymbol{X_{q+1}}^{-1}(\boldsymbol{r}') \cdot \hat{\mathrm{a}}_{\mathrm{n}}^{\mathrm{t}}]\tau_\delta{}^0(\mathbf{r}')d\mathbf{r}' \tag{31}$$

This allows for smooth expression of the qth order of the target function $\tau_\delta{}^0(\mathbf{r}')$ in terms of the target function $\tau_\delta(\mathbf{r}')$ for the linear solution of the first-order Born approximation. Finally, the linear relationship of the scattered field and the dielectric profile is provided with:

$$\mathbf{E}^S(\boldsymbol{r_n^t}, \boldsymbol{r_m^r}) = \mathbf{L}(\tau_\delta(\mathbf{r}')) \tag{32}$$

The linear operator L must be inverted for computation of the unknown dielectric profile $\tau_\delta(\mathbf{r}')$. The first-order Born approximation is providing accurate results if the target was near the transmitter and had no contrast. In the following section, resolution improvement will be affected as it is essential to be sure of the target's nature, i.e., if it is a landmine or not. As the multipath frequency increases, the target contrast and the first-order Born approximation becomes less accurate, with the electrical field demonstrating notable spatial variations in the scattered. Thus, the Born approximation is invalidated as a result of multiple-scattering effects.

3. SIMULATION AND RESULTS

The electromagnetic computational software FEKO© was used to obtain the simulation of the scattered field $\mathbf{E^S}$, with MATLAB© being employed for calculation of the total electric field. The data is processed to produce a reconstruction of the buried target's image. The electric field's numerical computation was chosen to undergo comparison with the results obtained through experimentation in the Mumma lab facilities employed for the simulation; FEKO© software was employed, providing electromagnetic simulation for calculation and simulation of the desert field. We operate the simulation at ultra-narrowband 10.8 GHz single frequency to exploit the tomographic radar scanning's gematrical diversity. The ultra-narrowband's operating frequency has gained the scattered signal attenuation immunity due to the bandwidth reduction to increase the resolution. We collected data using 51 receivers and 19 transmitters located equally spaced in a circular manner around the

The orientation of the transmitter is given by $\hat{a}_n^t$ at the location $\boldsymbol{r_n^t}$ while the receiver orientation is given by $\widehat{\boldsymbol{a}}_{\boldsymbol{m}}^{\boldsymbol{r}}$ at location $\boldsymbol{r_m^r}$. By substitute Eq.(13) and Eq.(17)

$$\boldsymbol{E}^S(\boldsymbol{r}_n^t, \boldsymbol{r}_m^r) = Qk_0^2 \iiint_{V_i} [\widehat{\boldsymbol{a}}_m^r \bar{\boldsymbol{G}}(\boldsymbol{r}_m^r, \boldsymbol{r}')][\bar{\boldsymbol{G}}(\boldsymbol{r}', \boldsymbol{r}_n^t)\hat{a}_n^t]\tau_\delta(\boldsymbol{r}')d\boldsymbol{r}' \quad (18)$$

When higher-order extended Born approximation is introduced, the accuracy of the reconstruction of the target is enhanced. Research has been undertaken into the convergence of nonlinear approximations with high contrast targets provided through:

$$\mathbf{E}(\mathbf{r}') = \boldsymbol{X}(\boldsymbol{r}')^{-1} \cdot \mathbf{E}^{\boldsymbol{I}}(\mathbf{r}') \quad (19)$$

With $\boldsymbol{X}(\boldsymbol{r})$ being the reflectivity coefficient; clearly, if $X(r) = 1$, we arrive at a first-order Born approximation in Eq.(13), but High-order Extended Born approximation for their general form is provided as q-th order, thus

$$\boldsymbol{X_q}(\boldsymbol{r}') \cdot \mathbf{E}(\mathbf{r}', \boldsymbol{r_n^t}) = \mathbf{E}^{\boldsymbol{I}}(\mathbf{r}', \boldsymbol{r_n^t}), \text{ where q} = 0,1,2, \ldots \quad (20)$$

The reflectivity coefficient $\boldsymbol{X_q}(\boldsymbol{r'})$ The definition of the zeroth-order of the approximation becomes:

$$\boldsymbol{X_0}(\boldsymbol{r}') = \boldsymbol{I} + \boldsymbol{A^0}(\boldsymbol{r}') \quad (21)$$

in which ***I*** **is** unity matrix, and $A^0(r)$ is a matrix with a definition of

$$\boldsymbol{A^0}(\boldsymbol{r_m^r}) = k_0^2 \iiint_{V_i} \hat{a}_m^r \cdot \bar{\mathbf{G}}(\boldsymbol{r_m^r}, \mathbf{r}') \cdot {\tau_\delta}^0(\mathbf{r}')d\mathbf{r}' \quad (22)$$

$$\begin{bmatrix} X_1^0 \\ \vdots \\ X_M^0 \end{bmatrix} = I + \begin{bmatrix} A_1^0 \\ \vdots \\ A_M^0 \end{bmatrix} = \begin{bmatrix} \bar{\mathbf{G}}_{\mathbf{11}}(\mathbf{r}_1^r, \mathbf{r}_1) & \ldots & \bar{\mathbf{G}}_{\mathbf{1P}}(\mathbf{r}_1^r, \mathbf{r}_P) \\ \vdots & \ddots & \vdots \\ \bar{\mathbf{G}}_{\mathbf{M1}}(\boldsymbol{r_m^r}, \mathbf{r}_1) & \ldots & \bar{\mathbf{G}}_{\mathbf{MP}}(\boldsymbol{r_m^r}, \mathbf{r}_P) \end{bmatrix} \begin{bmatrix} {\tau_\delta}^0(\mathbf{r}_1) \\ \vdots \\ {\tau_\delta}^0(r_P) \end{bmatrix} \quad (23)$$

$$\boldsymbol{E}^S(\boldsymbol{r}_n^t, \boldsymbol{r}_m^r) = Qk_0^2 \iiint_{V_i} [\widehat{\boldsymbol{a}}_m^r \bar{\boldsymbol{G}}(\boldsymbol{r}_m^r, \boldsymbol{r}')][\bar{\boldsymbol{G}}(\boldsymbol{r}', \boldsymbol{r}_n^t)\hat{a}_n^t]{\tau_\delta}^1(\boldsymbol{r}')d\boldsymbol{r}' \quad (24)$$

For the first-order of the approximation, we have a definition of

$$\boldsymbol{X_1}(\boldsymbol{r}') = \boldsymbol{I} + \boldsymbol{A^1}(\boldsymbol{r}')\boldsymbol{X_0}(\boldsymbol{r}') \quad (25)$$

with $\boldsymbol{A^1}(\boldsymbol{r}')$ having a definition of

$$\boldsymbol{A^1}(\boldsymbol{r_m^r}) = k_0^2 \iiint_{V_i} \hat{a}_m^r \cdot \bar{\mathbf{G}}(\boldsymbol{r_m^r}, \mathbf{r}') \cdot \boldsymbol{X_0}^{-1}(\boldsymbol{r}'){\tau_\delta}^1(\mathbf{r}')d\mathbf{r}' \quad (26)$$

$$\begin{bmatrix} A_1^1 \\ \vdots \\ A_M^1 \end{bmatrix} = \begin{bmatrix} \bar{\mathbf{G}}_{\mathbf{11}}(\mathbf{r}_1^r, \mathbf{r}_1) & \ldots & \bar{\mathbf{G}}_{\mathbf{1P}}(\mathbf{r}_1^r, \mathbf{r}_P) \\ \vdots & \ddots & \vdots \\ \bar{\mathbf{G}}_{\mathbf{M1}}(\boldsymbol{r_m^r}, \mathbf{r}_1) & \ldots & \bar{\mathbf{G}}_{\mathbf{MP}}(\boldsymbol{r_m^r}, \mathbf{r}_P) \end{bmatrix} \begin{bmatrix} X_1^0 \\ \vdots \\ X_M^0 \end{bmatrix}^{-1} \begin{bmatrix} {\tau_\delta}^1(\mathbf{r}_1) \\ \vdots \\ {\tau_\delta}^1(r_P) \end{bmatrix} \quad (27)$$

The *q*th -order solution of Eq.(27) is defined as

$$\boldsymbol{X_{q+1}}(\boldsymbol{r}') = \boldsymbol{I} + \boldsymbol{A^{q+1}}(\boldsymbol{r}')\boldsymbol{X_q}(\boldsymbol{r}') \quad \mathbf{(28)}$$

$$\tau_\delta(\mathbf{r}') = \varepsilon_r(\mathbf{r}') - \varepsilon_D + j\,\frac{\sigma(\mathbf{r}')-\sigma_D}{2\pi f \varepsilon_0} \quad (1)$$

With $\tau_\delta(\mathbf{r}')$ being the target function and the wavenumber expression in the investigation domain V_i being

$$k^2(\mathbf{r}') = \omega^2\mu_0\varepsilon_0\varepsilon_r(\mathbf{r}') + j\omega\mu_0\sigma(\mathbf{r}') \quad (2)$$

$$= k_D^2 + k_0^2\varepsilon_\delta(\mathbf{r}') \quad (3)$$

$$k_D = \omega\sqrt{\mu_0\varepsilon_0\varepsilon_r(\mathbf{r}') + j\omega\mu_0\sigma_D/\omega} \quad (4)$$

$$k_0 = \omega\sqrt{\mu_0\varepsilon_0\varepsilon_r(\mathbf{r}')} \quad (5)$$

The vector wave equation at each point of the investigation domain V_i derives from:

$$\nabla\times\nabla\times\mathbf{E}(\mathbf{r}') = [k_D^2 + k_0^2\tau_\delta(r')]\mathbf{E}(\mathbf{r}'). \quad (6)$$

Thus the scattered field $\mathbf{E^S}(\mathbf{r}')$ is expressed in terms of total field $\mathbf{E}(\mathbf{r}')$ for the investigation domain as the integral form

$$\mathbf{E^S}(\boldsymbol{r}') = k_0^2 \iiint_{V_i} \bar{\mathbf{G}}(\mathbf{r},\mathbf{r}')\cdot\mathbf{E}(\mathbf{r}')\tau_\delta(\mathbf{r}') \quad (7)$$

in which the vector point $r \in V_i$, (6) is a nonlinear integral equation because $\tau_\delta(\mathbf{r}')$ incorporated the total electric field. $\mathbf{E}(\mathbf{r}')$; $\bar{G}(r,r')$ is the Green's dyadic function due to the current source arrived at with Eq.(6),

$$\bar{\mathbf{G}}(\mathbf{r},\mathbf{r}') = \frac{1}{4\pi}\left[\bar{\mathbf{I}} + \frac{1}{k^2}\nabla\nabla\right]\frac{e^{-jk|\mathbf{r}-\mathbf{r}'|}}{|\mathbf{r}-\mathbf{r}'|}. \quad (8)$$

The Green's dyadic function correlates with the radiation emitted by a single transmitter (L. L. Monte, Soldovieri, Akduman, & Wicks, 2010), which offers a solution for the partial differential equation boundary condition Eq.(1),

$$\nabla\times\nabla\times\bar{\mathbf{G}}(\mathbf{r},\mathbf{r}') - k(\mathbf{r})^2\bar{\mathbf{G}}(\mathbf{r},\mathbf{r}') = \bar{\mathbf{I}}\delta(\mathbf{r}-\mathbf{r}') \quad (9)$$

Born approximation minimizes unknown variables in Eq.(6) to be simply $\tau_\delta(\mathbf{r}')$ through linearization of the inverse scattering problem under the approximation; thus, the inverse scattering problem is resolved for $\tau_\delta(\mathbf{r}')$ with the total field $\mathbf{E}(\mathbf{r}')$ expressed as an operator form Eq.(4),

$$\mathbf{E}(\mathbf{r}') - \mathbf{E^I}(\mathbf{r}') = \boldsymbol{A}(\boldsymbol{r}')\mathbf{E}(\mathbf{r}') \quad (10)$$

$$\mathbf{E}(\mathbf{r}') = [\mathbf{I} - \boldsymbol{A}(\boldsymbol{r}')]^{-1}\mathbf{E^I}(\mathbf{r}') \quad (11)$$

With $\mathbf{I}$ referring to the identity vector and the convolution and multiplication for $\tau_\delta(\mathbf{r}')$ are shown by Γ and Ψ, in that order. Subsequently, Eq.(10) may be expanded if the norm is below one, thus:

$$\mathbf{E}(\mathbf{r}') = (\mathbf{I} - \boldsymbol{A^0}(\boldsymbol{r}') + \boldsymbol{A^1}(\boldsymbol{r}') - \boldsymbol{A^2}(\boldsymbol{r}')\ldots)\mathbf{E^I}(\mathbf{r}') \quad (12)$$

Thus, the first-order Born approximation is described as:

$$\mathbf{E}(\mathbf{r}') = \mathbf{E^I}(\mathbf{r}') \quad (13)$$

The initial term in Eq.(11) is regarded as substituting the total field $\mathbf{E}(\mathbf{r}')$ with the incident field $\mathbf{E^I}(\mathbf{r}')$ in accordance with first-order Born approximation Eq.(4), thus:

$$\mathbf{E^S}(\boldsymbol{r}') \cong k_0^2 \iiint_{V_i} \bar{\mathbf{G}}(\mathbf{r},\mathbf{r}')\cdot\mathbf{E^I}(\mathbf{r}')\tau_\delta(\mathbf{r}')d\mathbf{r}' \quad (14)$$

We can now express the incident field in terms of Green's function as

$$\boldsymbol{E^I}(\boldsymbol{r}',\boldsymbol{r_n^t}) = \bar{\boldsymbol{G}}(\boldsymbol{r}',\boldsymbol{r_n^t})\hat{\boldsymbol{a}}_{\boldsymbol{n}}^{\boldsymbol{t}}. \quad (15)$$

$$\mathbf{E^I}(\mathbf{r}',\boldsymbol{r_n^t}) = \bar{\mathbf{G}}(\mathbf{r}',\boldsymbol{r_n^t})\cdot\hat{\mathrm{a}}_{\mathrm{n}}^{\mathrm{t}} \quad (16)$$

$$\boldsymbol{E^S}(\boldsymbol{r_n^t},\boldsymbol{r_m^r}) = k_0^2 \iiint_{V_i} \hat{\boldsymbol{a}}_{\boldsymbol{m}}^{\boldsymbol{r}}\bar{\boldsymbol{G}}(\boldsymbol{r_m^r},\boldsymbol{r}')\boldsymbol{E}^{\boldsymbol{I}}(\boldsymbol{r}',\boldsymbol{r_n^t})\tau_\delta(\boldsymbol{r}')d\boldsymbol{r}' \quad (17)$$

ed by GPS; in this way no human operator is put at risk. Nevertheless, standard ground-penetrating radar does not work well over rough surfaces such as rocky or mountainous terrain as the radar has to be positioned directly over the target for detection, which cannot be achieved on uneven terrain; a further consideration is that an area that has been subjected to missile attack will inevitably be uneven.

2. THE MATHEMATICAL MODEL FOR THE BURIED TARGET

For the buried target, the electric field model was expressed as a single frequency being the investigation domain V_i.

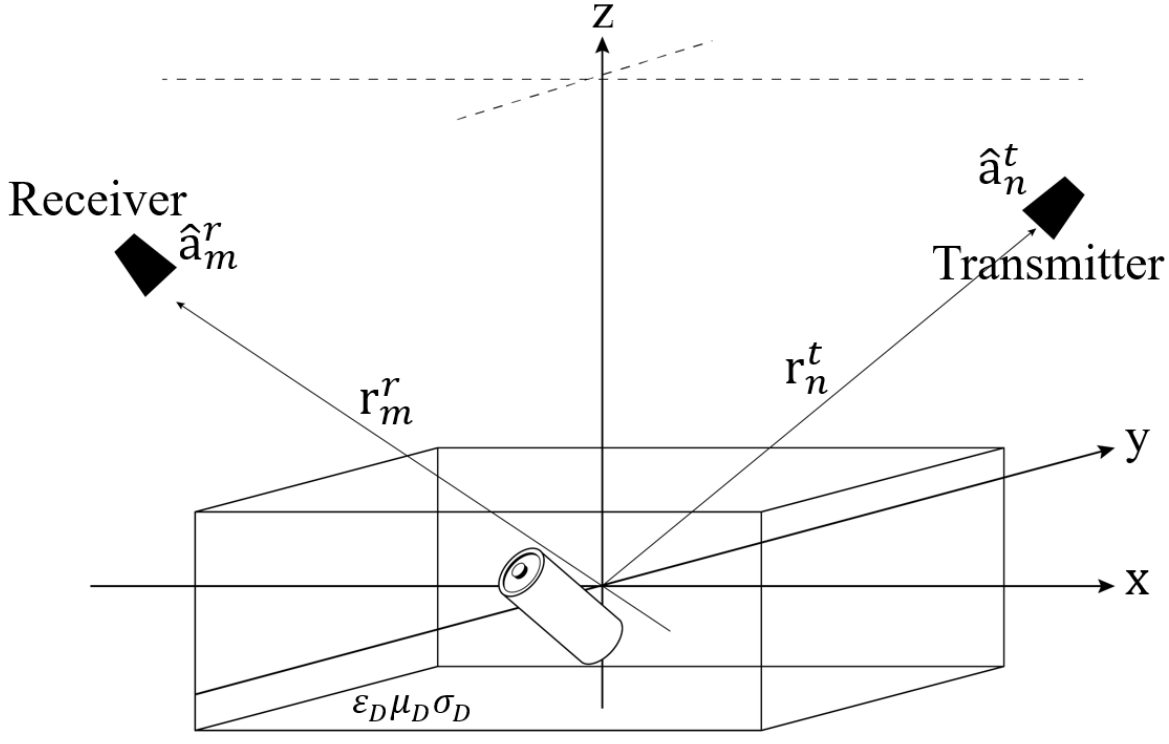

Figure 1: 3-D model of the buried target.

Figure 1 illustrates a 3-D geometric view of the model. The area of investigation where it is assumed the buried target will be discovered is a homogenous medium of estimated permeability μ_0, conductivity σ_D, and dielectric permittivity ε_D. It is assumed that the homogenous medium has identical properties to earth. Transmitters and receivers were positioned just above the ground. The dielectric permittivity profile $\varepsilon_r(r')$ for the investigation domain V_i is unknown; the conductivity profile $\sigma(r')$, when r' is the separate position vector, the unknown dielectric permittivity contrast reframes the inverse problem thus:

landmines and unexploded missiles, however, GPR is not as efficient in terms of detection because these objects tend to be just a short distance below the surface (Ambrosanio et al., 2019; Gurbuz, 2012; Sato, 2009). Over the last ten years, there have been a number of suggestions about using first-order Born approximation with RF tomography for underground detection (Cui et al., 2003; Fornaro, Lombardini, & Serafino, 2005; Guzel, Tran, Wicks, & Monte, 2015; L. Lo Monte, Erricolo, Picco, Soldovieri, & Wicks, 2009; L. Lo Monte, Erricolo, Soldovieri, & Wicks, 2010, 2010; L. Lo Monte, Patton, & Wicks, 2010; Meincke, 2001; Norgard et al., 2007; Vitebskiy, Carin, Ressler, & Le, 1997). Employing ground-penetrating radar throws up several problems in terms of its detection specifications, e.g., it is desirable to bring the transmitters/receivers as near to the search area as can be permitted; for optimal detection, the radar device must be directly over the object being sought (Kasban, Zahran, Elaraby, El-Kordy, & Abd El-Samie, 2010). Clearly, this is highly dangerous in terms of the probability of touching off the landmine or other buried ordnance, and it also makes for insuperable difficulties when direct access to a territory is not available(Carevic, 2000). A new form of detection will be introduced for discovering landmines and unexploded ordnance in such terrain. The GPR system will employ wideband to procure additional information regarding targets buried underground and therefore supply high-resolution imaging. Because of this, there will be significant propagation losses around the end of the operating band, which will impose limits upon penetration depth. Due to the electromagnetic spectrum being crowded and extremely narrow, this research employs ultra-narrowband signals to ensure that the detection process is free of interference. This system provides an economic architecture and ensures no noise levels and low-frequency dispersion by employing ultra-narrowband and adaptive waveforms. Thermal noise increases signal bandwidth, degrading the signal-to-noise ratio; this can be resolved by employing discrete ultra-narrowband tones.

1.1. Radio Frequency Tomography

Radio Frequency Tomography is a promising technology for generating 3D imagery of buried objects, e.g., landmines or unexploded ordnance. It is crucial to achieve a proper object resolution to be confident that the detected object is the desired target. In this method, the transmitters and receivers undergo arbitrary spatial dispersion over the area under investigation. N transmitters and M receivers are transported using unmanned ground vehicles. One transmitter will operate with the other transmitters are being silent, with every transmitter radiating a defined waveform employing appropriate polarization (Picco, Erricolo, & Lo Monte, 2010), so that we know a defined quantity of receivers have undergone activation in a defined location. These transmitters and receivers are selected to prevent forward scattering. Having various transmitters/receivers enables us to obtain a unique perspective of the target object(Desai & Jenkins, 1992). The data harvested through each receiver has its noise and clutter removed and then is stored. When selecting an active receiver antenna, the active transmitter antenna's main lobe's beamwidth angle is considered (Karlovšek, Scheuermann, & Willimas, 2012). The inverse scattering problem was employed to provide a superior means of creating imagery of buried targets employing high contrast dielectric media or even anomaly-conducting media. Experiments will take place over both homogenous and inhomogeneous rough surfaces. Two methods were employed to derive the scattered field's expression on the target, first by employing the wave equation and Born approximation and then employing the wave equation and high order extended Born approximation. A comparative study between both methods in terms of how efficient they are and the resolution provided. For both method, geometrical measurements have been taken to provide estimations of the target as a function of the scattered field. RFT, employing multiple transmitters/receivers for the achievement of geometric diversity(Baker & Hume, 2003), naturally provides high levels of information regarding the area being searched, which makes it easier to identify the void; furthermore, the resolution and the possibilities of detection are increased by each transmitter and receiver being transported by autonomous ground vehicles guid-

1. INTRODUCTION

Radar imaging is an instrumental means of exploring the underground. RFT for ground-penetrating radar imaging (RFT-GPR) application is the most frequently employed radar imaging technique(Wicks, 2007). This form of imaging is exceptionally prevalent in commercial operations, e.g., gas/oil exploration; it returns a grayscale mapping of the amplitude (brightness) of echoes related to a location within the scanned area(Ambrosanio, Bevacqua, Isernia, & Pascazio, 2019). Nevertheless, this technique cannot resolve structures below the size of one-third of the incident wave's wavelength. This difficulty could be overcome by employing an inverse scattering technique founded in RFT-GPR. If incident electromagnetic waves come across an inhomogeneity, a percentage of the energy is broadcast in all directions. Several electromagnetics parameters can be employed for the recognition of weak non-metallic scatterer, e.g., landmines. This means that quantitative information regarding the examined objects could be returned using RFT-GPR.

For environmental monitoring and assessment, near-surface geophysical explorations, and the discovery of landmines and other unexploded ordinance, electromagnetic (EM) inverse scattering methodologies to find submerged dielectric objects are frequently employed. EM inverse scattering is a nonlinear one, as there will be a multiplicity of scattering effects within objects. With substantial 3D problems, it is challenging to employ nonlinear inversion methodologies due to the competing demands they impose(Chew & Wang, 1990). When there is a low level of contrast between the buried object and its background, the Born approximation is generally employed for linearization of the nonlinear inverse scattering. Lilia inversion is frequently used to detect buried objects on-site due to its simplicity and the demand for computational resources. However, when there is a significant contrast between the buried object and the surroundings, inaccuracies appear with the Born approximation, and accurate detection is impossible with the linear inversion. However, a fast measurement for brain stroke diagnosis at the emergency room was proposed for fluctuations of biological tissue dielectric function using the Born iterative method (BIM) (Afsari, Abbosh, & Rahmat-Samii, 2019). Solving the computational cost issue was proposed at (Han et al., 2019) by proposing a new inversion algorithm—a multifrequency inversion algorithm as proposed by minimizing the cost function (Qiu et al., 2019).

To harvest acceptable resolution imagery of buried objects without having to resolve nonlinear inverse scattering problems, it has been suggested that with 2D scalar problems quasilinear approximations (Zhdanov & Hursan, 2000; Zhou & Liu, 2000) and high-order approximations (Gao & Torres-Verdin, 2006) should be employed. This research suggests an efficient method of imaging 3D objects buried employing First-order Born approximation to update each iteration object's object profile function (Cui et al., 2005). The proposed method shows that first iteration solutions match that of Born approximations, correspondent to linear inverse scattering. High-older solutions for object profile functions with inverse scattering problems can be found, having closed-form relationships while keeping the linearity of inversion(Cui, Aydiner, Chew, Wright, & Smith, 2003). The Fast Fourier Transform can be employing the evaluation of the simplicity of the relationship. This high-order solution is of an order of simplicity compared to the Born approximation. When the object profile function has a significant contrast, high-order solutions have far greater accuracy due to approximate considerations of the object's internal multiple-scattering effect. Thus, high contrast object profile function acceptable resolution images can be created employing the proposed methodology only through linear inverse problem solution. With this linear inversion, we have employed a conjugate gradient, offering superior reconstruction outcomes. Numerical experimentation has demonstrated that the suggested means of employing ground-penetrating radar and radiofrequency tomography is both valid and efficient when they are combined to provide improved estimations of the detection parameters in reconstructing a target image, incorporating geolocation. In the case of

المملكة العربية السعودية
جامعة الحدود الشمالية (NBU)
مجلة الشمال للعلوم الأساسية والتطبيقية (JNBAS)
طباعـــة - ردمد: 1658-7022 / الكتروني - ردمد: 1658-7014
www.nbu.edu.sa
http://jnbas.nbu.edu.sa

الكشـف عـن الأجسـام المدفونـة باسـتخدام التصويـر المقطعـي الراديـوي تحـت افتـراض تقريـب بـورن ذو الرتبـة العاليـة

مهند سالم المطيري

(قدم للنشر في 1441/11/05هـ؛ وقبل للنشر في 1442/03/24هـ)

ملخص: يُستخدم التصوير المقطعي للترددات الراديوية عادة لاكتشاف وإعادة بناء صور الأهداف المدفونة بعمق والمرافق الأرضية تحت الأرض. يجمع هذا البحث بين رادار الاختراق الأرضي والتصوير المقطعي للترددات اللاسلكية (RFT) ولتقييم البيئة ، وتحديد موقع الهدف ، وإنشاء صورة مستهدفة لأشياء متنوعة مثل الألغام الأرضية أو الذخائر غير المنفجرة. بعد جمع البيانات من عدد من أجهزة الإرسال والاستقبال ، يتم استخدام مبدأ الانتشار العكسي لحساب الخصائص العازلة. لحل صعوبة الانتشار العكسي غير الخطي ، يتم استخدام تقريب Born عالي الترتيب. يرسل جهاز الإرسال أشكالاً موجية ضيقة النطاق منخفضة التردد مناسبة على سطح الأرض ؛ وهكذا فإن واجهة الموجة خلقت أجسامًا تحت الأرض ، والتي تبدد الطاقة الكهرومغناطيسية في كل اتجاه. تأخذ أجهزة الاستقبال عينة من الإشارة المتناثرة ، وتسترد أطوارها ، ويتم ترحيل هذه المعلومات إلى معالج مركزي. بمجرد وضع البيانات الملتقطة من خلال المعالجة التكيفية ، يمكن إنشاء صورة للأهداف تحت الأرض. تقترح هذه الورقة تقليل التعقيدات الحسابية وإعادة بناء الصورة المحسنة من خلال شكل بسيط وفعال لتقريب Born الأعلى رتبة. وهذا يسمح ببناء صور عالية الدقة عند العمل مع أهداف التباين العالية ببساطة من خلال حل مشكلة التشتت العكسي الخطي. تم استخدام خوارزمية متدرجة متقاربة للانقلاب الخطي. و لقد أظهر الاختبار العددي أن هذه المنهجية المقترحة صالحة وفعالة.

كلمات مفتاحية: رادار الاختراق الأرضي، التصوير المقطعي، الترددات الراديوية، الانتشار العكسي، التشتت العكسي الخطي.

* **للمراسلة:**
أستاذ مساعد، قسم الهندسة الكهربائية، كلية الهندسة، جامعة الحدود الشمالية، ص ب: 1321، رمز بريدي: 91431، المدينة عرعر، المملكة العربية السعودية.

e-mail: Muhannad.almutiry@nbu.edu.sa

jnbas.nbu.edu.sa
DOI: 10.12816/0058335

KINGDOM OF SAUDI ARABIA
Northern Border University (NBU)
Journal of the North for Basic and Applied Sciences (JNBAS)
p- ISSN: 1658 - 7022 / **e- ISSN:** 1658 - 7014
www.nbu.edu.sa
http://jnbas.nbu.edu.sa

Detection of Buried Object Using RF Tomography Under High-Order Born Approximation Assumption

Muhannad S. Almutiry

(Received 26/06/2020; Accepted 09/11/2020)

Abstract: Radiofrequency tomography (RFT) is frequently employed for the detection and reconstruction of images of deeply buried targets and underground facilities. This research combines ground penetrating radar with RFT for assessment of the environment, pinpointing the location of a target, and creating a target image of suc buried objects as landmines or unexploded ordnance. Following data collection from a number of transmitters and receivers, the inverse scattering principle is employed for the computation of dielectric properties. For the resolution of the nonlinear inverse scattering difficulty, a high-order Born approximation is employed. The transmitters beam appropriate low-frequency narrowband waveforms at the earth's surface; the wave front thus created encounters underground objects, which scatters electromagnetic energy in every direction. Receivers take a sample of the scattered signal, retrieving their phases, and this information is relayed to a central processor. Once the captured data has been put through adaptive processing, an image of the underground object can be constructed. This paper proposes the reduction in computational complexities and an improved image reconstruction through a simple and efficient form of higher-order Born approximation. The proposed method is based on updating the reconstructing domain at each Born approximation process. This allows high-quality resolution imagery to be constructed when working with significant contrast objects simply through the resolution of a linear inverse-scattering problem. A Conjugate Gradient algorithm has been employed for the linear inversion. Numerical testing has demonstrated that this suggested methodology is both valid and efficient.

Keywords: GPR, RFT, RFT-GPR, RFT Born Approximation.

* **Corresponding Author:**

Assistant Professor, Dept. of Electrical Engineering, College of Engineering, Northern Border University, P.O. Box: 1321, Code: 91431, City of Arar, Kingdom of Saudi Arabia..

e-mail: Muhannad.almutiry@nbu.edu.sa

jnbas.nbu.edu.sa

DOI: 10.12816/0058335

Manuscripts in English Language

Journal of the North for Basic and Applied Sciences (JNBAS)
p-ISSN: 1658- 7022 e-ISSN: 1658- 7014

Vol. 6, Issue 1 May 2021 - Ramadan 1442 H

CONTENTS

Manuscripts in Arabic Language

Manuscripts in English Language

Citation from a book of more than one author:

Timothy, N., Stepich, D., & James, R. (2014/1434 H) *Instructional technology for teaching and learning.* Riyadh, Kingdom of Suadi Arabia: University of King Saud Publications.

Citation from Periodicals:

Al Nafaa, A. H. (1427 H). Effect of driving off–road on wild vegetation parks: A study in environmental protection, in the center of the Kingdom of Saudi Arabia. *Saudi Journal of Life Sciences, 14*(1), 35-72.

Citation from M.A. or Ph.D. Thesis:

AlQadi, I. A. (1429 H). *Natural Plants in a Coastal Environment between Rassi Tanoura and Elmalouh in the Eastern Region: A Study in Botanical Geography and the Protection of Environment.* Unpublished Ph.D. Dissertation, College of Arts for Girls, Dammam, Kingdom of Suadi Arabia: King Faisal University.

Citation from Internet References:

Citing an online book:

Almazroui, M .R. & Madani, M. F. (2010). *Evaluation of performance in Higher Education Institutions.* Digital Object Identifier (doi:10.xxxx/xxxx-xxxxxxxx-x), or the Hypertext Transfer Protocol (http://www...), or the International Standard Book Number (ISBN: 000-0-00-000000-0) must be mentioned.

Citing an article in a periodical:

Almadani, M. F. (2014). The definition of debate in reaching consensus. *The British Journal of Educational Technology, 11*(6), 225-260. Digital Object Identifier (doi:10.xxxx/xxxx-xxxxxxxx-x) or the Hypertext Transfer Protocol (http://onlinelibrary.wiley.com/journal/10.1111), or the International Standard Serial Number of the journal (ISSN: 1467- 8535) must be mentioned.

15. It is the researcher's responsibility to translate into English the Arabic bibliography.

Example:

الجبر، سليمان. (1991م). تقويم طرق تدريس الجغرافيا ومـدى اختلافها باختلاف خبـرات المدرسين وجنسياتهم وتخصصاتهم في المرحلة المتوسطة بالمملكة العربية السعودية. ***مجلة جامعة الملك سعود- العلوم التربوية، 3***(1)، 143-170.

Al-Gabr, S. (1991). The evaluation of geography instruction and the variety of its teaching concerning the experience, nationality, and the field of study in intermediate schools in Kingdom of Saudi Arabia *(in Arabic). Journal of King Saud University- Educational Sciences, 3*(1), 143-170.

16. Numerals should be the original Arabic numbers (0, 1, 2, 3 ...) in the manuscript.

Required Documents

Researchers are required to submit the following:

1. An electronic copy of their submissions in two formats: Microsoft Word Document (WORD) and Portable Document Format (PDF), to be sent to the following email:

s.journal.nbu@gmail.com

&

s.journal@nbu.edu.sa

2. The researcher's CV, including his/her full name in Arabic and English, current work address, email, and academic rank.
3. The researcher must fill out and submit the application for publishing in the Journal of the North, along with the Pledge Statement that his/her submission has not been published before or has not been submitted for publishing elsewhere.

NB

1. The submissions received by the Journal of the North will not be returned whether they are published or not.
2. The published papers reflect only the author's points of view.
3. All accepted manuscripts devolve their property to *the Journal of the North for Basic and Applied Sciences (JNBAS)*.

PUBLICATION INSTRUCTIONS FOR AUTHORS

Submission Guidelines

1. Manuscript must not exceed 35 pages of plain paper (A4).
2. Manuscript must have a title and an abstract in both Arabic and English on one page; the abstract should not be more than 250 words. The manuscript should include, in both languages, keywords that indicate the field of specialization. The keywords are written below each summary and should not be more than six.
3. The author(s) name(s), affiliation(s) and address(es) must be written immediately below the title of the article, in Arabic and English.
4. The Arabic manuscript is typed in Simplified Arabic, in 14-font size for the main text, and 12-font size for notes.
5. The English manuscript is typed in Times New Roman, in 12- font size for the main text, and 9-font size for notes.
6. The manuscript is typed only on one side of the sheet, and line spacing should be single. Margins should be 2.5 cm (or 1.00 inches) on all four sides of the page.
7. The manuscript must have the following organization:

   Introduction: It should indicate the topic and aims of the research paper, and be consistent with its ideas, information and the established facts. The research problem(s) and importance of the literature review should also be introduced.

   Body: The manuscript body includes all necessary and basic details of research approach, tools and methods. All stated information should be arranged according to priority.

   Findings and Discussion: Research findings should be clear and brief, and the significance of these findings should be elucidated without repetition.

   Conclusion: It is a brief summary of the research topic, findings, recommendations and suggestions.
8. Figures, diagrams and illustrations should be included in the main text and consecutively numbered and given titles, with explanatory notes beneath them.
9. Tables should also be included in the main text, consecutively numbered and given titles at the top, with explanatory notes below.
10. Footnotes should be added at the bottom of each page, when necessary. They are to be indicated by numbers or asterisks, in 12-font size for Arabic and 9-font size for English.
11. The Journal of the North does not publish research and measurement tools (instruments). However, they must be included in the submission(s).
12. Citations must follow the American Psychological Association (APA) reference style in which both the author's name and year of publishing are mentioned in the main text, i.e. (name, year). Numbering the references inside the main text and adding footnotes are not allowed.

    Researchers' documentation must be as follows:

    - For single author, the author's family name, followed by a comma, and the publishing year, such as (Khayri, 1985). Page numbers are indicated in the main text in case of quotations, such as (Khayri, 1985, p. 33).
    - If a manuscript has two authors, they must both be cited as shown previously, e.g. (AL-Qahtani & AL-Adnani, 1426 H).
    - If there are multiple (more than two) authors, their family names must be mentioned the first time only, e.g. (Zahran, Al-Shihri, & Al-Dusari, 1995); if the researcher is quoting the same work several times, the family name of the first author followed by *"et al."*[for papers in English] and by "وآخرون" [for papers in Arabic] must be used, e.g. (Zahran *et al.*, 1995) / (زهران وآخرون، 1995) Full publishing data must be mentioned in the bibliography.
13. Hadith documentation must follow the following example: (Sahih Al-Bukhari, vol.1, p.5, hadith number 511).
14. The bibliography, list of all the sources used in the process of researching, must be added in alphabetical order using the author's last name according to the APA reference style (6th edition) in 12-font size for Arabic and 9-font size for English.

    The bibliography should be organized as follows:

    Citation from books:

    Citation from a one-authored book:

    Shotton, M. A. (1989). *Computer education? A study to computer dependency.* London, England: Taylor & Francis.

Journal of the North for Basic and Applied Sciences (JNBAS)

About the Journal

The Journal of the North is concerned with the publication of original, genuine scholarly studies and researches in Basic and Applied Sciences in Arabic and English. It publishes original papers, review papers, book reviews and translations, abstracts of dissertations, reports of conferences and academic symposia. It is a biannual publication (May and November).

Vision

The journal seeks to achieve leadership in the publication of refereed scientific papers and rank among the world's most renowned scientific periodicals.

Mission

The mission of the journal is to publish refereed scientific researches in the field of Basic & Applied Sciences according to well-defined international standards.

Objectives

1. Serve as a scholarly academic reference for researchers in the field of Basic & Applied Sciences.
2. Meet the needs of researchers, publish their scientific contributions and highlight their efforts at the local, regional and international levels.
3. Participate in building a knowledge community through the publication of research that contributes to the development of society.
4. Cover the refereed works of scientific conferences.

Terms of Submission

1. Originality, innovation, and soundness of both research methodology and orientation.
2. Sticking to the established research approaches, tools and methodologies in the respective discipline.
3. Accurate documentation.
4. Language accuracy.
5. The contribution must be unpublished or not submitted for publication elsewhere.
6. The research extracted from a thesis/dissertation must be unpublished or not submitted for publishing elsewhere and the researcher must indicate that the research submitted for publishing in the journal is extracted from a thesis/dissertation.

Correspondence

Editor-in-Chief
Journal of the North for Basic and Applied Sciences (JNBAS),
Northern Border University, P.O.Box 1321, Arar 91431,
Kingdom of Saudi Arabia.
Tel: +966(014)6615499
Fax: +966(014)6614439
email: *s.journal@nbu.edu.sa* & *s.journal.nbu@gmail.com*
Website: *http://jnbas.nbu.edu.sa*

Subscription & Exchange

Scientific Publishing Center,
Northern Border University,
P.O.Box. 1321, Arar 91431,
Kingdom of Saudi Arabia.

Journal of the North for Basic and Applied Sciences

(JNBAS)

Peer-Reviewed Scientific Journal

Published by

Scientific Publishing Center

Northern Border University

Vol. (6), Issue (1)

May 2021 – Ramadan 1442 H

Website & Email

http://jnbas.nbu.edu.sa

s.journal@nbu.edu.sa **&** *s.journal.nbu@gmail.com*

p-ISSN: 1658- 7022 / e-ISSN: 1658- 7014

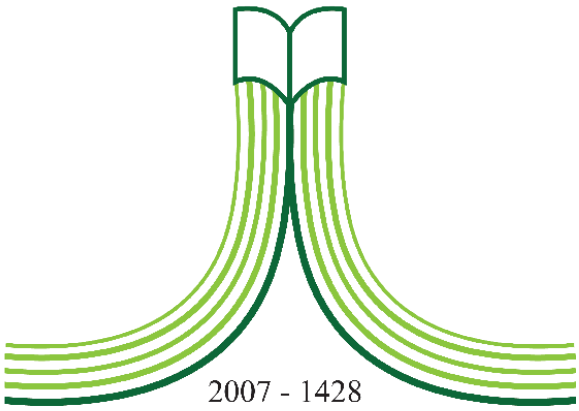

جامعة الحدود الشمالية

NORTHERN BORDER UNIVERSITY

Kingdom of Saudi Arabia

IN THE NAME OF ALLAH

THE MOST GRACIOUS, THE MOST MERCIFUL

مجلة الشمال للعلوم الأساسية والتطبيقية - المجلد (6) العدد (1) 1442 هـ
6(1)
Journal of the North for Basic and Applied Sciences Volume (6) Issue (1) 2021
JNBAS

2007 - 1428
جامعة الحدود الشمالية
NORTHERN BORDER UNIVERSITY

Volume (6)
Issue (1)
May
2021
Ramadan
1442 H

JNBAS

Journal of the North for Basic and Applied Sciences

Peer-Reviewed Scientific Journal

Northern Border University
www.nbu.edu.sa & jnbas.nbu.edu.sa

p- ISSN: 1658 - 7022
e- ISSN: 1658 - 7014